論文 / 著書情報
Article / Book Information

題目(和文)	
Title(English)	Pivotal roles of aminolevulinic acid (ALA) uptake transporters in ALA-photodynamic therapy
著者(和文)	Lai Hung Wei
Author(English)	Hung Wei Lai
出典(和文)	学位:博士(工学), 学位授与機関:東京工業大学, 報告番号:甲第12109号, 授与年月日:2021年9月24日, 学位の種別:課程博士, 審査員:小倉 俊一郎,西山 伸宏,小畠 英理,三重 正和,堤 浩
Citation(English)	Degree:Doctor (Engineering), Conferring organization: Tokyo Institute of Technology, Report number:甲第12109号, Conferred date:2021/9/24, Degree Type:Course doctor, Examiner:,,,,
学位種別(和文)	博士論文
Type(English)	Doctoral Thesis

Year 2021

Doctoral Thesis

Pivotal roles of aminolevulinic acid (ALA) uptake transporters in ALA-photodynamic therapy

Tokyo Institute of Technology

School of Life Science and Biotechnology

Life Science and Biotechnology Major

in

Life Science and Biotechnology Course

Lai Hung Wei

Academic Supervisor

Assoc. Prof. Dr. Ogura Shun-ichiro

Table of Contents

List of Abbreviations

%	Percentage
°C	Degree Celsius
ABAM	Antibiotic antimycotic
ABCG2	Adenosine triphosphate-binding cassette G2 transporter
ALA	Aminolevulinic acid
ALAD	ALA dehydratase
ANOVA	Analysis of variance
cDNA	Complementary DNA
CO_2	Carbon dioxide
CP III	Coproporphyrin III
CPgen III	Coproporphyrinogen III
DMEM	Dulbecco's modified Eagle medium
DMF	Dimethylformamide
DTT	Dithiothretiol
FBS	Foetal bovine serum
FECH	Ferrochelatase
GABA	Gamma-aminobutyric acid
GAT2	GABA transporter 2
HBBS	Hank's balanced salt solution
HCl	Hydrochloric acid
HPLC	High-performance liquid chromatography
LA	Levulinic acid
mL	Milliliter

mM	Millimolar
mRNA	Messenger RNA
NaOH	Sodium hydroxide
nm	Nanometer
nM	Nanomolar
O_2	Oxygen
OPTI-MEM	Optimized Eagle’s minimum essential medium
PAT1	Proton amino acid transporter 1
PBS	Phosphate buffered saline
PDD	Photodynamic diagnosis
PDT	Photodynamic therapy
PEPT1	Peptide transporter 1
PEPT2	Peptide transporter 2
PPB	Porphobilinogen
PpIX	Protoporphyrin IX
PrEGM	Prostate epithelial growth medium
qRT-PCR	Quantitative real-time polymerase chain reaction
RANK	Receptor associated nuclear factor-κB
RANKL	Receptor associated nuclear factor-κB ligand
ROS	Reactive oxygen species
RPMI 1640	Roswell Park Memorial Institute 1640
SDS-PAGE	SDS-polyacrylamide gel electrophoresis
siRNA	Small interfering RNA
SLC	Solute carrier

TauT	Taurine transporter
TBST	Tris-buffered saline with 0.05 % (v/v) Tween 20
YAP	Yes-associated protein
µL	Microliter
µM	Micromolar

CHAPTER 1
INTRODUCTION

1.1 GENERAL INTRODUCTION

1.1.1 History of photodynamic therapy

1.1.2 Mechanism of photodynamic therapy following light irradiation

1.2 AMINOLEVULINIC ACID IN PHOTODYNAMIC THERAPY AND DIAGNOSIS

1.2.1 Aminolevulinic acid as a prodrug

1.2.2 Mechanism of protoporphyrin accumulation following addition of aminolevulinic acid

1.2.3 Tailor-made therapy

1.3 TRANSPORTERS INVOLVED IN AMINOLEVULINIC ACID UPTAKE

1.3.1 Uptake transporters

1.3.1.1 Peptide transporter 1

1.3.1.2 Proton amino acid transporter 1

1.3.1.3 Taurine and GABA transporter 2

1.3.1.4 Transporters in normal cells

1.3.2 Efflux transporter

1.4 TRANSPORTERS' INVOLVEMENT IN THE EFFECTIVENESS OF PHOTODYNAMIC THERAPY UNDER DIFFERENT CANCER MALIGNANCY

1.4.1 Introduction to cancer malignancy

1.4.2 Relationship between transporters and cancer malignancy

1.5 AIMS & OBJECTIVES

1.1 GENERAL INTRODUCTION

1.1.1 History of photodynamic therapy

The concept of photodynamic therapy (PDT) was first found in 1900, where Oscar Raab, a medical student in Germany, accidentally found that paramecia incubated with certain dyes were dead following exposure to light but remain alive in the dark (Moan & Peng, 2003). This therapy was then quickly adapted in cancer research and several other fields such as dentistry and skin problems (Itoh *et. al.*, 2001; Konopka & Goslinski, 2007; Abrahamse & Hamblin, 2016). PDT has been an important therapy involved in various cancer clinical trials over the past decades (Dolmans *et. al.*, 2003; Huggett *et. al.*, 2014).

1.1.2 Mechanism of photodynamic therapy following light irradiation

This therapy utilized a photosensitizer to induce localized cell death and killing of solid tumors when irradiated with light (Peng *et. al.*, 1997; Krammer and Plaetzer, 2008). Photosensitizers enter a singlet-excited state when they absorbed a photon of light at specific wavelength, preferably between 650 nm to 800 nm (Agostinis *et. al.*, 2011). This is then followed by the conversion of the photosensitizer into a more stable excited triplet state with parallel spins where it transfers its energy by colliding with molecular oxygen (O_2), leading to formation of singlet oxygen ($^1O_2$) (Figure 1.1) (Abrahamse & Hamblin, 2016). This process is known as a Type II photochemical process whereby Reactive Oxygen Species (ROS) is generated and initiates the cell-killing action (Agostinis *et. al.*, 2011). PDT is believed to kill tumor cells via three main pathways, namely apoptosis, necrosis and autophagy. Although other factors such as the subcellular localization of photosensitizer in different organelles (e. g. mitochondria) and overall PDT doses were also possible candidates involved in this cell-killing action, it is generally believed that apoptosis is the

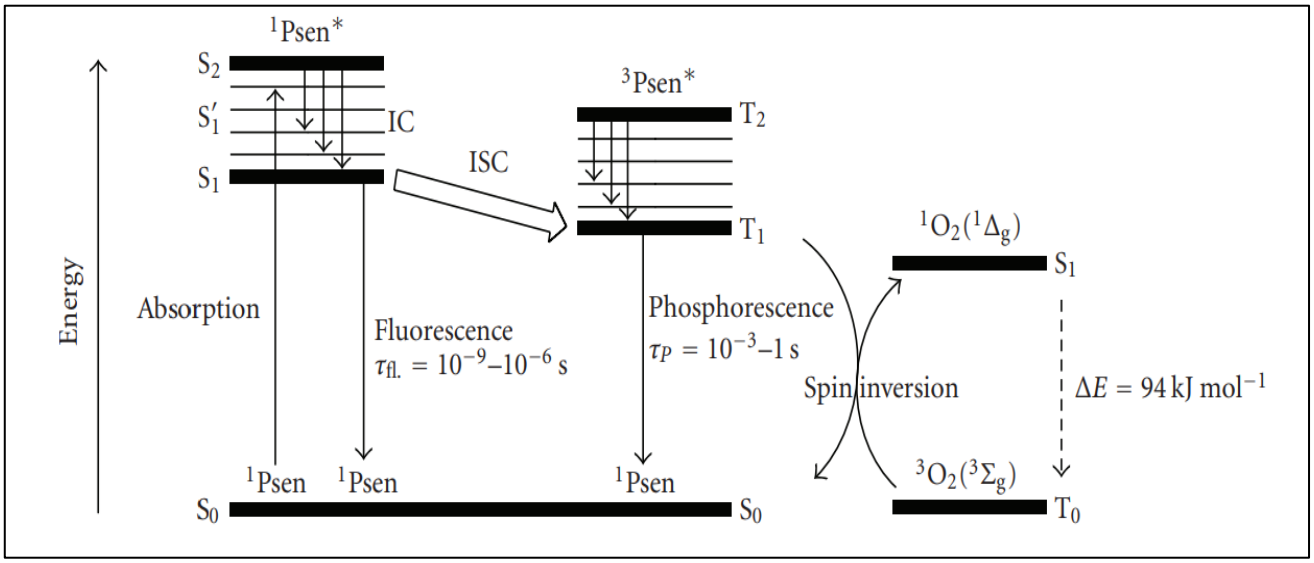

Figure 1.1 Conversion of singlet-excited photosensitizer into a more stable excited triplet state
(Leann & Ross, 2008)

main cell-death pathway following PDT (Abrahamse & Hamblin, 2016). However, since singlet oxygen have an unusually short lifetime (~10 – 320 ns), the maximum depth of cell diffusion is only approximately 10 – 55 nm, prompting the society to continue their effort in looking for new ways to enhance this therapy (Moan *et. al.*, 1989; Dysart & Patterson, 2005).

1.2 AMINOLEVULINIC ACID IN PHOTODYNAMIC THERAPY AND DIAGNOSIS

1.2.1 Aminolevulinic acid as a prodrug

5-aminolevulinic acid (ALA), a naturally-occurring heme precursor, is currently being used as a prodrug in PDT and PDD (Figure 1.2) (Krammer and Plaetzer, 2008). ALA and its derivatives are identified as prodrugs, as they need to be converted into protoporphyrin (PpIX) through the heme biosynthesis pathway metabolically before being able to function as an active photosensitizer (Figure 1.2 & 1.3) (Kennedy & Pottier, 1992; De Rosa & Bentley, 2000).The benefits of ALA include rapid clearance from the body, which is vital in reducing

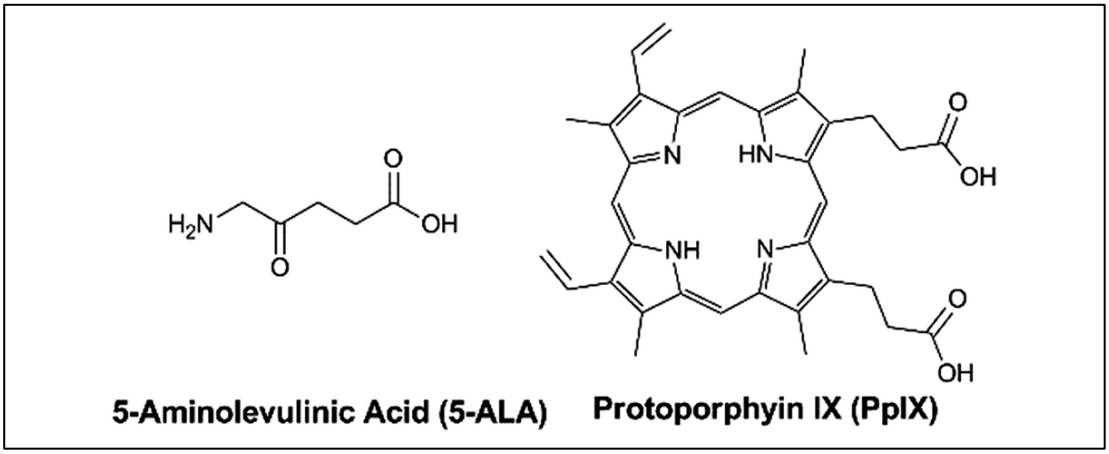

Figure 1.2 Diagram showing a 5-aminolevulinic acid (ALA) molecule (Plaunt *et. al.*, 2014)

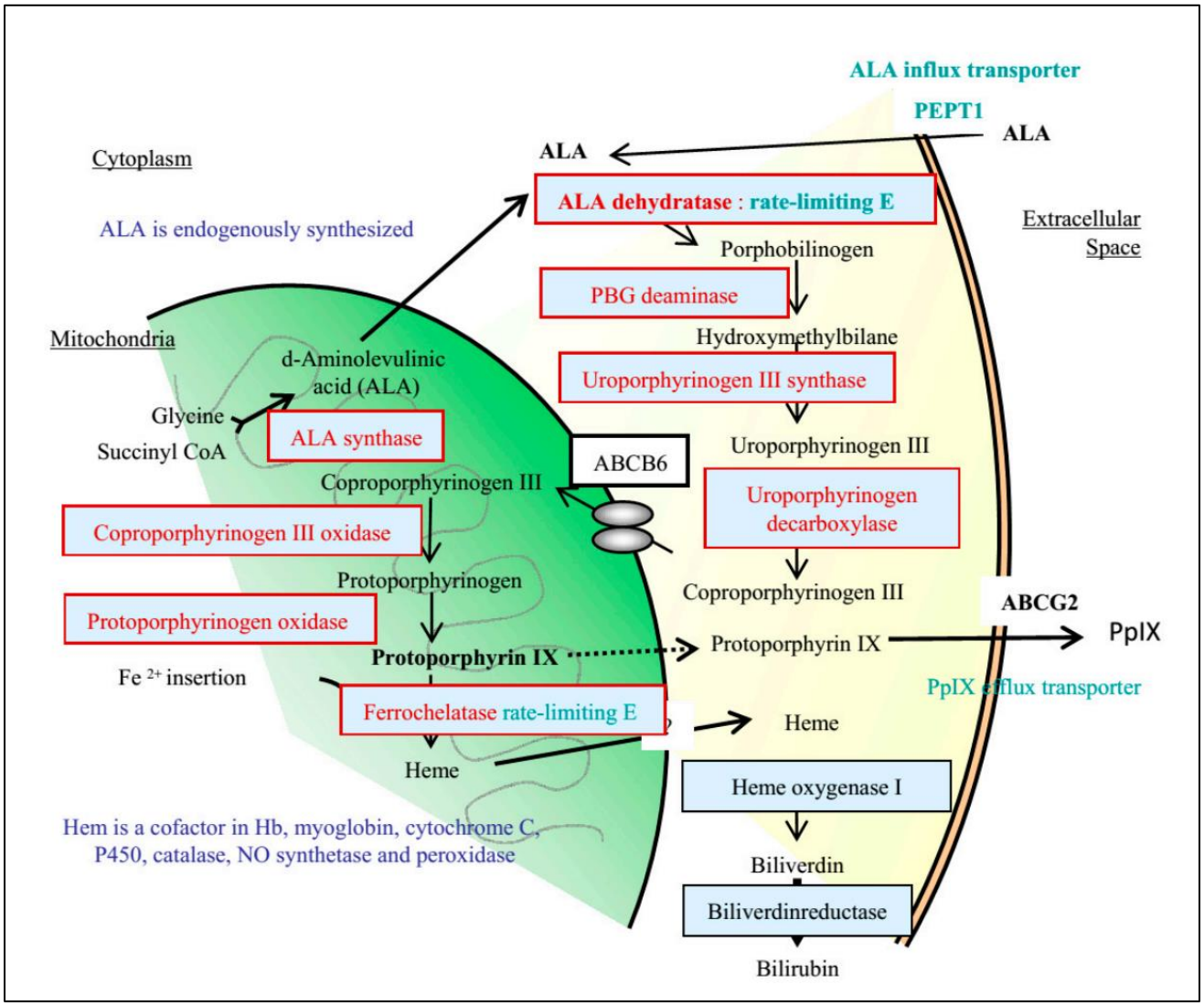

Figure 1.3 Diagram showing how exogenous 5-aminolevulinic acid is involved in the heme synthesis pathway (Yutaka *et. al.*, 2017)

possible side effects such as cutaneous photosensitivity following the therapy (Rick *et. al.*, 1997). Based on study by van den Boogert *et. al.*, 1998, ALA have a good oral bioavailability where it produces a plasma ALA level of similar dosage compared to that attained by intravenous delivery within an hour. It also exhibited outstanding results in diffusing into the blood brain barrier and tumor interface in brain tumors, where no other compound could achieve that (Ennis *et. al.*, 2003; Collaud *et. al.*, 2004; Valdés *et. al.*, 2011).

1.2.2 Mechanism of protoporphyrin accumulation following addition of aminolevulinic acid

Aminolevulinic acid is the natural precursor PpIX and heme whereby intrinsic ALA is produced from succinyl-CoA and glycine via the action of ALA synthase, which is regulated by heme through a feedback mechanism (Figure 1.3) (Rodriguez *et. al*., 2006). In the heme synthesis pathway, ALA dehydratase (ALAD), a rate-determining enzyme, converted ALA into porphobilinogen (PPB) where it undergoes a series a metabolic transformation before being entering the mitochondria as coproporphrinogen III (CPgen III). CPgen III is then converted into protoporphyrinogen and finally into PpIX (Jichlinski *et. al.*, 1997). Exogenous administration of ALA in excess contributes to an increase in intracellular PpIX production through uptake transporters, resulting in selective accumulation of PpIX within the cells (Kennedy & Pottier, 1992). These accumulated PpIX would then emit a red fluorescence under violet light at 405 nm (Jichlinski *et. al.*, 1997). Scientists manipulated this phenomenon to be applicable in photodynamic diagnosis (PDD) for fluorescent-guided resection of tumors (e.g., malignant glioma) under light irradiation (Stummer *et. al.*, 2006). Despite exact reasons of why PpIX excessively accumulated in cancer cells specifically still remain unknown, it is believed to be due to three main factors: malfunction ferrochelatase (FECH), uptake and efflux transporters in cancer cells. Ferrochelatase (FECH), an enzyme

responsible in conversion of PpIX to heme, played a significant role in the accumulation of PpIX in mitochondria (van Hillegersberg et al., 1992; Hunter *et. al.*, 2011; Yutaka *et. al.,* 2017). Enzymes, such as ALA synthase (ALAS) and heme oxygenase I (HO-1), in the heme synthesis pathway are also suggested to be influencing on PpIX accumulation via feedback inhibition (Nishio *et. al.*, 2014; Yang *et. al.*, 2015). Role of transporters in PpIX accumulation would be discussed in the next sub-chapter.

1.2.3 Tailor-made therapy

Similar to the name of the therapy, tailor-made therapy is a cancer therapy specially tailored or suited for a specific individual by predicting disease outcome through the identification of gene-expression signatures of that individual (Van't Veer *et. al.*, 2002). Based on a study by Van't Veer *et. al.* (2002), it was observed that over 5,000 genes had significant changes in expression levels out of isolated RNAs of 98 tumors from patients with lymph-node-negative, primary breast cancer. This is especially important as a diagnosis of breast cancer could result in a completely different long-term treatment. This is one of example why tailor-made therapies come in handy (Chung *et. al.*, 2001). These genes which were used in predicting tumor prognosis were usually genes involved in cell-cycle progression, invasion, metastasis, angiogenesis and signal transduction, which were usually upregulated in tumors with poor prognosis (Greenwood, 2002).

The effectiveness of tailor-made therapy was proven to be significantly higher compared to conventional methods of classifying tumors. Disease outcome was correctly predicted in 17 out of 19 patients using this therapy, which was a significant improvement of currently used prognostic factors, such as tumor size, grade and angioinvasion (Caldas & Aparicio, 2002). This method could be utilized in this study to enhance the mechanism of

action of ALA-PDT and ALA-PDD through the inhibition or activation of transporters in cancer cells by targeting highly expressed transporters using specific drugs.

1.3 TRANSPORTERS INVOLVED IN AMINOLEVULINIC ACID UPTAKE

Another factor causing the accumulation of PpIX is believed to be due to transporters. Solute carrier (SLC) and ATP-binding cassette (ABC) families drug transporters have received increasing attention in drug development as they are found to affect drug absorption and disposition (Giacomini *et. al.*, 2010). Studies suggest that exogenous ALA are being uptake into intracellular space through peptide transporter 1 (PEPT1/ *SLC15A1*), peptide transporter 2 (PEPT2/ *SLC15A2*), proton amino-acid transporter 1 (PAT1/ *SLC36A1*), taurine transporter (TauT/ *SLC6A6*) and gamma-aminobutyric acid (GABA) transporter 1 (GAT1/ *SLC6A13*) (Döring *et. al.*, 1998; Moretti *et. al.*, 2002; Rodriguez *et. al.*, 2006; Frølund *et. al.*, 2010; Tran *et. al.*, 2014). PpIX produced in the cells following ALA addition may also exit the cell due to expression of ATP-binding cassette sub-family G member 2 (ABCG2) transporters (Hagiya *et. al.*, 2012). High expression of these uptake transporters would induce an increase in ALA intake which in turn increased accumulation of PpIX in the cells, thus improving the efficiency of ALA-PDT and ALA-PDD (Xie *et. al.*, 2016). On the other hand, low expression of ABCG2, an efflux transporter, would lower the efflux of accumulated PpIX in the cell, resulting in rising of efficiency of ALA-PDT and ALA-PDD (Hagiya *et. al.*, 2012; Kobuchi *et. al.*, 2012). However, these transporters are not only expressed at different levels depending on the location of organs, but also vary in specificity and ALA transport rate among them. Table 1.1 shows where these transporters are being expressed in the human body while Figure 1.4 illustrate

the roles of these transporters in heme synthesis pathway. These transporters would be further discussed in sub-chapter 1.3.1 and 1.3.2.

Table 1.1 Different transporters found in various organs of the human body

Transporters	Organs Expressed	Citations
PEPT1 (*SLC15A1*)	Duodenum, jejunum, ileum, renal proximal tubule S1 region, pancreas, bile duct, liver	Smith *et. al.*, 2013
PEPT2 (*SLC15A2*)	Renal proximal tubule S3 region, brain choroid plexus, cerebral cortex, olfactory bulb, basal ganglia, hindbrain, lung, mammary gland, spleen	Smith *et. al.*, 2013
PAT1 (*SLC36A1*)	Esophagus, stomach, stomach, cecum, colon, rectum, kidney, placenta, liver, pancreas, cup, heart, brain, skeletal muscle, testes, spleen of the intestinal cells of the duodenum, jejunum, ileum	Thwaites & Anderson, 2007
TauT (*SLC6A6*)	Brain, retina, liver, kidney heart, spleen, pancreas	Kristensen *et. al.*, 2011
GAT2 (*SLC6A13*)	Brain, liver, kidney	Kristensen *et. al.*, 2011

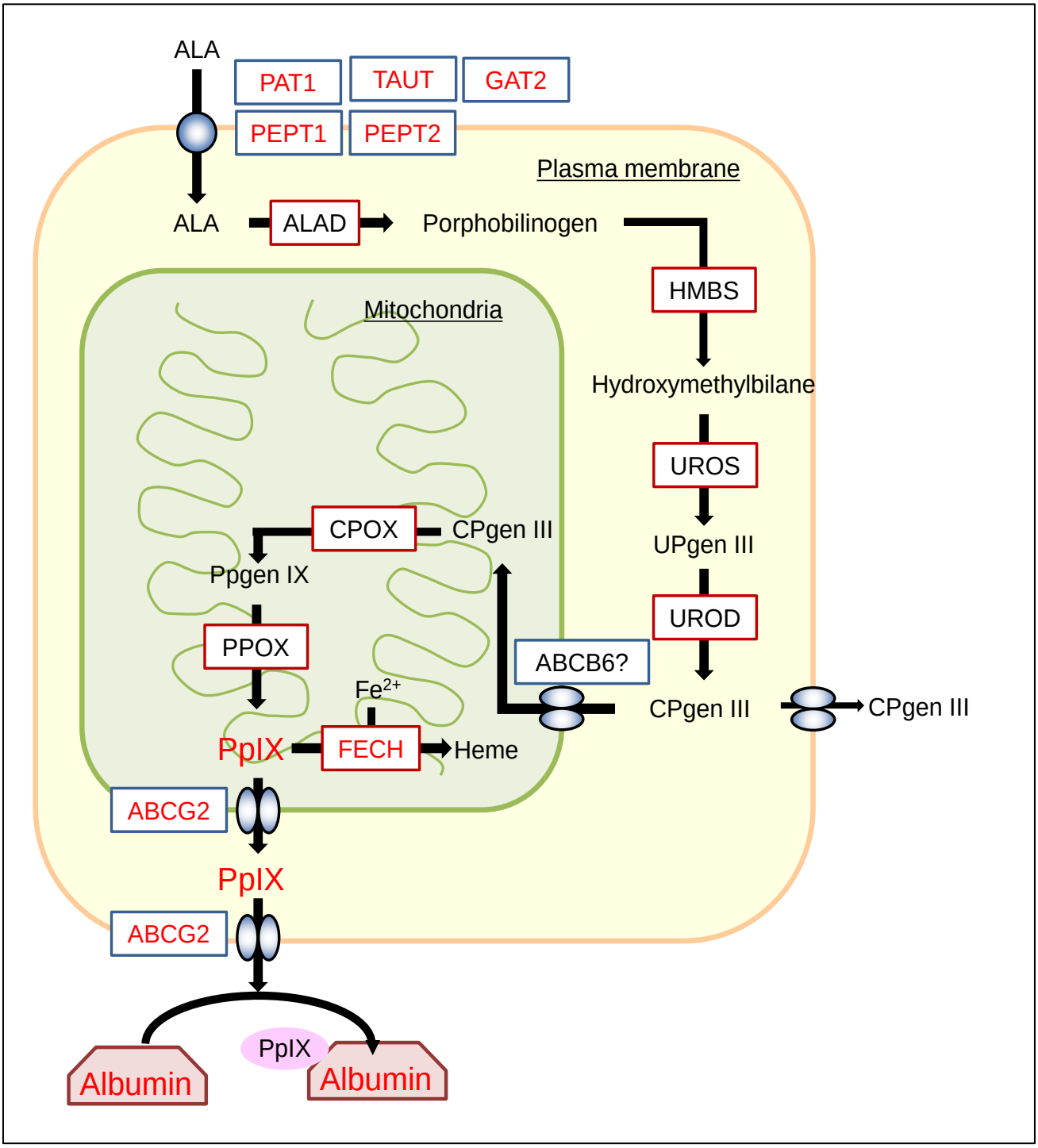

Figure 1.4 Diagram showing how transporters are involved in the heme synthesis pathway (Otsuka, 2017)

1.3.1 Uptake Transporters

1.3.1.1 Peptide transporter 1

While peptide transporter 1 (PEPT1) was known as the only peptide transporter in the small intestine, studies on this transporter were long carried out since the early 1970s (Rubio-Aliaga & Daniel, 2002). Research by Addison *et. al.* (1975) using glycylsarcosine (Gly-Sar) showed that only dipeptides and tripeptides could be transported across the membrane, thus giving rise to the current name of peptide transporter 1. This finding was further supported by Adibi & Morse (1977) where no uptake of tetra-Gly or larger peptides were observed, proving that dipeptide and tripeptide as the only substrate for PEPT1. Study by Döring *et. al.* in 1998 is one of the earliest evidence of the involvement of PEPT1 and PEPT2 in ALA cellular uptake by measuring the uptake of radiolabeled ALA in *Picia pastoris.* It was also found that this uptake action is coupled with the co-transport of H^+/H_3O^+ (Novotny *et. al.*, 2000). The role of PEPT1 in ALA uptake in cancer cells is further strengthened following findings by Rodriguez *et. al.* (2006) and Hagiya *et. al.* (2012), whereby the knockdown of PEPT1 decreased PpIX accumulation while overexpression of PEPT1 resulted in a significant increase in PpIX accumulation in cancer cells.

1.3.1.2 Proton amino acid transporter 1

Proton amino acid transporter 1 (PAT1) is an H^+ coupled amino acid transporter found to be involved in various small neutral amino acid uptake such as proline and GABA (Anderson *et. al.*, 2009). Coincidently, structure of ALA is highly similar to GABA, thus raising questions whether ALA might be involved with a GABA uptake system (Figure 1.4). Boll *et. al.* (2002) showed an increase in ALA uptake in mPAT1-expressing *Xenopus laevis* oocytes, suggesting the role of PAT1 in ALA influx. Several other studies also further strengthened

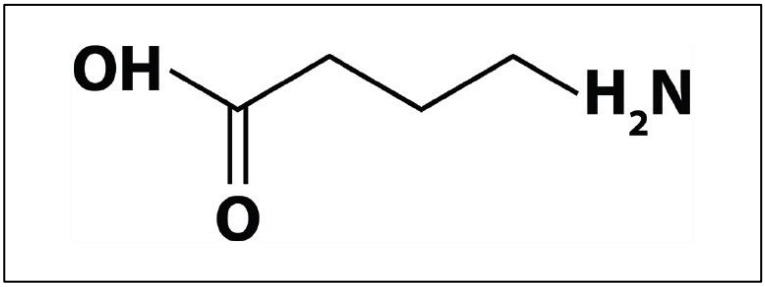

Figure 1.4 Diagram showing a gamma-aminobutyric acid (GABA) molecule (Boonstra *et. al.*, 2015)

this finding, showing that PAT1 is involved in the uptake of ALA through a competitive inhibition study against proline and Gly-Sar (Chen *et. al.*, 2003; Frølund *et. al.*, 2010). Despite many researches had shown that PEPT1 played a major role in ALA uptake, most of the available studies are carried out in gastrointestinal cell lines (Döring *et. al.*, 1998; Meredith *et. al.,* 2000; Casas & Batlle, 2002; Xie *et. al.*, 2016). Cell lines that express only PAT1, but lacking PEPT1 in expression, should be further studied to identify the role of this transporter in ALA uptake.

1.3.1.3 Taurine and GABA transporter 2

Similar to PAT1, GABA is also a substrate for TauT and GAT2, sparking questions on whether these two transporters are involved in ALA uptake (Gether *et. al.*, 2006; Tomi *et. al.*, 2008; Yahara *et. al.*, 2014). Both transporters are known to be highly expressed especially in brain and liver cells (Kristensen *et. al.*, 2011). ALA is also known as a substrate of TauT and GAT2 (Moretti *et. al.,* 2002; Tran *et. al.*, 2014) whereby studies by Tran *et. al.* (2014) showed that HEK293 cells, when overexpressed with either TauT or GAT2, induced a significant increase in PpIX production. Tran *et. al.* (2014) also further proved that the knockdown of TauT and GAT2 in DLD-1 and HeLa cells exhibited a significant drop in PpIX level,

suggesting these results to be a result of increase in ALA uptake through these two transporters.

1.3.1.4 Transporters in normal cells

All transporters, namely PAT1, TauT and GAT2, introduced in the previous sections were also found to be expressed in normal cells except PEPT1 (Ögmundsdóttir *et. al.,* 2012; Zhou *et. al.*, 2012; Scimemi, 2014). Past researches on liver and gastrointestinal cells showed that PEPT1 was known to be highly expressed only in cancer cells but not in normal cells (Rodriguez *et. al.*, 2006; Hagiya *et. al.*, 2012; Chung *et. al.*, 2013). PEPT1 was currently known as the specific transporter found only in cancer cells and is identified as the major contributor for selective accumulation of PpIX in tumors (Hagiya *et. al.*, 2012). In human normal cells, PAT1 was found to be involved in intestinal absorption of a wide range of amino acids in gastrointestinal cells and activates mammalian Target of Rapamycin Complex 1 (mTORC1) by forming complexes with Rag GTPases in late endosomal and lysosomal membranes (Ögmundsdóttir *et. al.,* 2012). On the other hand, TauT and GAT2 were essential transporters that are vital in maintaining normal taurine levels in liver and brain tissues (Zhou *et. al.*, 2012).

1.3.2 Efflux transporter

The only efflux transporter currently identified as the transporter responsible in causing PpIX efflux is the adenosine triphosphate-binding cassette G2 (ABCG2) transporter (Zhou *et. al.*, 2005, Hagiya *et. al.*, 2012; Kobuchi *et. al.*, 2012). ABCG2, formally known as breast cancer resistance protein 1, is a member of the ATP-binding cassette (ABC) family of cell surface transport proteins, which comprises of around 50 members and involved in the

transfer of various substrates around cellular membranes (de Paiva *et. al.*, 2005). Similar to its former nomenclature, ABCG2 is previously known to contribute to drug resistance in breast cancers (de Paiva *et. al.*, 2005). This transporter is also expressed in a variety of normal and cancerous tissues (Trosko & Ruch, 1998). Low expression of ABCG2 is believed to lower the efflux of accumulated PpIX in the cell, contributing to an increase in PDT and PDD efficiency. Past studies showed that PpIX efflux reduced significantly following the inhibition of ABCG2 using siRNA and inhibitors in cancers following the administration of ALA (Hagiya *et. al.*, 2012; Kobuchi *et. al.*, 2012). On the other hand, cells which have a high ABCG2 expression also caused problems in Hoechst 33342 dye in fluorescence microscopy (Kim *et. al.*, 2002). Solving unintended proteins efflux is important, however, had been proven difficult as ABCG2 transporter gene is a highly conserved evolutionary gene in most cells (Cooray *et. al.*, 2002; Kim *et. al.,* 2002).

1.4 TRANSPORTERS' INVOLVEMENT IN THE EFFECTIVENESS OF PHOTODYNAMIC THERAPY UNDER DIFFERENT CANCER MALIGNANCY

1.4.1 Introduction to cancer malignancy

The malignancy of cancer cells is defined as the degree of genetic stability in them, usually having reduced expression levels of DNA repair enzymes and higher proliferative capabilities (Wang & Wheeler, 2014). Cancer cells with higher malignancy would resembled later disease stage, which correlates to higher invasiveness and drug resistance (Chen *et. al.*, 2006). Receptor associated nuclear factor-κB ligand (RANKL) have been recently identified as a marker of cancer disease stage and functional regulation in prostate cancer (Chen *et. al.*, 2006). RANKL, originally known as TNF ligand superfamily member 11 (TNFSF11), is a type II membrane protein encoded by TNFSF11 gene in humans (Anderson *et. al.*, 1997). Study by Chen et. al., (2006) showed that RANKL is highly expressed in

malignant prostate cancer cells and the addition of RANKL could further increase proliferative capability of prostate cancer cells.

1.4.2 Relationship between transporters and cancer malignancy

As mentioned in Section 1.3 above, uptake transporters are essential in bringing ALA into the cell. Therefore, an increase in uptake capability of ALA by the cells would contribute to a higher production of PpIX, which would lead to the increase in cancer killing effect and efficiency of ALA-PDT (Hagiya *et. al.*, 2008). Nakayama *et. al.* (2016) showed that transporters involved in ALA, such as PEPT1, was found to be highly expressed when incubated in high cell density. This led scientists to believe that the relationship between malignancy and efficiency of ALA-PDT may be closely associated with the expression levels of these transporters.

Another study by Kraff *et. al.* (2012) has suggested a possible relationship between malignancy and cell density of tumours. This suggest the involvement of Yes-associated protein (YAP), which control tissue growth based on cell density, in the regulation of cancer malignancy. YAP is an oncoprotein known to be a transcription factor regulating various downstream processes such as proliferation and metastasis (Varelas *et. al.*, 2010). In addition, a recent study by Li *et. al.*, (2020), showed that inhibition of YAP significantly enhanced the efficiency of ALA-PDT, highlighting the importance of YAP in ALA-PDT (Li & Zhou, 2020). Several studies using highly malignant cancer cells, such as nerve sheath cancer cells, urothelial carcinoma and prostate cancer, have been carried out in the past and showed the effectiveness of ALA-PDT against highly malignant cancers (Lee *et. al.*, 2017; Fukuhara *et. al.*, 2020). All these findings suggest a possible relationship between uptake transporters and malignancy.

1.5 AIMS & OBJECTIVES

The main aim of this research is to study the roles of transporters involved in cellular uptake of ALA across cellular membrane in ALA-PDT *in vitro.* Studies on ALA uptake are carried out in order to improve the concentration of intracellular PpIX accumulation in cells which will lead to higher effectiveness of cancer killing effect in ALA-PDT. This research served as a fundamental study to increase the efficiency of PDT and PDD in clinical field in the future. The specific objectives were:

1. To investigate the role of transporters involved in cellular ALA uptake in cancer cells.
2. To clarify the effect caused by transporters on porphyrin production in normal human cells.
3. To improve selectivity and specificity of drugs for tumors by preventing ALA uptake in normal cells
4. To determine the effectiveness of ALA-PDT under different malignancy.
5. To evaluate the relationship of malignancy and ALA uptake transporters

At the end of this thesis, transporter(s) involved in cellular uptake of ALA only in normal cells but not in tumors would be identified. Targeting these transporter(s) using inhibitory drugs will further enhance the specificity of ALA-PDT and PDD to prevent unnecessary cytotoxic damage or PpIX accumulation in normal cells. The roles of uptake transporters on the effectiveness of ALA-PDT will also be evaluated. Results obtained from this thesis would serve as a fundamental knowledge for future *in vivo* and clinical studies.

CHAPTER 2
ROLE OF TRANSPORTERS IN CELLULAR ALA UPTAKE IN CANCER CELLS

2.1 INTRODUCTION

Past researches had suggested that peptide transporter 1 (PEPT1) as the dominant transporter in ALA uptake, as suggested by Hagiya *et. al.* & (2012) Xie *et. al.* (2016), whereby overexpression and knockdown of this transporter showed a visible influence on the cellular uptake of aminolevulinic acid (ALA). These data, however, were mostly based on gastric cancer cell models, raising doubts where the role of PEPT1 still remain significant in other organs of the human body (Faria, *et. al.*, 2004; Anderson *et. al.*, 2010; Hagiya *et. al.*, 2012; Xie *et. al.*, 2016). ALA-photodynamic therapy (PDT) and ALA-photodynamic diagnosis (PDD) could only be efficient with a high concentration of protoporphyrin (PpIX) accumulation. Therefore, the most direct method would be to identify the dominant transporter responsible in uptaking ALA, a precursor of PpIX, to induce a higher production of intracellular PpIX.

Being one of the most prominent cancers in developed countries such as the USA and Japan, prostate cancer still failed to accumulate at sufficient levels to induce photocytotoxicity in ALA-PDT, hindering scientists' efforts in eradicating the disease (Gheewala *et. al.*, 2017). A few papers on the cellular uptake of ALA had been published over the past few years and findings shown that different transporters were involved in ALA uptake in different parts of the body. Studies by Anderson *et. al.* (2010), for example, showed that proton amino acid transporter 1 (PAT1) was responsible in cellular uptake of ALA. Despite both PAT1 and PEPT1 were known to be expressed in gastric cancer cells, PEPT1 was believed to contribute more in ALA uptake gastric cancer cells (Xie *et. al.*, 2016). However, since PAT1 was also known to be relatively highly expressed in prostate cancer cells, it might be possible that this high expression level may result in a more dominant role in ALA uptake in prostate cancer (Okudaira *et. al.*, 2011). On the other hand,

neurotransmitter family transporters, taurine transporters (TauT) and gamma-aminobutyric acid transporter 2 (GAT2), were also found to be involved in ALA uptake in HeLa and HEK293T cancer cells, pushing further a need to identify the dominant ALA uptake transporter (Tran *et. al.*, 2014). In this chapter, the expression level of these transporters and the identity of the dominant transporter in ALA uptake would be evaluated as a fundamental knowledge in the cellular uptake of ALA into cancer cells.

2.2 MATERIALS & METHODS

Chemicals

RPMI-1640 culture medium, DMEM-high glucose culture medium and antibiotic-antimycotic mixed stock medium (ABAM) were purchased from Nacalai Tesque (Kyoto). Fetal bovine serum (FBS) was purchased from Equitech-Bi, Inc. (Kerrville, Texas, USA). Aminolevulinic acid (ALA) was purchased from Cosmo Oil Ltd. (Tokyo). Ibuprofen, tryptophan, taurine and gamma-aminobutyric acid (GABA), used in this study were purchased from Sigma Aldrich Corporation (Tokyo). All inhibitors used were of analytical grade.

Cell Culture

Human gastric cancer cell line, TMK1, was obtained from Assoc. Prof. Dr. Endo Yoshio from Kanazawa University, Japan. Human prostate cancer cell lines, DU145 and PC3, were obtained from Prof. Inoue Keiji from Kochi University, Japan. Human gastric cancer cell line, MKN45, was obtained from RIKEN, Japan. TMK1, MKN45 and PC3 cells were cultured in RPMI 1640 culture medium. DU145 cells were cultured in DMEM-high glucose culture medium. All cell lines were incubated with respective culture medium followed by the

-addition of 10% FBS and 10% ABAM, at 37°C in a 5% CO_2 incubator. Experiments were only carried out when cell density achieve 50% - 80% confluency. Cell number for seeding in various experiments is tabulated in Table 2.1.

Table 2.1 Amount of cell seeded for each cell line respectively in different experiment

Chapter	Experiment	Seeding cell number (cells / well)	
2.3.1	PpIX production of four selected cell lines	TMK1 MKN45, DU145, PC3	: 0.05×10^6 : 0.2×10^6
2.3.2	mRNA expression of various transporters in four selected cell lines	TMK1 MKN45, DU145, PC3	: 0.05×10^6 : 0.2×10^6
2.3.2	Protein expression of various transporters in four selected cell lines	TMK1 MKN45, DU145, PC3	: 0.05×10^6 : 0.2×10^6
2.3.3	PpIX and CPIII production of DU145 following different ALA concentration	DU145	: 0.2×10^6
2.3.3	ALA uptake inhibitors in DU145 cell	DU145	: 0.2×10^6
2.3.3	RNAi knockdown study in DU145 cell	DU145	: 0.02×10^6

Quantitative reverse transcription-polymerase chain reaction (qRT-PCR)

Total RNA extractions from cultured cells were carried out using RNA extraction kit NucleoSpin® RNA II (MACHEREY-NAGEL, Düren, Mannheim, Germany). Extracted RNA were transcript into 1 μg single stranded cDNA via a reverse transcription reaction using PrimeScript RT reagent Kit with gDNA Eraser (TaKaRa Bio, Shiga). The expression levels of PAT1, PEPT1, TauT and actin (internal control) were then quantified using Thermal Cycler Dice® Real Time System Single (TaKaRa Bio, Shiga). The primers used in amplification were tabulated in Table 2.2. Primers set specific to each gene were used in qRT-PCR. Expression

level of each targeted gene were then standardized by dividing with the expression level of actin which is used an internal control.

Table 2.2 Primers sequences used in gene amplification

Gene	Sense / Antisense	Sequence
PEPT1	Sense	5'-TCACCTGTGGCGAAGTGGTC-3'
	Antisense	5'-GCCACGATGAGCACAATGATG-3'
PAT1	Sense	5'-CATAACCCTCAACCTGCCCAAC-3'
	Antisense	5'-GGGACGTAGAACTGGAGTGC-3'
TauT	Sense	5'-TATCTGTATCCTGACATCACCCG-3'
	Antisense	5'-CCCAGGCAGATGGCATAAGAG-3'
Actin	Sense	5' -TGGCACCCAGCACAATGAA-3'
	Antisense	5'-CTAAGTCATAGTCCGCCTAGAAGCA-3'

Agarose gel electrophoresis

Total RNA was extracted from cultured cells, and first-strand cDNA was prepared from total RNA by RT reaction, based on methods by Hagiya *et. al.* (2008). Thereafter, the first-strand cDNA preparations encoding PAT1, PEPT1, TauT and actin were individually amplified by PCR in a Thermal Cycler Dice Mini (TaKaRa Bio, Otsu, Japan) with specific primer sets in Table 2.2. Actin is used as the internal control. The PCR reaction consisted of hot-start incubation at 95°C for 5 min and 35 cycles each of 95°C for 30 s and 60°C for 1 min. The resulting amplicons were separated by 2.5% agarose gel electrophoresis and detected with ethidium bromide under ultraviolet light.

Western blotting

Western blotting experiments were carried out to quantify the expression level of proteins in cells using modified methods based on Tamura *et. al.* (2007). Cells were first washed with PBS (-), followed by addition of Lysis Buffer A [50 mM Tris-HCl (pH 7.4), 20 mM N-methylmaleimide, 1 mM DTT, 1% (v/v) Triton X-100 and Protease inhibitor cocktail (Nacalai Tesque)]. The cell suspensions were homogenized using a 27 G syringe for at least 10 times and centrifuge at 1000×G for 10 minutes at 4°C. Protein samples were then recovered and stored at -80°C freezer for future use.

Protein samples were next treated with SDS-PAGE sample buffer where they were then separated through SDS-PAGE electrophoresis using 7.5% and 11.25% polyacrylamide gel. These separated proteins were then transferred onto an Immobilon-P PVDF membrane (Milipore Corp., M.A.) whereby blocking and antibody treatment would be carried out next. Blocking was carried out by incubating the membrane at room temperature for 60 minutes in 5% (w/v) skimmed milk dissolved in TBST [20 mM Tris-HCl (pH 7.4), 150 mM NaCl, 0.05% (v/v) Tween 20].

Anti-human PAT1 antibody (Novus Biologicals, Littleton, Colorado, USA; 1:1000), anti-human PEPT1 antibody (Abcam, Cambridge, Massachusetts, USA; 1:200), anti-human TauT antibody (Santa Cruz Biotechnology, Dallas, Texas, USA; 1:500), anti-human GAT2 antibody (Medical & Biological Laboratories, Naka-ku, Nagoya, Japan; 1:1000) and human actin antibody (MP Biomedicals, Santa Ana, CA; 1:200 dilution), which served as internal control, were used in primary antibody treatment. Secondary antibody used in this study were horseradish peroxidase (HRP)-conjugated anti-mouse (Cell Signalling Technology, Beverly, MA) and anti-rabbit IgG (Santa Cruz Biotechnology, Dallas, Texas, USA) concentrate, which were diluted 3000 times in TBST solution. Substrate for HRP used in this

study were Western Lightning Chemiluminescent Reagent Plus、Western Lightning Chemiluminescent Reagent Pro (PerkinElmer Life and Analytical Sciences, Waltham, MA), Western BLoT Ultra-Sensitive HRP Substrate (TaKaRa Bio, Inc., Shiga, Japan). Chemiluminescent were used to quantify protein expression levels using Lumino Imaging Analyzer LAS-4000 mini (GE Healthcare UK, Amersham Place, England).

ALA uptake inhibition assay

Ibuprofen and tryptophan were utilized to suppressed PEPT1 and PAT1 transporter activity via non-competitive inhibition and competitive inhibition respectively. Taurine and GABA were used as TauT and GAT2 inhibitors. Ibuprofen was dissolved in DMSO (Final concentration: 0.2 M). Tryptophan was dissolved in 0.5 M HCl (Final concentration: 0.25 M). Taurine and GABA were dissolved in distilled water with a final concentration of 0.4 M and 0.25 M respectively. 1 mM ALA was added together with respective inhibitors for 24 hours for the reaction to occur.

RNAi knockdown

Cells were transfected using transfection medium comprising of small interfering RNA (siRNA) and 0.1% Dharmafect 4 solution (Dharmacon, Lafayette, Colorado, USA). PAT1 and PEPT1 siRNA were designed using siRNA template designing tools (Sigma Genosys siRNA service). Sequence of these siRNA can be found in Table 2.3. Both siRNAs, together with Opti-MEM™ reduced serum medium (OPTI-MEM) (Thermo Fisher Scientific, Minato-ku, Tokyo, Japan) were mixed at specific proportion to give rise to a final concentration of 10 nM while Dharmafect 4 were prepared by mixing with OPTI-MEM to produce a 0.1% Dharmafect 4 solution. Both solutions were incubated at room temperature for 10 minutes before mixing

both solutions at a 1: 1 proportion. The transfection medium is then incubated again for 20 minutes to allow formation of siRNA-liposome complex. This transfection medium is then added into seeded cells containing 1.6 mL ABAM-free DMEM high glucose culture medium and incubated for 48 hours before recovering the cells.

Table 2.3 siRNA duplex sequence for PAT1 and PEPT1

siRNA	Sequence
PEPT1	5'-CAAGAGUGGGAAAGUUUA-3'
	5'-UAAACUUUCCCACUCAUUG-3'
PAT1	5'-GCGCUUUGGUCAAAGCAAU-3'
	5'-AUUGCUUUGACCAAAGCGC-3'

Porphyrin production quantification using High Performance Liquid Chromatography (HPLC)

Cells were first seeded at specific cell number (As stated in Table 2.1) in 35 mm dishes and incubated at 37°C under 5% CO_2 in a CO_2 incubator for 24 hours. Experiments were carried out in triplicates per sample. Co-addition of ALA and inhibitors (if applicable), were carried out and cells were further incubated under the same condition for another 24 hours. For RNAi knockdown study, siRNAs were first added and incubated under the same condition for 24 hours, followed by another 24 hours of incubation with 1 mM ALA.

Extracellular porphyrins were then extracted first by recovering all culture medium, followed by a 3000×G centrifugation for 10 minutes in order to separate dead cells. A volume of 50 µL of the supernatant from each sample were then taken out and added into a new 1.5 mL centrifuge tube containing 150 µL Dimethylformamide (DMF): 2-propanol solution (100: 1, v/v). This step is essential for the denaturation of unwanted proteins and to ensure pure extraction of porphyrins. Separation of denatured proteins were then carried out

by centrifuging at 10000×G for 10 minutes. Supernatants were recovered and pellets were discarded.

In order to isolate intracellular porphyrins, cells were first washed using PBS (-) twice, followed by addition of 150 μL of 0.1 M NaOH. A volume of 50 μL of cell suspension from each sample were taken out and added into a new 1.5 mL centrifuge tube containing 150 μL of DMF: 2-propanol solution (100: 1, v/v) as mentioned in the previous paragraph. Cell suspensions then underwent centrifugation under 10000×G for 10 minutes. Supernatants were recovered and pellets were discarded.

HPLC analysis of porphyrin was carried out using Type Promonence System (Shimadzu Manufacturing Co., Kyoto) equipped with reverse phase C18 column (CAPCELL PAK, C18, SG300, 5 μm, 4.6 mm × 250 mm, Osaka Soda Co. Ltd., Osaka) while maintaining at a temperature of 40°C. Mobile phase A, comprising of 1 M ammonium acetate solution containing 12.5% acetonitrile (adjusted to pH 5.2), and mobile phase B, made up of 50 mM ammonium acetate solution containing 80% acetonitrile, were used in elution of porphyrin. 50% mobile phase B was first directed at a flow rate of 1.0 mL / min for 10 minutes following by driving mobile phase B into the column from a linear gradient ranging from 90% for 10 minutes and finally 90% mobile phase B at a flow rate of 2.0 mL / min for another 10 minutes in the elution program. 100μL of each eluate was injected and detected using with a detector equipped with a fluorescence spectrometer at an excitation wavelength of 404 nm and a detection wavelength of 624 nm. The protein concentrations of each samples were -determined using Bradford's method using Quickstart Bradford 1×Dye Reagent (Biorad Laboratories, Inc., Hercules, California, USA). Coproporphyrin I dihydrochloride, Coproporphyrin I dihydrochloride, Protoporphyrin I dihydrochloride, used as standard material for porphyrin were purchased from Frontier Scientific, Inc. (Logan, Utah, USA).

Chromatograms and standard curves using each porphyrin standard are shown in Figure 2.1 and Figure 2.2, respectively.

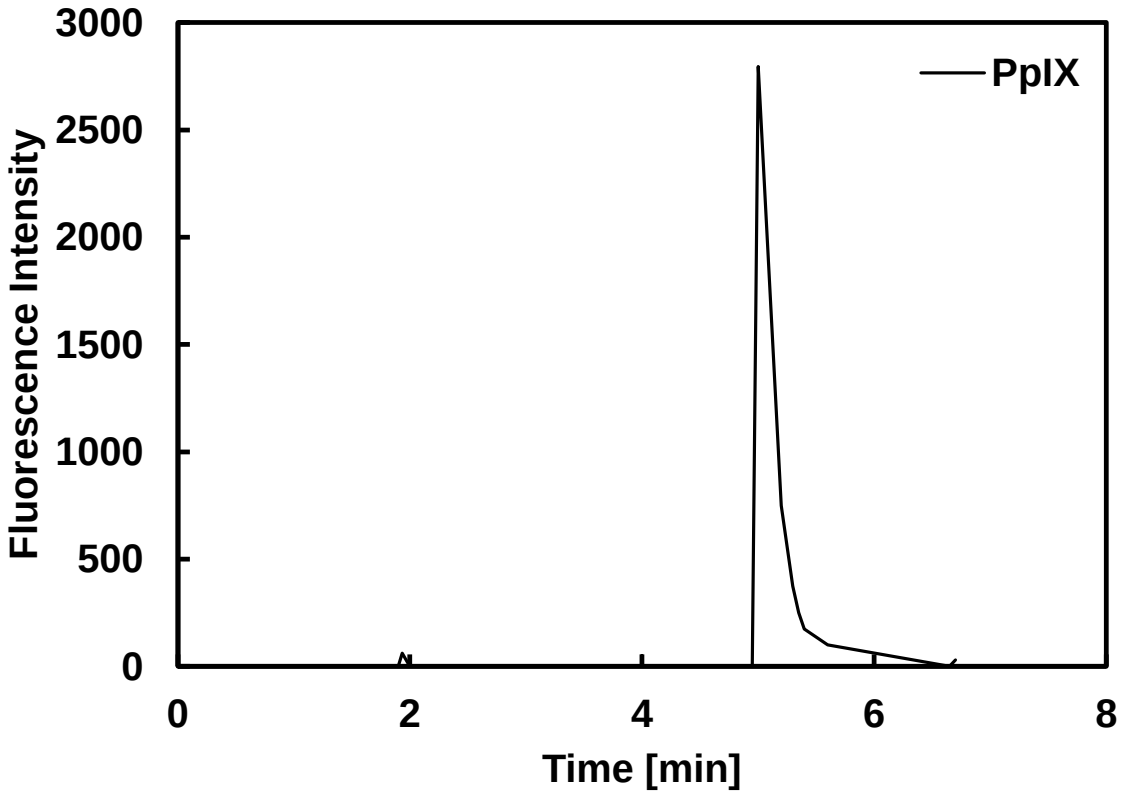

Figure 2.1 Chromatogram for each porphyrin molecule

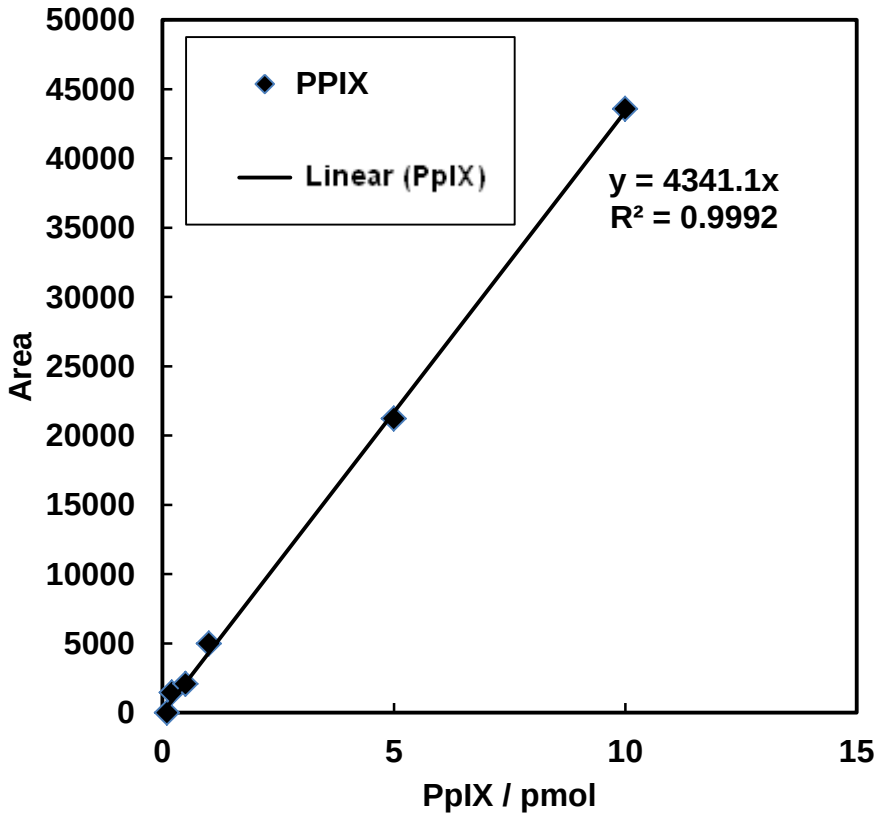

Figure 2.2 Standard curve using CPIII and PpIX standard substrate

Statistical analysis of data

Microsoft Excel 2010 was used for data analysis in this study. One-way ANOVA (Tukey's Test) were performed for each set of data to show that there were significant differences in mean values between treated and non-treated samples, $p < 0.05$.

2.3 RESULTS

2.3.1 PpIX production in selected cell lines

The concentration of PpIX was first evaluated on gastrointestinal cancer cells, TMK1 and MKN45, and prostate cancer cells, DU145 and PC3 cell lines. This study is required to identify which cell lines could take in most ALA following the addition of a fixed ALA concentration, which in turn resulted in production of PpIX. All four cell lines were administered with 1 mM ALA for 24 hours at 37°C under 5% CO_2 condition. These cells were then collected where concentration of both intracellular and extracellular PpIX were analyzed using high-performance liquid chromatography (HPLC). The results were recorded and a graph was plotted (Figure 2.3). TMK1 cell line showed the lowest total PpIX production (0.21 nmol / mg-protein), followed by PC3 at 0.23 nmol / mg-protein. On the other hand, DU145 cell line produced the highest amount of PpIX (0.29 nmol / mg-protein) whereas MKN45 cell line produced around 0.25 nmol / mg-protein of PpIX. No significant difference were observed for these graphs ($p > 0.05$). The high production of PpIX in DU145 cells

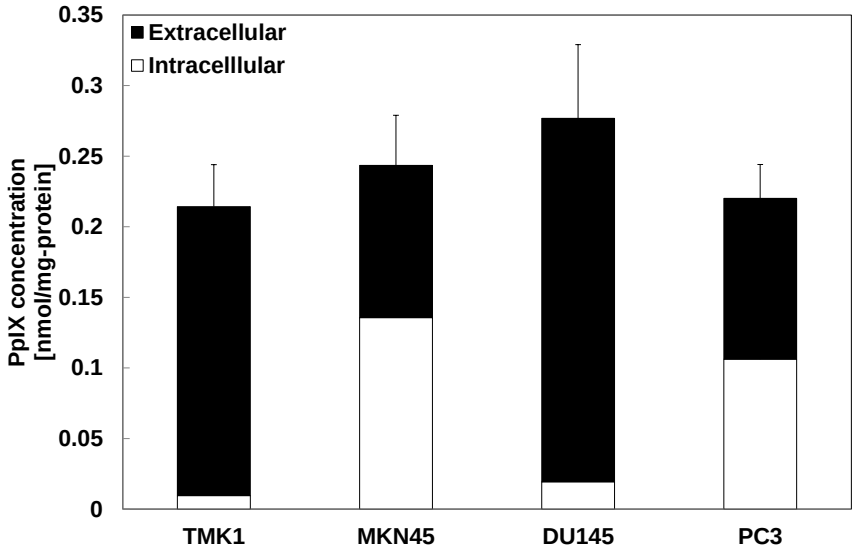

Figure 2.3 Concentration of PpIX produced following addition of 1 mM aminolevulinic acid (ALA) in four selected cancer cell lines (*; $p < 0.05$)

suggested that a different transporter(s), which is not found or lowly expressed in the remaining cell lines, were involved and thus enabling a higher uptake of ALA, which subsequently leaded to a rise in PpIX production. The expressions of various transporters involved in ALA uptake were then evaluated in sub-chapter 2.3.2 in order to identify the possible reasons for high PpIX production in DU145 cell line.

2.3.2 Expression of transporters in selected cell lines

The expression levels of ALA transporters, namely PEPT1, PAT1 and TauT, were studied to identify the possible dominant transporter(s) in cellular uptake of ALA. mRNA and protein expression levels of these transporters were studied in four selected cancer cell lines (namely TMK1, MKN45, DU145 and PC3) in the presence or absence of 1 mM ALA addition for 24 hours at 37°C in a 5% CO_2 incubator. The samples were then collected and being analyzed using agarose gel electrophoresis, quantitative reverse transcriptase-polymerase chain reaction (qRT-PCR) and Western blotting as stated in page 18-20. Results of mRNA expression levels of these transporters using agarose electrophoresis and qRT-PCR were shown as in Figure 2.4 and Figure 2.5 respectively whereas results of Western blotting and band intensity graphs were plotted as in Figure 2.6 and 2.7.

Findings from agarose gel electrophoresis and qRT-PCR generally showed very similar results (Figure 2.4 and Figure 2.5). mRNA expression of PAT1 was observed to be around 5 times higher in DU145 cell line compared to other cell lines, where PEPT1 was almost exclusively found to be expressed only in MKN45 cell line. TauT, on the other hand, was found to be highly expressed in TMK1 and DU145, but lowly expressed in MKN45 and PC3. The results here also indicated that expressions of these transporters were slightly lowered following the addition of ALA, although the effect appears to be larger in PEPT1.

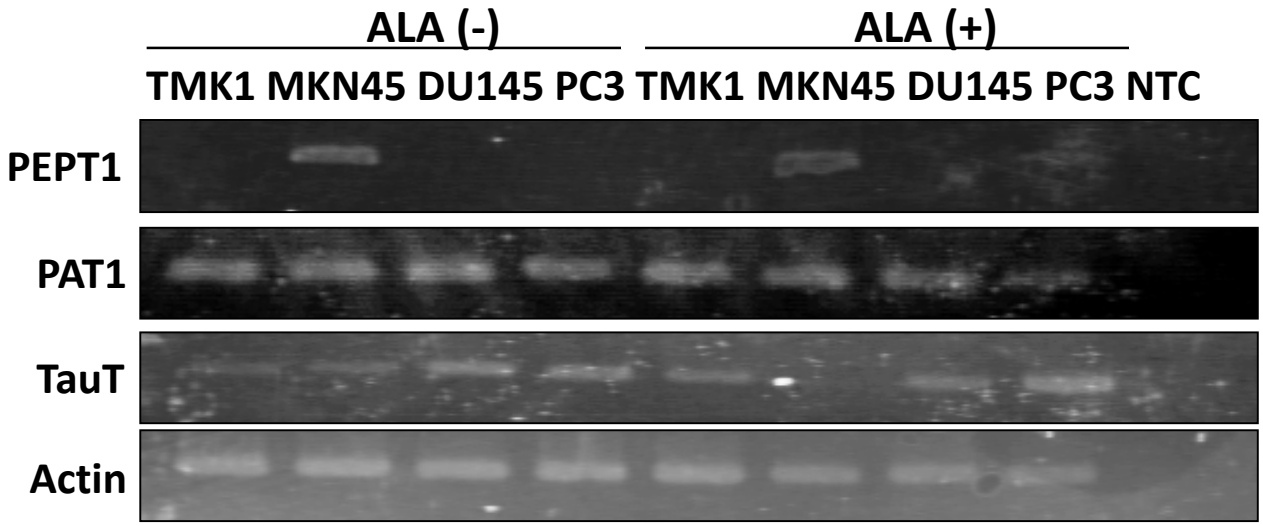

Figure 2.4 Comparison of mRNA expression of various transporters in the presence or absence of aminolevulinic acid (ALA) addition in four selected cancer cell lines using agarose gel electrophoresis

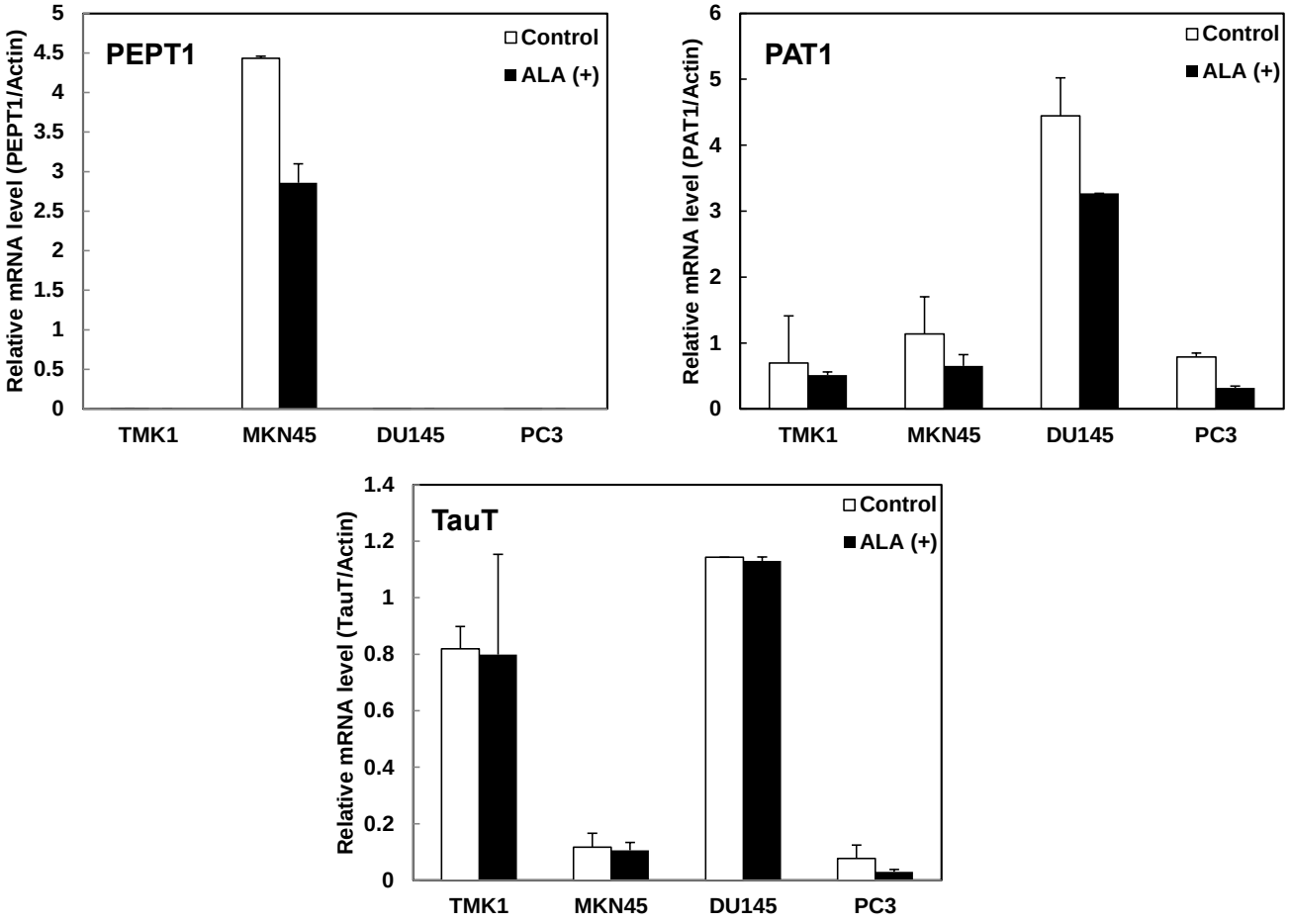

Figure 2.5 Comparison of mRNA expression of various transporters in the presence or absence of aminolevulinic acid (ALA) addition in four selected cancer cell lines using quantitative real time-polymerase chain reaction (qRT-PCR)

Results of Western blotting (Figure 2.6) did not completely correlate with findings from mRNA expression study in Figure 2.4 and Figure 2.5. This is believed to be due to the difference in decomposition rate of mRNA following the translation into protein transporters (Gygi *et. al.*, 1999; Yang *et. al.*, 2003; Chen *et. al.*, 2008). Studies using mammalian cell models also shown that the decomposition rate of the same mRNA also varied among cell lines (Chen *et. al.*, 2008). Protein expression of PAT1 was observed to be highest in DU145 cell line compared to other cell lines. PEPT1, whose mRNA expression was almost exclusively only in MKN45 cell line, was found out to be equally highly expressed in MKN45, DU145 and PC cell line. TauT was found to be highly expressed in TMK1 cell line, followed by MKN45 cell line. DU145 and PC3 both exhibited relatively low expression level of TauT despite DU145 cell line showed equally high mRNA expression with TMK1 cell line. On the other hand, GAT2 was found to be highly expressed only in DU145 cell line. The results here indicated that expressions of PEPT1 and TauT transporters were slightly lowered following the addition of ALA, although the effect is reversed in the case of PAT1.

Study on protein expression was believed to be more accurate as transporters were generally translated proteins. The band intensities from Figure 2.6 were plotted as in Figure 2.7. Based on this figure, PEPT1, PAT1 and GAT2 appeared to be possible candidates that might play a significant role in cellular ALA uptake in DU145 cell line. The significance of these transporters was studied in the next sub-chapter to identify the dominant transporter for cellular ALA uptake in this cell line.

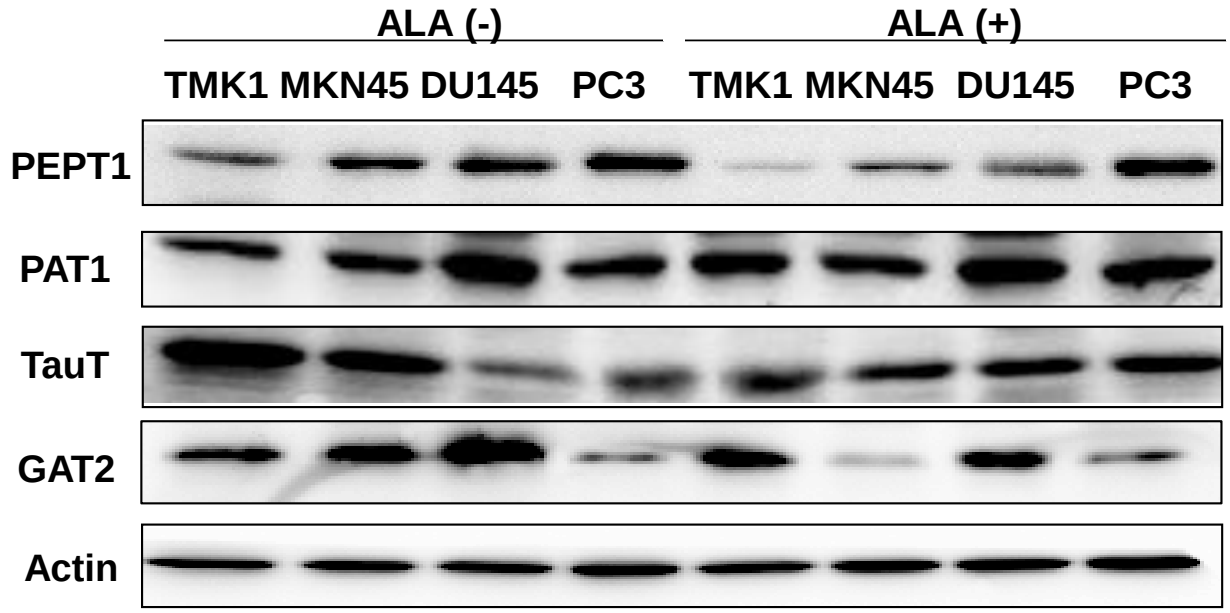

Figure 2.6 Protein expressions of PEPT1, PAT1, TauT & GAT2 in four selected cell lines using Western blotting in the absence or presence of aminolevulinic acid

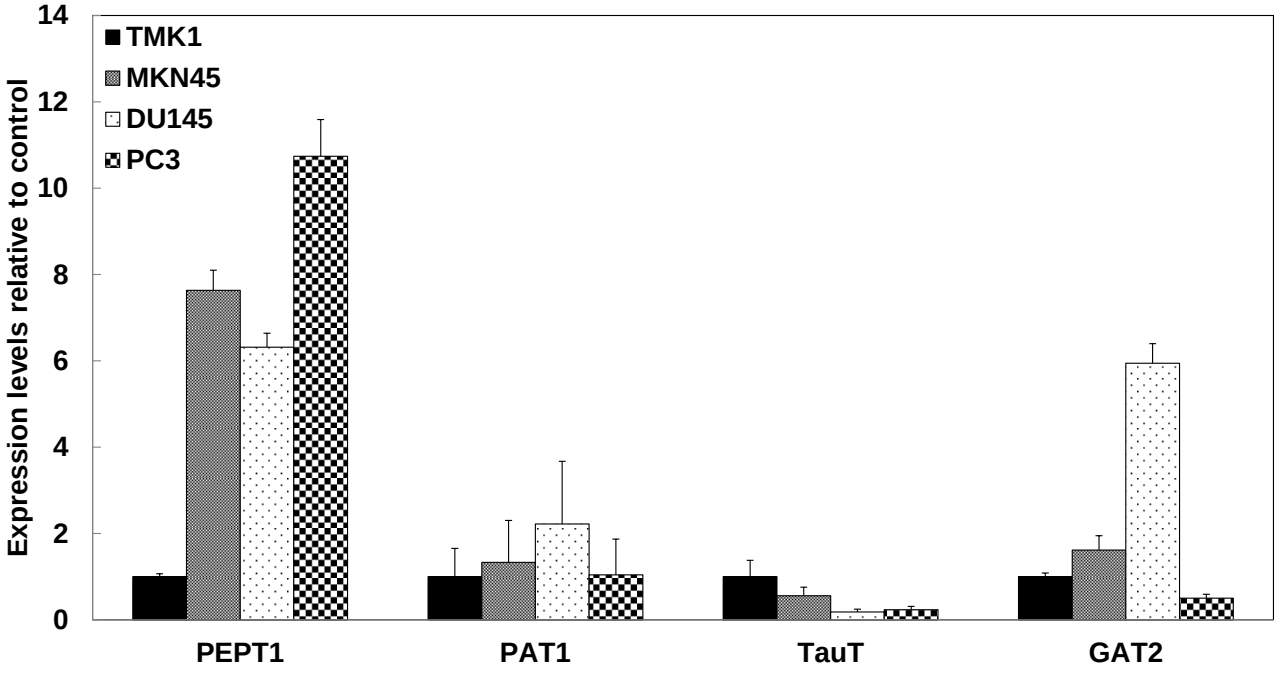

Figure 2.7 Band intensity of protein expressions of PEPT1, PAT1, TauT & GAT2 in four selected cell lines using Western blotting without ALA administration

2.3.3 Roles of transporters in ALA uptake

PEPT1 and PAT1 gene knockdown studies were carried out to identify the dominant transporter(s) responsible in the role of ALA uptake in in DU145 cells. Cells were seeded at 0.02×10^6 cells / mL for 24 hours with ABAM-free DMEM high glucose culture medium. This is to prevent ABAM substrates from inhibiting the formation of complex in transfection medium. Transfection medium were prepared and inserted into each dish for 48 hours. 1 mM ALA was added into each dish after the first 24 hours of inoculation of transfection medium. The cell samples were collected and total PpIX production levels were analyzed using HPLC. Proteins of these cell samples were also extracted and Western blotting was carried out to show the change in expression levels of PEPT1 and PAT1 after gene knockdown.

Optimum concentration for knocking down PAT1 and PEPT1 were first determined using Western blotting as described in page 19 & 20. Figure 2.8 showed the expression level of PEPT1 and PAT1 under different concentration. Band intensity graphs were also plotted (Figure 2.8). The bands showed more than 60% decrease in the expression of PAT1 at a concentration of 100 nM siPAT1. There were no observable changes in PAT1 expression level at concentration lower than 100 nM. On the other hand, a concentration of 10 nM siPEPT1 decreased PEPT1 expression by 40% when compared to the control. A 60% decrease in PEPT1 expression were observed at 50 nM siPEPT1 and a staggering 95% decrease at 100 nM.

The production of total PpIX production (intracellular and extracellular PpIX) following the knockdown of mRNA using siRNAs (siPEPT1 and siPAT1) were plotted in Figure 2.9. PpIX produced following PEPT1 or PAT1 knockdown showed a significant reduction of 70 % and 60%, respectively, compared to the siNC control ($p < 0.05$). No

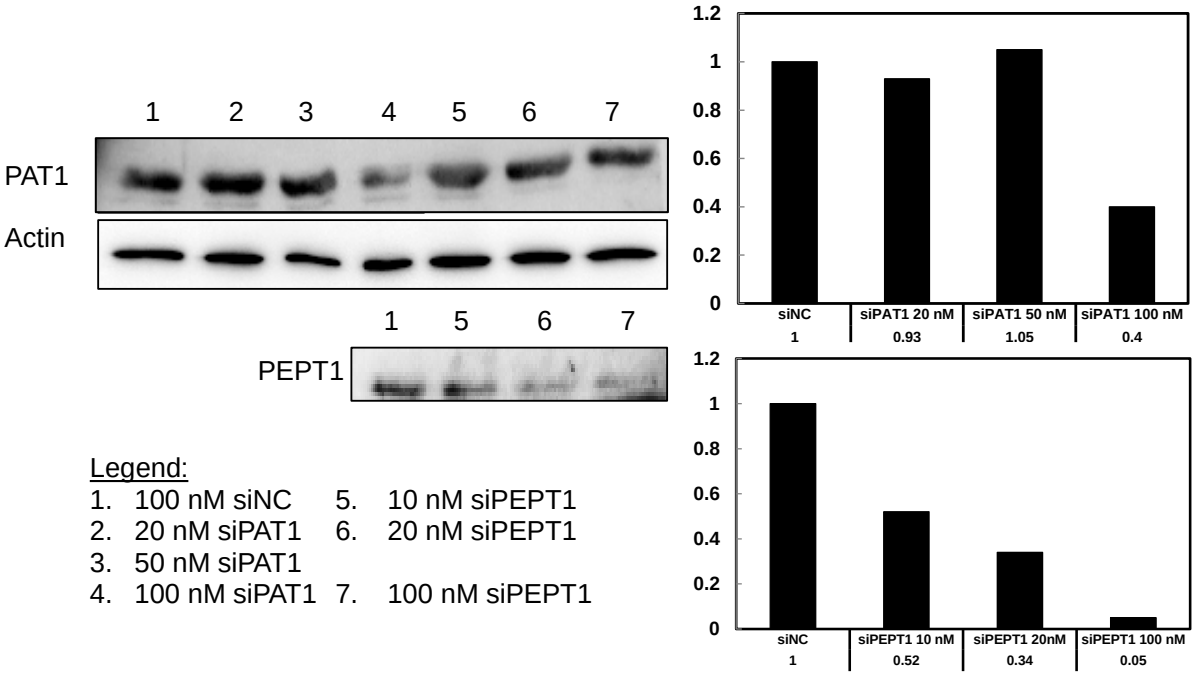

Figure 2.8 Expression of transporters following knockdown of PAT1 and PEPT1 in DU145 cancer cell line

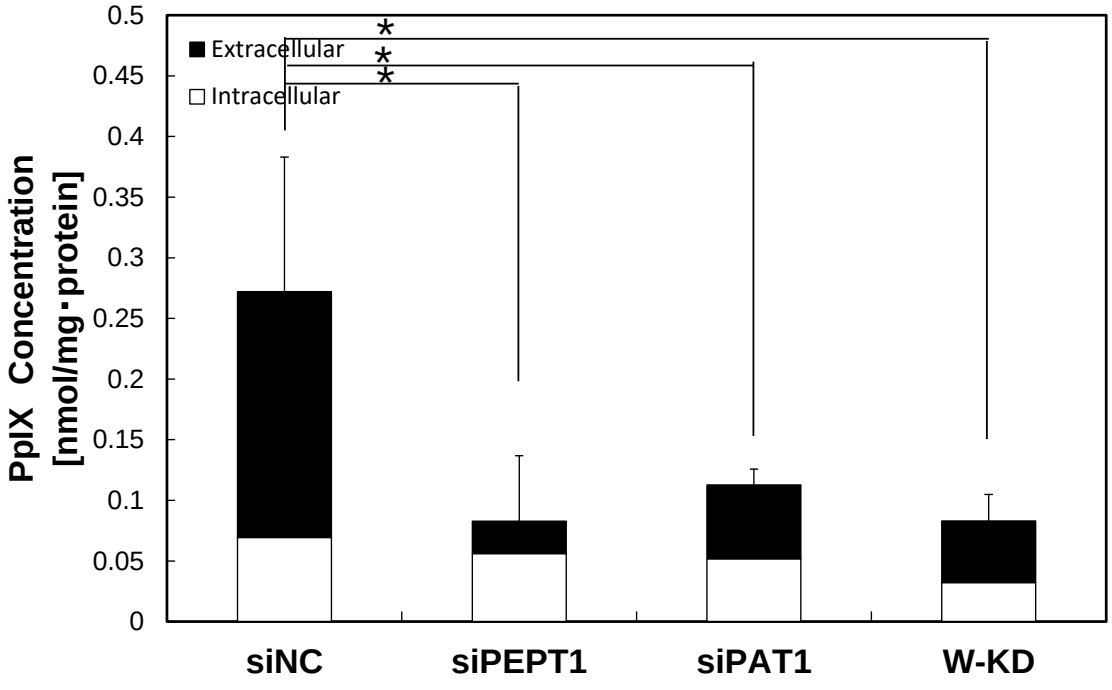

Figure 2.9 Production of intracellular and extracellular protoporphyrin (PpIX) following knockdown of PAT1 and PEPT1 in DU145 cancer cell line (*; $p < 0.05$)

significant difference was found between the siPAT1 and siPEPT1 samples ($p > 0.05$). A double-gene knockdown study (W-KD) was also carried out using both siPAT1 and siPEPT1 at 100 nm each. It exhibited a 70% drop in PpIX production when compared to the control ($p < 0.05$). No significant difference was observed between the PpIX production of siPAT1, siPEPT1 and W-KD samples ($p > 0.05$). This result showed that inhibition of PAT1 and PEPT1 decreased PpIX production significantly in DU145 cells, suggesting that both transporters played a significant role in cellular uptake of ALA in this cell line, which coincided with their high expression levels in DU145 cells.

After showing both PAT1 and PEPT1 were involved in ALA uptake, inhibitors of PEPT1, PAT1, TauT and GAT2 were added to evaluate the effect on PpIX production following the suppression of each transporter's activity respectively. Studies were carried out by carrying out co-administration of ALA and inhibitors at least two different concentrations, followed by 24 hours of incubation at 37°C in a 5% CO_2 incubator. Cell samples were then collected for HPLC analysis. Findings of these studies were plotted into graphs in Figure 2.10.

Addition of ibuprofen, a non-competitive inhibitor of PEPT1, showed a 40% decrease in PpIX production in DU145 cells ($p < 0.05$) (Figure 2.10A). No significant difference in PpIX production was observed among the three different concentration of ibuprofen ($p > 0.05$). This result correlated with previous studies by past researchers where PEPT1 played a significant role in the cellular uptake of ALA. On the other hand, study using tryptophan, taurine and GABA, competitive inhibitors of PAT1, TauT and GAT2, respectively, were also carried out in DU145 cells. Production of PpIX showed a gradual decrease as the concentration of inhibitors increased. PpIX production halved when co-administered with 1 mM ALA and 5 mM tryptophan ($p < 0.05$) and dropped sharply by 75% at 10 mM

tryptophan ($p < 0.05$) (Figure 2.10B). This result also indicated the importance of PAT1 in cellular uptake of ALA. Similar trends were also observed after the addition of taurine and GABA, suggesting TauT & GAT2 may also play significant roles in ALA uptake (Figure 2.10C & 2.10D).

Inhibition studies of all four transporters in the remaining cell lines, TMK1, MKN45 and PC3, were also studied and the data were plotted in a bar chart as in Figure 2.11. In general, all these results correlated with expression of all four transporters in all cell lines (except PAT1 inhibition in TMK1, where it was lowly expressed), whereby inhibition of transporters which were highly expressed resulted in a significant drop in PpIX production.

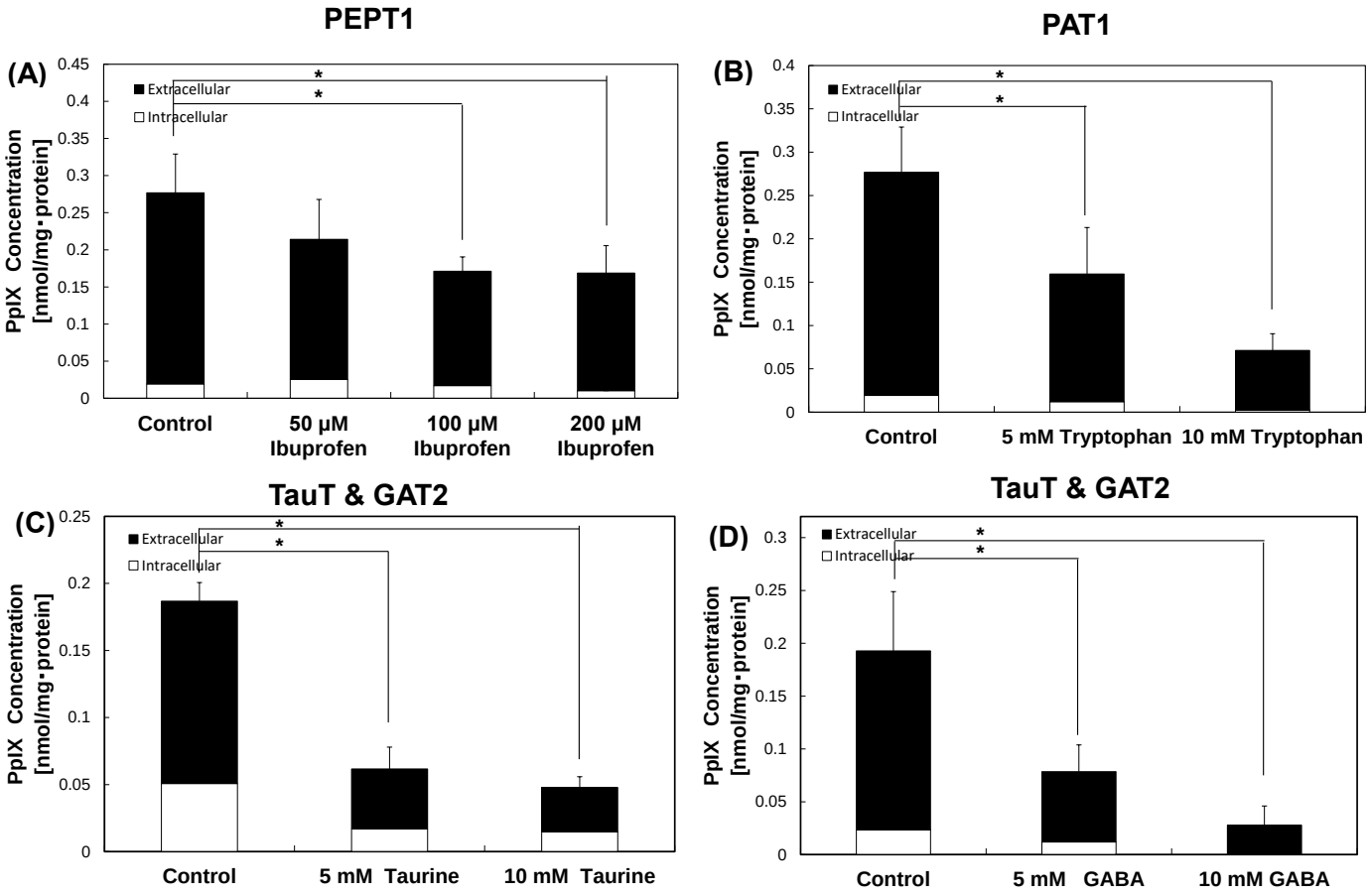

Figure 2.10 PpIX production of DU145 cells following the co-addition of 1 mM ALA and 5 mM inhibitors, namely (A) ibuprofen, (B) tryptophan, (C) taurine and (D) GABA (*; $p < 0.05$)

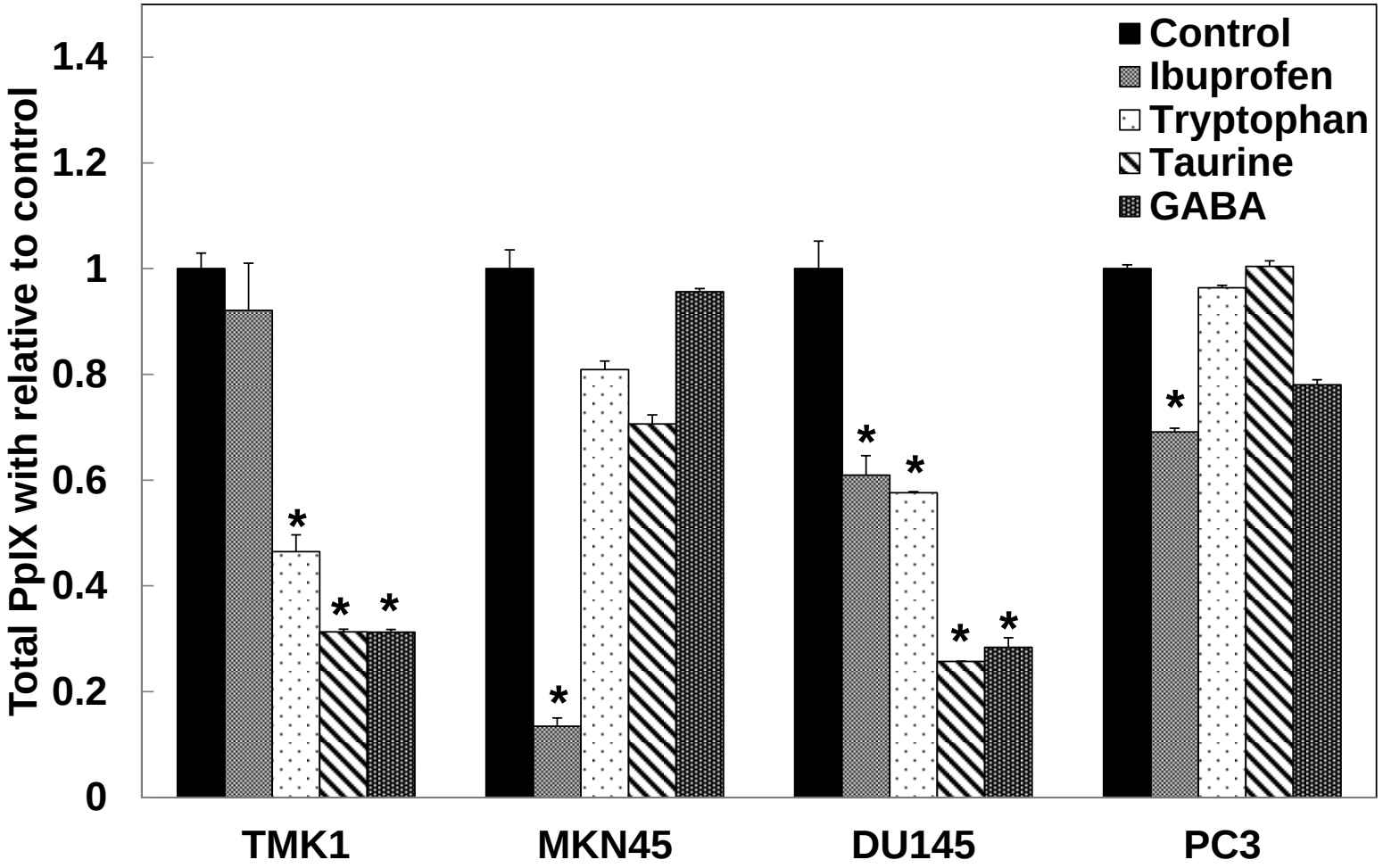

Figure 2.11 Production of intracellular and extracellular protoporphyrin (PpIX) following co-administration of aminolevulinic acid (ALA) and inhibitors in DU145 cancer cell line; (A) ibuprofen as PEPT1 inhibitor; (B) tryptophan as PAT1 inhibitor; (C) (D) taurine and GABA as TauT and GAT2 inhibitor
(*; $p < 0.05$)

In short, results obtained in this sub-chapter showed that factors affecting cellular uptake is highly dependent on the expression levels of transporters and is not fixed to a specific transporter.

2.4 DISCUSSION

The definition of cellular uptake varies under different circumstances. In medicine, it is defined as the absorption and incorporation of a substance by living tissue (Uptake, 2003). Understanding the cellular uptake of ALA, such as identifying dominant uptake transporters and possible naturally occurring inhibitors, is important in enhancing the efficacy of ALA-PDT and ALA-PDD.

Results from the protein expression levels of various transporters, namely PEPT1, PAT1, TauT and GAT2, in four selected cancer cell lines from Figure 2.6 and 2.7 were quantified and tabulated in Table 2.4. It is seen that correlation between the trend of mRNA and protein expression levels were observed only in PAT1, but not in the other three transporters. However, the trend observed is not surprising as expression levels of mRNA and protein of a gene do not often correlate which one another and have only around 40% explanatory correlations across many studies as reported in Koussounadis *et al.* (2015). In this study, protein expression levels were given priority over the expression level of mRNAs as transporters exist as protein complex structure on the cellular membrane instead of the mRNA form. DU145 was identified as the only cell line that highly expressed PEPT1, PAT1 and GAT2, emerging as a valuable model for transporters study.

Table 2.4 showed the expressions of these transporters were independent of organ origins, where TMK1 and MKN45 did not expressed similar transporter expression trends despite both originating from stomach. Prostate cancer cells, DU145 and PC3 also failed to

Table 2.4 Summary on protein expression of various transporters in selected cell lines

Low → High

	TMK1	MKN45	DU145	PC3
PEPT1	0.39	0.88	0.93	1
PAT1	0.45	0.65	1	0.53
TauT	1	0.55	0.17	0.21
GAT2	0.24	0.33	1	0.34

Table 2.5 Effect on PpIX production following the co-addition of inhibitors and ALA

Low → High

Inhibitors	Cell lines			
	TMK1	MKN45	DU145	PC3
Ibuprofen	-	↓	↓	↓
Tryptophan	↓	-	↓	-
Taurine	↓	-	↓	-
GABA	↓	-	↓	-

		Inhibitor / ALA ratio
Ibuprofen	: PEPT1 non-competitive inhibitor	0.1
Tryptophan	: PAT1 competitive inhibitor	5
Taurine	: TauT & GAT2 competitive inhibitor	5
GABA	: TauT & GAT2 competitive inhibitor	5

exhibit similar trends in transporter expression. These findings suggested that the expression levels and activity of these four transporters, namely PEPT1, PAT1, TauT and GAT2, might be independent of their origin. Sensitivity of ALA uptake in different cell lines are believed to be dependent on their expression levels as shown in Table 2.5. On the other hand, the results showed that expressions of various transporters were only slightly or not affected following the addition of ALA (Figure 2.6). The reason of this phenomenon remained unknown but coincided with mRNA expression levels (Figure 2.4 & 2.5). Further studies were essential to determine if there is a possibility of addition of ALA affects the expression and activity of uptake transporters.

Inhibition of PAT1 and PEPT1 via siRNA showed a significant drop in PpIX production, suggesting a decrease in uptake of ALA by these two transporters (Figure 2.9).

No significant differences in PpIX production were observed between PAT1 and PEPT1–knocked-downed samples, suggesting both transporters were equally important in ALA uptake, which is different from previous studies (Hagiya *et. al.,* 2012; Xie *et. al.*, 2016). The decrease in uptake of ALA is believed to result in a lower ALA pool within the cell, which in turn reduced the production of porphyrin intermediates and lastly, lowered the production of PpIX. These findings were further verified and validated by the inhibition studies of all four transporters using DU145 cells (Figure 2.10). Inhibition studies on the remaining three cell lines, TMK1, MKN45 and PC3, in general, also showed similar trends whereby inhibition of highly expressed transporters caused a drop in cellular uptake of ALA, leading to a lower production level of PpIX.

Identifying the dominant transporter is essential in understanding the sensitivity of cells towards ALA-induced PpIX accumulation. Different from past studies from various researchers, this chapter proved that not only the expression level of PEPT1, but PAT1, TauT and GAT2 also showed a correlation with the response to ALA-induced PpIX accumulation in these four cell lines *in vitro* although further tests are necessary to discover the actual contribution of each transporter (Anderson *et. al.*, 2010; Hagiya *et. al.,* 2012; Xie *et. al.*, 2016).

In conclusion, these results showed that role of transporters involved in ALA uptake differed among different cell lines and were highly dependent of expression levels of respective transporters. The study also proved, for the first time that, all four transporters could be dominant transporters responsible in cellular uptake of ALA, dependent on cell lines. This findings overwritten past studies which raised doubts on transporters besides PEPT1 having a significant role in ALA uptake in cancer cells. However, definitive evidence using knock-out models are required to obtain an accurate answer.

CHAPTER 3
ROLE OF TRANSPORTER INHIBITORS TO INCREASE SPECIFICITY OF ALA UPTAKE IN TUMORS

3.1 INTRODUCTION

Specificity has always been a problem for cancer treatment as cancer cells often showed highly similar genetic structure with normal cells (Morgan *et. al.*, 2010). An ideal treatment would exhibit high killing effect on cancer cells while keeping side effect to minimal to the surrounding normal cells (Delaney *et. al.*, 2005). Cancer cell treatment with such therapeutic qualities is relatively uncommon and thus future complicates the efficacy of treatment. More in-depth researches should be carried out to solve this problem.

Results from previous chapter on cancer cells from different origins suggested that PEPT1, PAT1, TauT and GAT2 played a role in aminolevulinic acid (ALA) uptake as long as they were highly expressed; suggesting tailor-made therapy might be the best way to cure cancer as different patients might exhibit tumors with different genetic materials. Therefore, in this chapter, the focus will be on the usage of chemical compounds to target specific transporters in various normal and cancer cells of the same organ origin with different expression levels of various transporters in cellular uptake of ALA. Identifying the roles of all four transporters would be important in determining the suitable drug (s) used in treatment especially in tailor-made therapy.

3.2 MATERIALS & METHODS

Chemicals

DMEM-high glucose culture medium, antibiotic-antimycotic mixed stock medium (ABAM) and prostate epithelial growth medium (PrEGM) and its supplements, were purchased from Nacalai Tesque (Kyoto). Fetal bovine serum (FBS) was purchased from Equitech-Bi, Inc. (Kerrville, Texas, USA). Aminolevulinic acid (ALA) was purchased from Cosmo Oil Ltd. (Tokyo). Ibuprofen, tryptophan and gamma-aminobutyric acid (GABA), used in this study were purchased from Sigma Aldrich Corporation (Tokyo). All inhibitors used were of analytical grade.

Cell Culture

Human lung carcinoma cell line, A549, and human lung normal cell line, WI38, were obtained from RIKEN, Japan. Human prostate cancer cell line, DU145, was obtained from Prof. Inoue Keiji from Kochi University, Japan. PrEC cells were obtained from SBI Pharmaceuticals Ltd., Tokyo, Japan. All cells (except PrEC cells) were cultured in DMEM-high glucose culture medium. PrEC cells were cultured in and routinely grown in PrEGM culture medium, supplemented with BPE, hydrocortisone, hEGF, epinephrine, transferring, insulin, retinoic acid, triidothyronine, GA-1000. All cell lines were incubated with respective culture medium followed by the addition of 10% FBS and 10% ABAM, at 37 °C in a 5% CO_2 incubator. Experiments were only carried out when cell density achieve 50% - 80% confluency. All cells were seeded at 0.2×10^6 cells / well and incubated for 24 hours before treatment.

Western blotting

Western blotting experiments were carried out to quantify the expression level of proteins in cells using modified methods based on Tamura *et. al.* (2007). Cells were first washed with PBS (-), followed by addition of Lysis Buffer A [50 mM Tris-HCl (pH 7.4), 20 mM N-methylmaleimide, 1 mM DTT, 1% (v/v) Triton X-100 and Protease inhibitor cocktail (Nacalai Tesque)]. The cell suspensions were homogenized using a 27 G syringe for at least 10 times and centrifuge at 1000×G for 10 minutes at 4°C. Protein samples were then recovered and stored at -80°C freezer for future use.

Protein samples were next treated with SDS-PAGE sample buffer where they were then separated through SDS-PAGE electrophoresis using 7.5% and 11.25% polyacrylamide gel. These separated proteins were then transferred onto a Immobilon-P PVDF membrane (Milipore Corp., M.A.) whereby blocking and antibody treatment would be carried out next. Blocking was carried out by incubating the membrane at room temperature for 60 minutes in 5% (w/v) skimmed milk dissolved in TBST [20 mM Tris-HCl (pH 7.4), 150 mM NaCl, 0.05% (v/v) Tween 20].

Anti-human PAT1 antibody (Novus Biologicals, Littleton, Colorado, USA; 1:1000), anti-human PEPT1 antibody (Abcam, Cambridge, Massachusetts, USA; 1:200), anti-human TauT antibody (Santa Cruz Biotechnology, Dallas, Texas, USA; 1:500), anti-human GAT2 antibody (Medical & Biological Laboratories, Naka-ku, Nagoya, Japan; 1:1000) and human actin antibody (MP Biomedicals, Santa Ana, CA; 1:200 dilution), which served as internal control, were used in primary antibody treatment. Secondary antibody used in this study were horseradish peroxidase (HRP)-conjugated anti-mouse (Cell Signalling Technology, Beverly, MA) and anti-rabbit IgG (Santa Cruz Biotechnology, Dallas, Texas, USA) concentrate, which were diluted 3000 times in TBST solution. Substrate for HRP used in this

study were Western Lightning Chemiluminescent Reagent Plus、Western Lightning Chemiluminescent Reagent Pro (PerkinElmer Life and Analytical Sciences, Waltham, MA), Western BLoT Ultra-Sensitive HRP Substrate (TaKaRa Bio, Inc., Shiga, Japan). Chemiluminescent were used to quantify protein expression levels using Lumino Imaging Analyzer LAS-4000 mini (GE Healthcare UK, Amersham Place, England).

ALA uptake inhibition assay

Ibuprofen and tryptophan were utilized to suppressed PEPT1 and PAT1 transporter activity via non-competitive inhibition and competitive inhibition respectively. Taurine and GABA were used as TauT and GAT2 inhibitors. Ibuprofen was dissolved in DMSO (Final concentration: 0.2 M). Tryptophan was dissolved in 0.5 M HCl (Final concentration: 0.25 M). Taurine and GABA were dissolved in distilled water with a final concentration of 0.4 M and 0.25 M respectively. 1 mM ALA was added together with respective inhibitors for 24 hours for the reaction to occur.

Porphyrin production quantification using High Performance Liquid Chromatography (HPLC)

Cells were first seeded at 0.2×10^6 cells / mL in 35 mm dishes and incubated at 37°C under 5% CO_2 in a CO_2 incubator for 24 hours. Experiments were carried out in triplicates per sample. Co-addition of ALA and inhibitors, were carried out and cells were further incubated under the same condition for another 24 hours.

Extracellular porphyrins were then extracted first by recovering all culture medium, followed by a 3000×G centrifugation for 10 minutes in order to separate dead cells. A volume of 50 µL of the supernatant from each sample were then taken out and added into a new 1.5 mL centrifuge tube containing 150 µL Dimethylformamide (DMF): 2-propanol

solution (100: 1, v/v). This step is essential for the denaturation of unwanted proteins and to ensure pure extraction of porphyrins. Separation of denatured proteins were then carried out by centrifuging at 10000×G for 10 minutes. Supernatants were recovered and pellets were discarded.

In order to isolate intracellular porphyrins, cells were first washed using PBS (-) twice, followed by addition of 150 µL of 0.1 M NaOH. A volume of 50 µL of cell suspension from each sample were taken out and added into a new 1.5 mL centrifuge tube containing 150 µL of DMF: 2-propanol solution (100: 1, v/v) as mentioned in the previous paragraph. Cell suspensions then underwent centrifugation under 10000×G for 10 minutes. Supernatants were recovered and pellets were discarded.

HPLC analysis of porphyrin was carried out using Type Promonence System (Shimadzu Manufacturing Co., Kyoto) equipped with reverse phase C18 column (CAPCELL PAK, C18, SG300, 5 µm, 4.6 mm × 250 mm, Osaka Soda Co. Ltd., Osaka) while maintaining at a temperature of 40 °C. Mobile phase A, comprising of 1 M ammonium acetate solution containing 12.5% acetonitrile (adjusted to pH 5.2), and mobile phase B, made up of 50 mM ammonium acetate solution containing 80% acetonitrile, were used in elution of porphyrin. 50% mobile phase B was first directed at a flow rate of 1.0 mL / min for 10 minutes following by driving mobile phase B into the column from a linear gradient ranging from 90% for 10 minutes and finally 90% mobile phase B at a flow rate of 2.0 mL / min for another 10 minutes in the elution program. 100µL of each eluate was injected and detected using with a detector equipped with a fluorescence spectrometer at an excitation wavelength of 404 nm and a detection wavelength of 624 nm. The protein concentrations of each sample were determined using Bradford's method using Quickstart Bradford 1×Dye Reagent (Biorad Laboratories, Inc., Hercules, California, USA). Coproporphyrin I

dihydrochloride, Coproporphyrin I dihydrochloride, Protoporphyrin I dihydrochloride, used as standard material for porphyrin were purchased from Frontier Scientific, Inc. (Logan, Utah, USA). Chromatograms and standard curves using each porphyrin standard are shown in Figure 2.1 and Figure 2.2, respectively.

Statistical analysis of data

Microsoft Excel 2010 was used for data analysis of this study. One-way ANOVA were performed for each set of data to show that there were significant differences in mean values between treated and non-treated samples, $p < 0.05$.

3.3 RESULTS

3.3.1 PpIX production in selected cell lines

Studies in chapter involved sets of normal and cancer cell lines of the same origin, namely, WI38 (normal) and A549 (cancer) from lungs, PrEC (normal), PC3 and DU145 (cancer) from prostate gland. The concentration of PpIX was first evaluated on all these cell lines. This study is required to identify which cell lines could take in most ALA following the addition of a fixed ALA concentration, which in turn resulted in production of PpIX. Both cell lines were administered with 1 mM ALA for 24 hours at 37°C under 5% CO_2 condition. These cells were then collected and concentrations of both intracellular and extracellular PpIX were analyzed using high-performance liquid chromatography (HPLC). The results was recorded and a graph was plotted (Figure 3.1). WI38 cells (~0.09 nmol / mg-protein) exhibited lower PpIX production by around 35% compared to its cancerous counterpart, A549 (~0.16 nmol / mg-protein) ($p < 0.05$). No significant differences were observed between the total PpIX produced in PrEC-PC3 pair and PrEC-DU145 pair ($p > 0.05$). These accumulations of PpIX in normal cells may result in unwanted cytotoxicity in treatment using ALA. Therefore, the expressions of various transporters involved in ALA uptake were then evaluated in sub-chapter 3.3.2 in order to identify the potential dominant transporters for ALA uptake in all these cell lines.

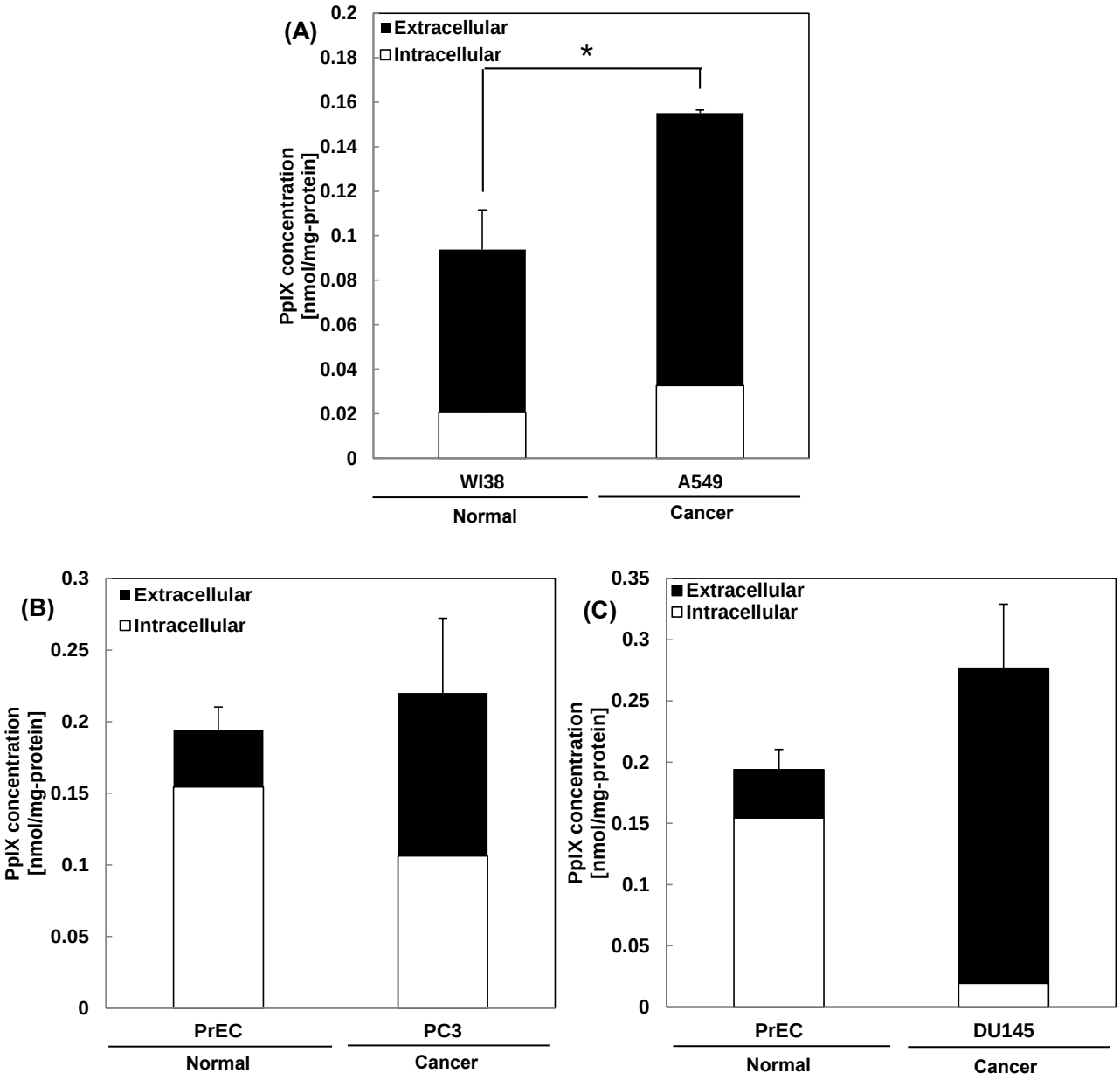

Figure 3.1 Concentration of PpIX produced following addition of 1 mM aminolevulinic acid (ALA) in WI38 and A549 cell lines
(*; $p < 0.05$)

3.3.2 Expression of transporters in selected cell lines

As discussed in the previous chapter (page 36), study on protein expression was believed to be more accurate than mRNA as transporters were generally translated proteins. Therefore, only protein expressions of PEPT1, PAT1, TauT and GAT2 transporters were studied in this chapter. Protein expression levels of these transporters were studied in all five cell lines in the absence of ALA addition for 48 hours at 37°C in a 5% CO_2 incubator. The samples were then collected and being analyzed using Western blotting as stated in page 42 and 43. Results of Western blotting and band intensity graphs were plotted as in Figure 3.2 and 3.3.

Protein expression of PAT1 and GAT2 were observed to be higher in A549 compared to WI38 while PEPT1, was found to be highly expressed in WI38 over A549. PAT1 and GAT2 bands in WI38, together PEPT1 bands in A549 were barely visible, suggesting they have very low abundance in respective cell lines. On the other hand, TauT was found to be lowly expressed in both WI38 and A549 cells. Unlike in previous chapter, expression levels of various transporters following ALA addition were not examined as no significant changes were observed previously (Figure 2.6).

In the case of prostate cells, PEPT1 was the only highly expressed transporter found in PC3 cells (Figure 3.3). PrEC showed high expression levels of PAT1 and PEPT1. PAT1, PEPT1 and GAT2 were highly expressed in DU145 cells. GAT2 was found to be the only transporter expressed in DU145 cells among the three cell lines. Similar to results from previous chapter (Figure 2.6 & 2.7), PC3 and DU145 did not exhibit similar transporters expressions patterns despite both are cancerous and originates from the same organ, further highlighted the importance of a tailor-made therapy.

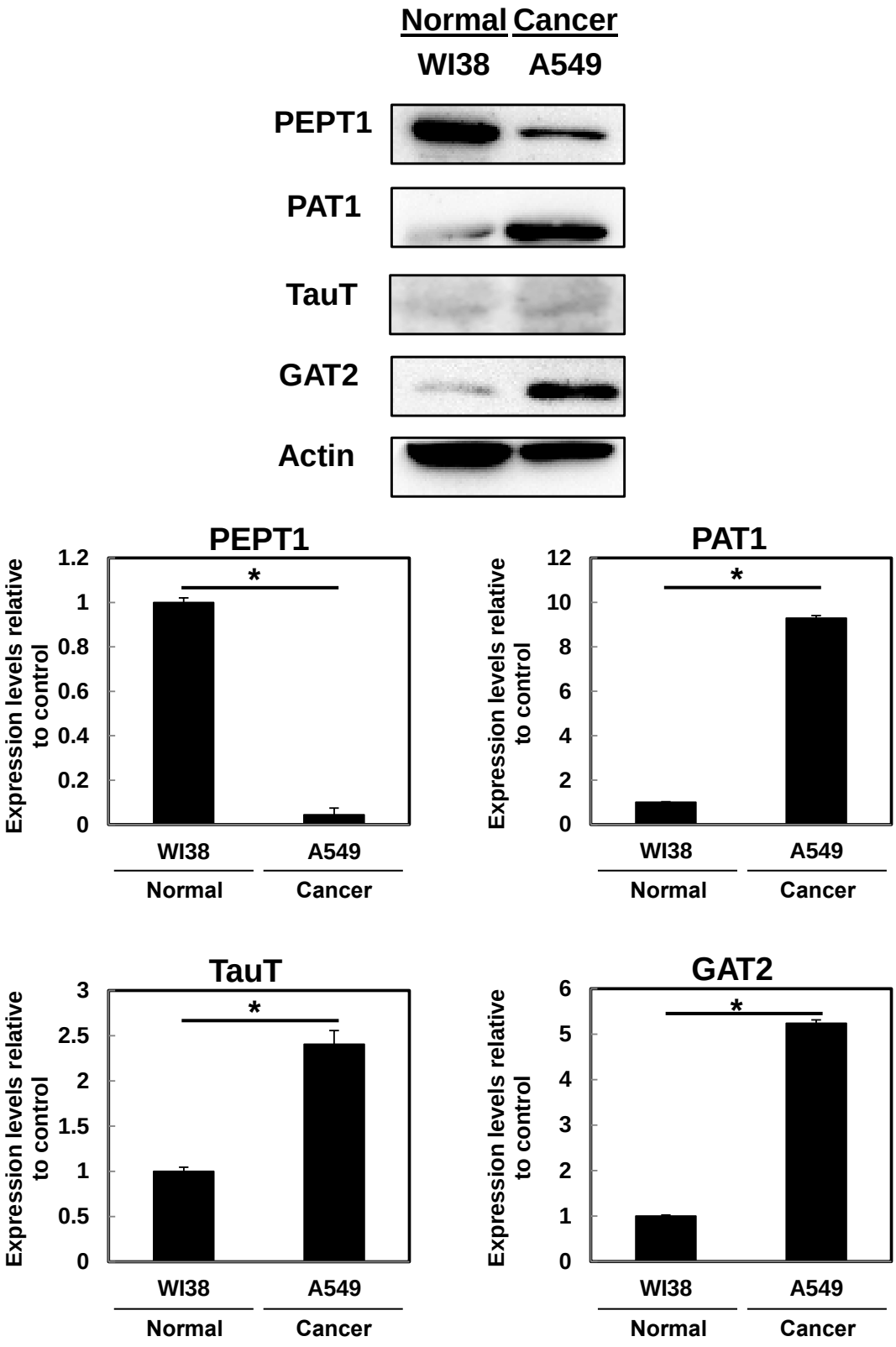

Figure 3.2 Protein expressions of PEPT1, PAT1, TauT & GAT2 and band intensity graphs in WI38 and A549 cell lines

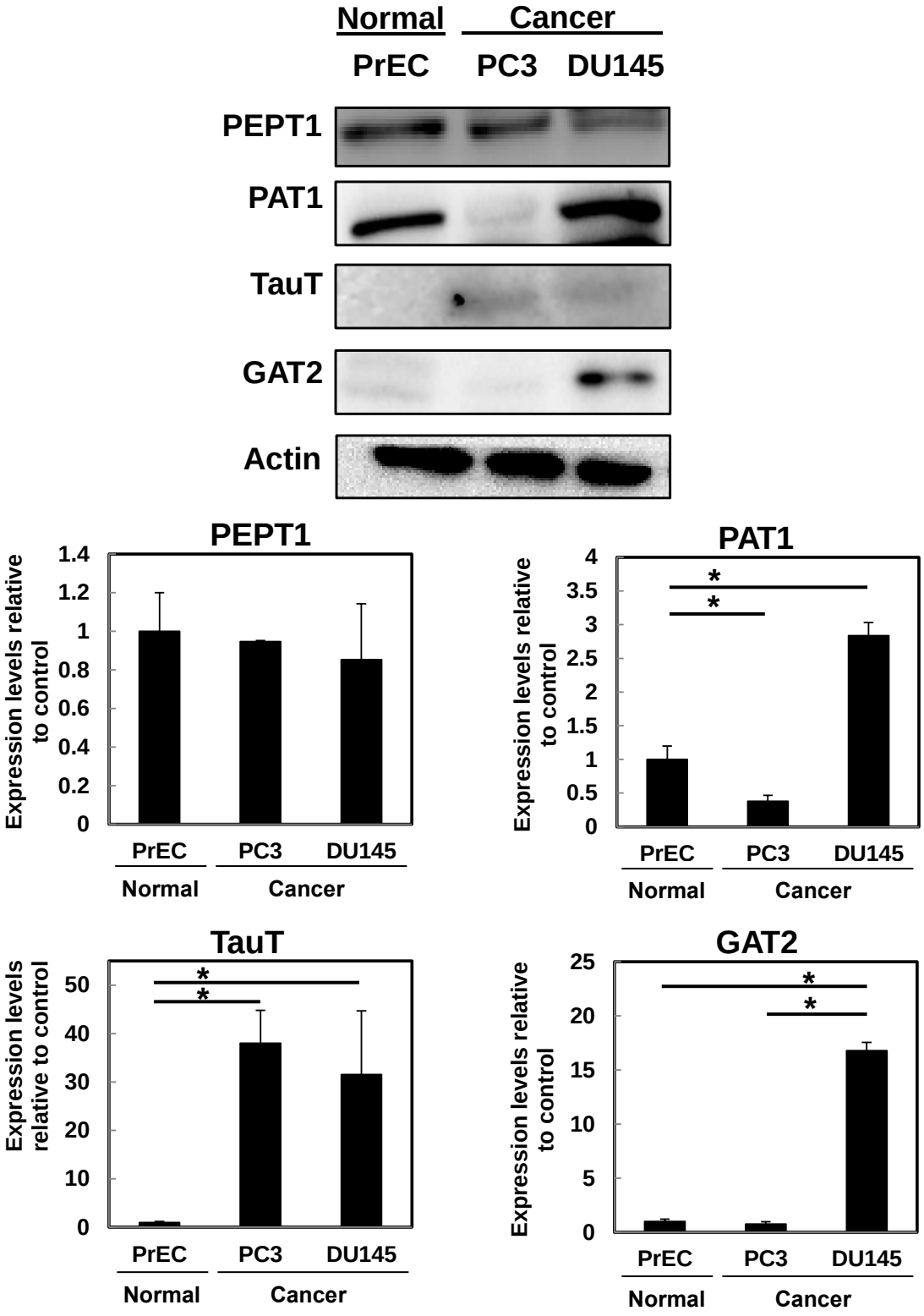

Figure 3.3 Protein expressions of PEPT1, PAT1, TauT & GAT2 and band intensity graphs in PrEC, PC3 and DU145 cell lines

Based on the results obtained above and findings from the previous chapter, it is believed that transporters which were highly expressed would play a significant role in ALA uptake. Therefore, inhibiting the actions of these highly expressed-transporters would result in a significant decrease in PpIX production. The significance of these transporters was studied in the next sub-chapter to identify the dominant transporter for cellular ALA uptake in these cell lines.

3.3.3 Roles of transporters in ALA uptake

Ibuprofen, tryptophan, taurine and GABA were used to evaluate the effect on PpIX production following the suppression of each transporter's activity respectively. Ibuprofen and tryptophan were inhibitors of PEPT1 and respectively, while taurine and GABA were inhibitors of both TauT and GAT2. Studies were carried out by carrying out co-administration of 1 mM ALA and inhibitors at a concentration of 5 mM for tryptophan, taurine and GABA, followed by 24 hours of incubation at 37°C in a 5% CO_2 incubator. Similar to studies in previous chapter, concentration of ibuprofen, a non-competitive inhibitor of PEPT1, was fixed at 100 μM. Cell samples were then collected for HPLC analysis. Findings of these studies were plotted into graphs in Figure 3.4, 3.5 and 3.6.

Addition of ibuprofen, a non-competitive inhibitor of PEPT1, showed more than 40% drop in PpIX production in WI38 cells but not in A549 cells (Figure 3.4). No significant difference in PpIX production was observed when tryptophan, taurine and GABA were co-administered with ALA, suggesting PAT1, TauT and GAT2 were not involved in ALA uptake in WI38 cells ($p > 0.05$). These results coincided with Western blotting results from Figure 3.2, where transporters other than PEPT1 were lowly expressed in WI38 cells. The level of PpIX produced following the addition of ibuprofen in both WI38 and A549 cells

.

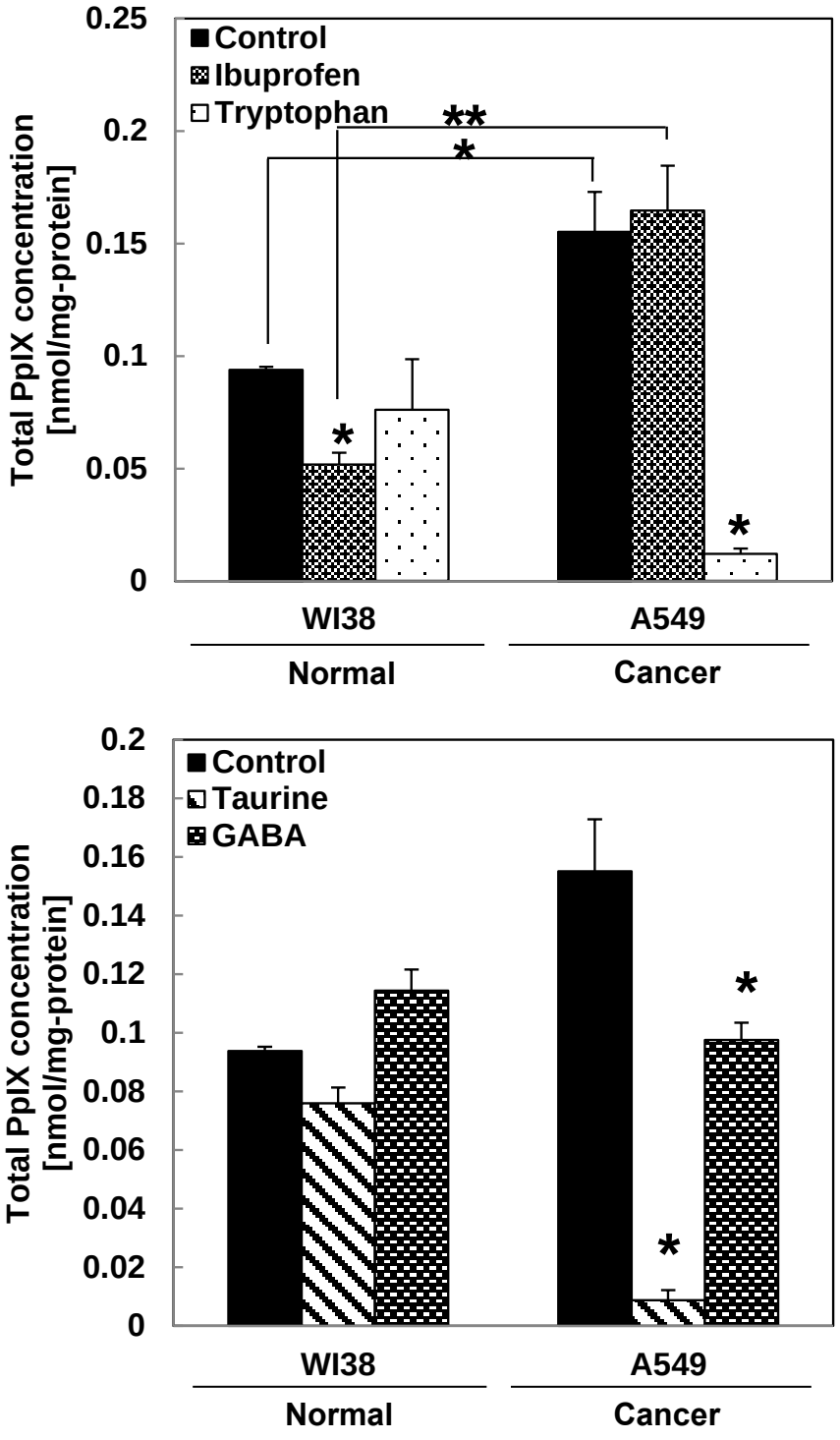

Figure 3.4 Production of intracellular and extracellular protoporphyrin (PpIX) following co-administration of aminolevulinic acid (ALA) and inhibitors in WI38 and A549 cells (*; $p < 0.05$; **; $p < 0.01$)

showed a higher degree of significance ($p < 0.01$) compared to the control ($p < 0.05$). On the other hand, studies using tryptophan, taurine and GABA in A549 cells showed significant decrease in PpIX production but not ibuprofen ($p < 0.05$), which again coincided with their protein expression results (Figure 3.2), suggesting the three transporters except PEPT1 were involved in ALA uptake in this cell line.

This inhibition assay was then repeated using the same methods in PrEC and PC3 cells originating from the prostate gland (Figure 3.5). Inhibition of PEPT1 in PrEC and PC3 resulted in a significant drop in PpIX production ($p < 0.05$). PpIX level dropped significantly following addition of tryptophan in PrEC but the trend was not observed in PC3 ($p < 0.05$). No significance difference was observed following the addition of taurine and GABA in both PrEC and PC3. These results coincided with protein expression levels stated in Figure 3.3.

Studies were carried out again in another pair of prostate cell lines, PrEC and DU145 as shown in Figure 3.6. PpIX production of both cell lines decreased significantly following the inhibition of PEPT1 and PAT1 ($p < 0.05$). No significant change in PpIX levels in PrEC cells following the addition of taurine and GABA. An observable drop in PpIX production were observed in DU145 following the inhibition of TauT and GAT2 ($p < 0.05$). Similar to the previous two studies, the inhibition results correlated with protein expression levels in Figure 3.3.

In general, all these results correlated with expression of all four transporters in both cell lines, whereby inhibition of transporters which were highly expressed resulted in a significant drop in PpIX production, possibly due to decrease in cellular uptake of ALA. Results obtained in this sub-chapter showed that factors affecting cellular uptake is independent of organ origins and the possibility usage of these drugs for tailor-made therapy to increase tumor specificity in ALA-PDT and ALA-PDD.

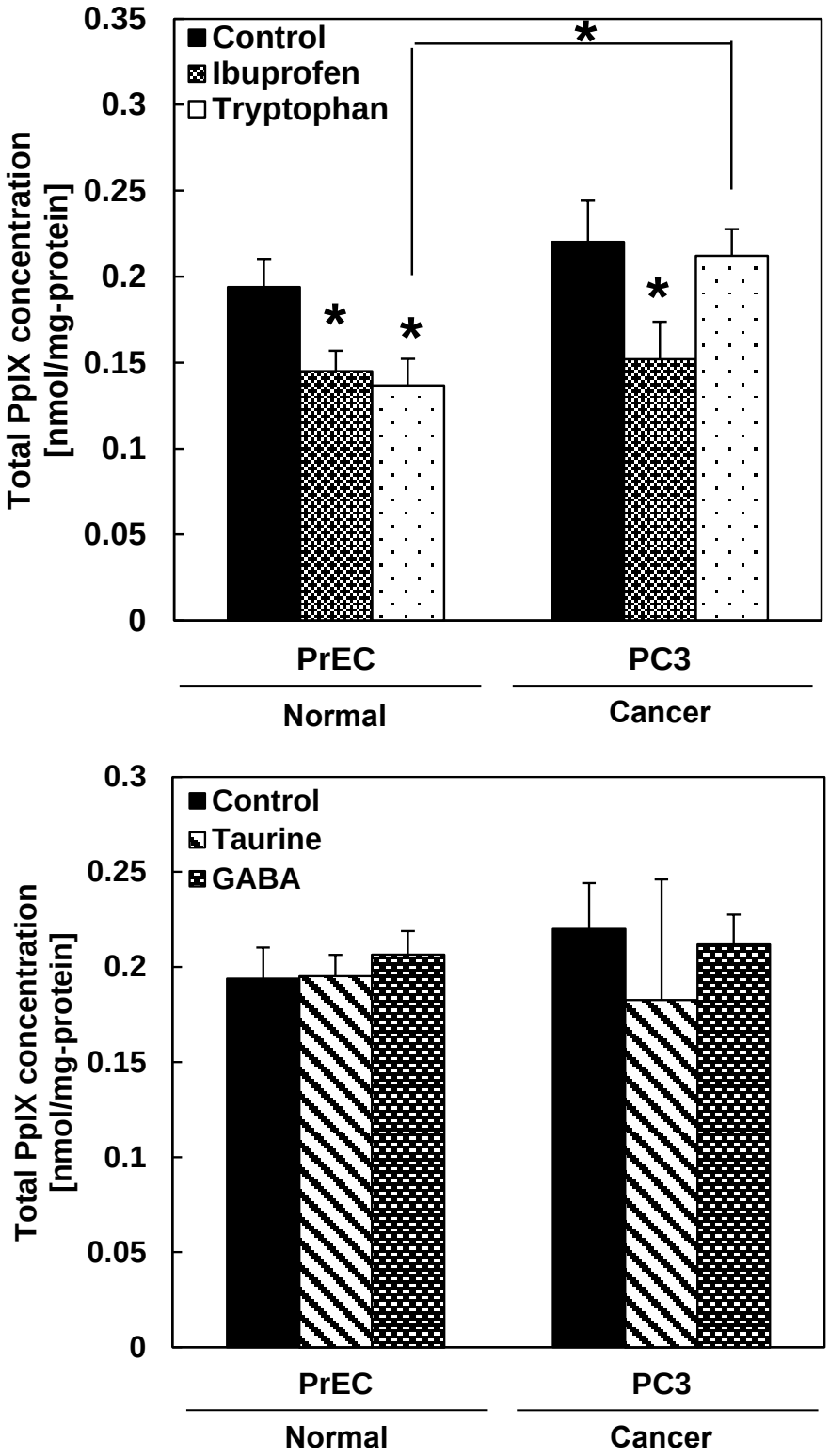

Figure 3.5 Production of intracellular and extracellular protoporphyrin (PpIX) following co-administration of aminolevulinic acid (ALA) and inhibitors in PrEC and PC3 cells (*; $p < 0.05$)

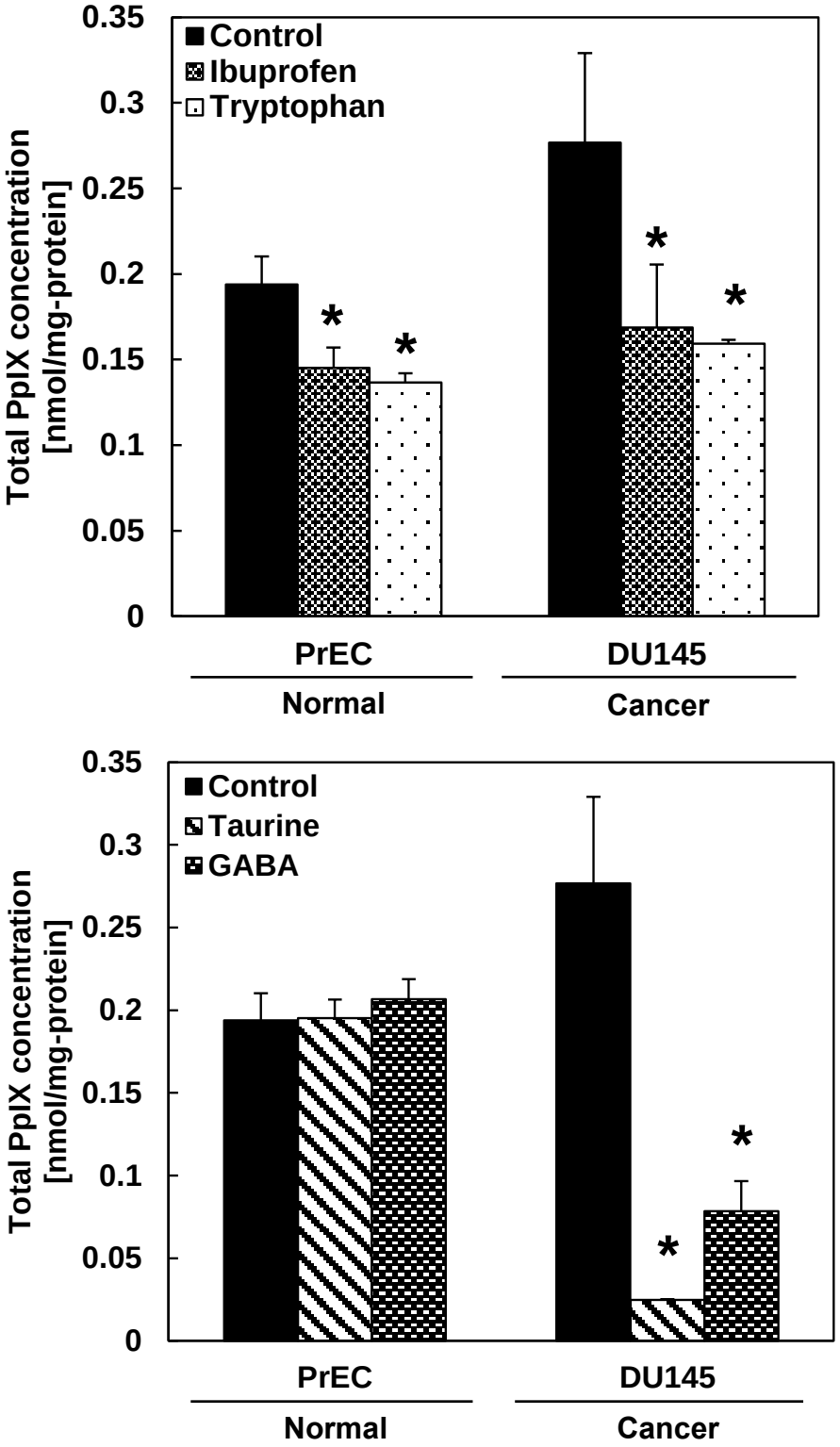

Figure 3.6 Production of intracellular and extracellular protoporphyrin (PpIX) following co-administration of aminolevulinic acid (ALA) and inhibitors in PrEC and DU145 cells (*; $p < 0.05$)

3.4 DISCUSSION

The study of relationship between the four transporters, namely PEPT1, PAT1, TauT and GAT2, and cellular uptake of ALA in cancer cells had been discussed in Chapter 2. However, it is more important to address the specificity of target transporters in order to allow maximum exogenous ALA-induced PpIX accumulation only in cancer cells but not in normal cells. Three sets of cell lines, from two different origins, were studied in order to obtain more comprehensive results on the cellular uptake of ALA by transporters.

Similar to results obtained from previous chapter, Table 3.1 also showed the expressions of these transporters were independent of organ origins, where all five cell lines studied in this chapter did not expressed similar transporter expression trends despite originating from the same organ, suggesting again that the expression levels and activity of these four transporters may be independent of their origin. Sensitivity of ALA uptake in different cell lines were believed to be dependent on their expression levels as shown in Table 3.2 and their expression levels would be vital in a tailor-made therapy. Two major findings were obtained from these studies, PEPT1 being expressed only in normal lung cells but not in its cancerous counterpart; and PAT1, which was expressed only in normal prostate cells but not in its cancerous counterpart (Figure 3.2 & 3.3). The inhibition of these transporters in these cell lines saw a significant drop in PpIX production in normal cells but not in cancer cells (Figure 3.3.4 & 3.3.5). This suggests ibuprofen and tryptophan might be useful in tailor-made therapy by increasing its specificity towards tumors.

Using mathematical calculations, the production of PpIX in the controls of A549 and WI38 cells were different, whereby A549 cells produced approximately 1.7 times more PpIX than the latter (Figure 3.4A). However, the difference in PpIX production of these cell lines increased further to about 3.2 times following the inhibition of PEPT1 using ibuprofen,

Table 3.1 Summary on protein expressions of various transporters in selected cell lines

Low — Medium — High

	Lung		Prostate			Stomach
	Normal	Cancer	Normal	Cancer		Cancer
	WI38	A549	PrEC	PC3	DU145	TMK1
PEPT1	1	0.03	0.98	0.90	1	0.42
PAT1	0.09	1	0.34	0.11	1	0.45
TauT	0.01	0.19	0.01	0.21	0.17	1
GAT2	0.07	1	0.06	0.04	1	0.24

Table 3.2 Effect on PpIX production following co-addition of inhibitors and ALA

Low — Medium — High

Inhibitors	Lung		Prostate		
	Normal	Cancer	Normal	Cancer	
	WI38	A549	PrEC	PC3	DU145
Ibuprofen	↓	-	↓	↓	↓
Tryptophan	-	↓	↓	-	↓
Taurine	-	↓	-	-	↓
GABA	-	↓	-	-	↓

		Inhibitor/ALA ratio
Ibuprofen	: PEPT1 non-competitive inhibitor	0.1
Tryptophan	: PAT1 competitive inhibitor	5
Taurine	: TauT & GAT2 competitive inhibitor	5
GABA	: TauT & GAT2 competitive inhibitor	5

indicating a significant decrease in PpIX production in WI38 cells but not in A549 cells ($p < 0.05$) (Figure 3.4 & Figure 3.7A). In the case of prostate cells, despite no significant difference in PpIX production was observed between PrEC and PC3 cells, difference in PpIX production was approximately 1.6 times higher in PC3 compared to PrEC cells following the addition of tryptophan, proving that inhibition of ALA uptake occurred only in PrEC cells ($p < 0.05$) (Figure 3.5 & Figure 3.7B). The increase in ratio values of both cases indicated that these two drugs are specifically targeted to normal cells, and could be used as a tailor-made therapy together with ALA treatment to increase specificity of ALA-induced PpIX

accumulation in tumors. The flow of a tailor-made therapy for ALA-PDT or PDD was stated in Figure 3.8. ALA-induced PpIX accumulation in cells is important in identifying or killing cancer cells and administration of these drugs could increase specificity of the therapy by preventing cellular uptake of ALA in normal cells.

In addition, this study also pointed out the abundance of PEPT1 in cancer and normal cells. Based on research by Chung *et. al.* (2013), PEPT1 is highly expressed in gastric cancer cells compared to normal cells, prompting that normal cells might exhibit a much lower production of PpIX. Results in this chapter suggested otherwise, whereby normal lung cell (WI38) expressed much more PEPT1 compared to its cancerous counterpart (A549) (Table 3.1). Normal prostate cells, PrEC, also exhibited equal levels of PEPT1 together with its cancerous counterparts, PC3 and DU145 (Table 3.1).

(A)

$$\text{ALA: } \frac{\text{PpIX(A549)}}{\text{PpIX(WI38)}} = \frac{0.155}{0.094} = 1.7$$

$$\text{ALA \& Ibuprofen: } \frac{\text{PpIX(A549)}}{\text{PpIX(WI38)}} = \frac{0.165}{0.052} = 3.2$$

(B)

$$\text{ALA: } \frac{\text{PpIX(PC3)}}{\text{PpIX(PrEC)}} = \frac{0.220}{0.194} = 1.1$$

$$\text{ALA \& Tryptophan: } \frac{\text{PpIX(PC3)}}{\text{PpIX(PrEC)}} = \frac{0.212}{0.137} = 1.6$$

Figure 3.7 Ratio on the differences between production of PpIX between ALA-only and ALA-inhibitor treatment samples among (A) WI38 and A549 cells; and, (B) PrEC and PC3 cells

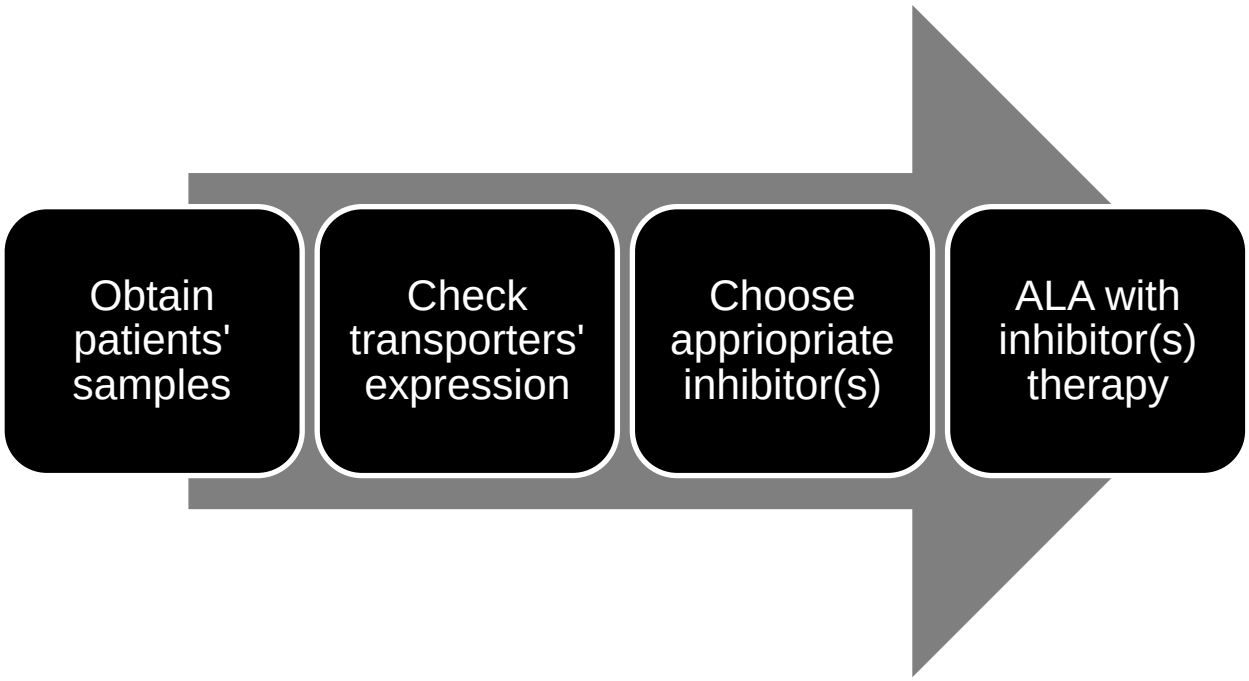

Figure 3.8 Flow chart showing chronological order of tailor-made therapy to enhance the specificity of ALA-PDT and ALA-PDD

In conclusion, these results showed that usage of drugs targeted specifically to transporters in normal cells is essential in reducing the PpIX accumulation in normal cells in order to increase the specificity of ALA-PDT and ALA-PDD in tumors. This study also showed the role of transporters involved in ALA uptake differ among different cell lines (even of the same origin) and are highly dependent of expression levels of respective transporters. These findings also overwritten past studies which suggested PEPT1 may be not highly expressed in normal cells.

CHAPTER 4
EFFICIENCY OF ALA-PDT BASED ON ALA UPTAKE TRANSPORTERS IN A CELL DENSITY-DEPENDENT MALIGNANCY MODEL

4.1 INTRODUCTION

Wang *et. al.* (2014) stated that the definition of cancer malignancy is the degree of genetic stability in cancer cells, primarily reduced expression levels of DNA repair enzymes and higher proliferative capabilities. This change in genetic stability and advance in malignancy level result in acquirement of drug resistance of cancer cells, leading to a significant reduction in effectiveness of conventional cancer chemotherapy. Cancer cells or tumours with higher malignancy typically resemble later disease stage which possess higher invasiveness, density and drug resistance (Chen *et. al.*, 2006). Highly malignant cells have been problematic to researchers and medical doctors in treating patients.

Previous chapters have shown the role of ALA uptake transporters, such as PEPT1 and PAT1, in uptaking ALA into cells, leading to accumulation of PpIX. The amount of PpIX accumulation in the cell is important in determining the effectiveness of ALA-PDT. Study by Nakayama *et. al.* (2016) has shown that the expression levels of PEPT1 is significantly higher when incubated under high density. Therefore, in this chapter, the study will be focused on the discovering the relationship between the efficiency of ALA-PDT and ALA uptake transporters using a cell density-dependent malignancy model. The relationship between ALA uptake transporters and cell density-induced malignancy will also be determined.

4.2 MATERIALS & METHODS

Chemicals

DMEM-high glucose culture medium and antibiotic-antimycotic mixed stock medium (ABAM) were purchased from Nacalai Tesque (Kyoto). Fetal bovine serum (FBS) was purchased from Equitech-Bi, Inc. (Kerrville, Texas, USA). Aminolevulinic acid (ALA) was purchased from Cosmo Oil Ltd. (Tokyo). Ibuprofen, tryptophan and verteporfin used in this study were purchased from Sigma Aldrich Corporation (Tokyo). All inhibitors used were of analytical grade.

Cell Culture

Human prostate cancer cell line, DU145, was obtained from Prof. Inoue Keiji from Kochi University, Japan. Cells are cultured in DMEM-high glucose culture medium. These cells are incubated with respective culture medium followed by the addition of 10% FBS and 10% ABAM, at 37 °C in a 5% CO_2 incubator. In this study, a cell density-dependent malignancy model using DU145 cancer cell line was established.

Western blotting

Western blotting experiments were carried out to quantify the expression level of proteins in cells using modified methods based on Tamura *et. al.* (2007). Cells were first washed with PBS (-), followed by addition of Lysis Buffer A [50 mM Tris-HCl (pH 7.4), 20 mM N-methylmaleimide, 1 mM DTT, 1% (v/v) Triton X-100 and Protease inhibitor cocktail (Nacalai Tesque)]. The cell suspensions were homogenized using a 27 G syringe for at least 10 times and centrifuge at 1000×G for 10 minutes at 4°C. Protein samples were then recovered and stored at -80°C freezer for future use.

Protein samples were next treated with SDS-PAGE sample buffer where they were then separated through SDS-PAGE electrophoresis using 7.5% and 11.25% polyacrylamide gel. These separated proteins were then transferred onto a Immobilon-P PVDF membrane (Milipore Corp., M.A.) whereby blocking and antibody treatment would be carried out next. Blocking was carried out by incubating the membrane at room temperature for 60 minutes in 5% (w/v) skimmed milk dissolved in TBST [20 mM Tris-HCl (pH 7.4), 150 mM NaCl, 0.05% (v/v) Tween 20].

Anti-human PAT1 antibody (Novus Biologicals, Littleton, Colorado, USA; 1:1000), anti-human PEPT1 antibody (Abcam, Cambridge, Massachusetts, USA; 1:200), anti-human TauT antibody (Santa Cruz Biotechnology, Dallas, Texas, USA; 1:500), anti-human GAT2 antibody (Medical & Biological Laboratories, Naka-ku, Nagoya, Japan; 1:1000), anti-human RANKL antibody (NSJ Bioreagents, San Diego, California, USA; 1:500), anti-human RANK antibody (Biorbyt Ltd., Cambridge, UK; 1:500), anti-human YAP antibody (Cell Signaling Technology, Chiyoda-ku, Tokyo, Japan; 1:1000) and human actin antibody (MP Biomedicals, Santa Ana, California; 1:200 dilution), which served as internal control, were used in primary antibody treatment. Secondary antibody used in this study were horseradish peroxidase (HRP)-conjugated anti-mouse (Cell Signaling Technology, Beverly, MA) and anti-rabbit IgG (Santa Cruz Biotechnology, Dallas, Texas, USA) concentrate, which were diluted 3000 times in TBST solution. Substrate for HRP used in this study were Western Lightning Chemiluminescent Reagent Plus、Western Lightning Chemiluminescent Reagent Pro (PerkinElmer Life and Analytical Sciences, Waltham, MA), Western BLoT Ultra-Sensitive HRP Substrate (TaKaRa Bio, Inc., Shiga, Japan). Chemiluminescent were used to quantify protein expression levels using Lumino Imaging Analyzer LAS-4000 mini (GE Healthcare UK, Amersham Place, England).

Porphyrin production quantification using High Performance Liquid Chromatography (HPLC)

Cells were first seeded at specific cell densities in 35 mm dishes and incubated at 37°C under 5% CO_2 in a CO_2 incubator for 24 hours. Experiments were carried out in triplicates per sample. Co-addition of ALA and inhibitors, were carried out and cells were further incubated under the same condition for another 24 hours.

Extracellular porphyrins were then extracted first by recovering all culture medium, followed by a 3000×G centrifugation for 10 minutes in order to separate dead cells. A volume of 50 µL of the supernatant from each sample were then taken out and added into a new 1.5 mL centrifuge tube containing 150 µL Dimethylformamide (DMF): 2-propanol solution (100: 1, v/v). This step is essential for the denaturation of unwanted proteins and to ensure pure extraction of porphyrins. Separation of denatured proteins were then carried out by centrifuging at 10000×G for 10 minutes. Supernatants were recovered and pellets were discarded.

In order to isolate intracellular porphyrins, cells were first washed using PBS (-) twice, followed by addition of 150 µL of 0.1 M NaOH. A volume of 50 µL of cell suspension from each sample were taken out and added into a new 1.5 mL centrifuge tube containing 150 µL of DMF: 2-propanol solution (100: 1, v/v) as mentioned in the previous paragraph. Cell suspensions then underwent centrifugation under 10000×G for 10 minutes. Supernatants were recovered and pellets were discarded.

HPLC analysis of porphyrin was carried out using Type Promonence System (Shimadzu Manufacturing Co., Kyoto) equipped with reverse phase C18 column (CAPCELL PAK, C18, SG300, 5 µm, 4.6 mm × 250 mm, Osaka Soda Co. Ltd., Osaka) while maintaining at a temperature of 40 °C. Mobile phase A, comprising of 1 M ammonium acetate solution containing 12.5% acetonitrile (adjusted to pH 5.2), and mobile phase B, made up of

50 mM ammonium acetate solution containing 80% acetonitrile, were used in elution of porphyrin. 50% mobile phase B was first directed at a flow rate of 1.0 mL / min for 10 minutes following by driving mobile phase B into the column from a linear gradient ranging from 90% for 10 minutes and finally 90% mobile phase B at a flow rate of 2.0 mL / min for another 10 minutes in the elution program. 100μL of each eluate was injected and detected using with a detector equipped with a fluorescence spectrometer at an excitation wavelength of 404 nm and a detection wavelength of 624 nm. The protein concentrations of each sample were determined using Bradford's method using Quickstart Bradford 1×Dye Reagent (Biorad Laboratories, Inc., Hercules, California, USA). Coproporphyrin I dihydrochloride, Coproporphyrin I dihydrochloride, Protoporphyrin I dihydrochloride, used as standard material for porphyrin were purchased from Frontier Scientific, Inc. (Logan, Utah, USA). Chromatograms and standard curves using each porphyrin standard are shown in Figure 2.1 and Figure 2.2, respectively.

ALA-PDT assay

The assay was carried out as previously described with slight modifications [16]. DU145 cells were first seeded for 24 h and incubated with 1 mM ALA in culture media under 5% CO_2 gas at 37 ºC in the dark for 4 h. The samples were then exposed to light irradiation (635 nm, 1080 mJ/cm^2) for 5 min by placing the dishes under an LED irradiation unit (provided by SBI Pharma CO., Ltd., Tokyo, Japan). Cells were then further incubated again in the dark under 5% CO_2 at 37 ºC for 24 h. Cell viability was determined with trypan blue and the number of living cells were quantified using Countess II FL cell counter (Thermo Fisher Scientific, Waltham, MA, USA).

Confocal Microscopy

Cells were cultured in 35 mm dishes under specific cell densities in the dark under 5% CO_2 at 37 ºC for 24 h. 1 mM ALA were added and the dishes were incubated for another 24 h. The ALA-containing dishes were washed twice with PBS solution and 3 mL of HBBS solution were added. Zeiss LSM 780 upright laser scanning confocal microscope (Carl Zeiss SAS, Jena, Germany) was used for cell imaging. The excitation for PpIX was set at a wavelength of 405 nm while emission wavelength was maintained at 620-700 nm. Laser illumination was set at 2.0 % power for all experiments. Images were acquired using a 40X water immersion lens for PpIX and later analyzed using ZEN 3.3 (Blue) software.

***In silico* analysis**

In order to analyze the overall survival of RANKL, the PrognoScan platform (http://www.prognoscan.org) was utilized on patient samples with the probe name, “210643_at [HG-U133A]”, under the DUKE-OC dataset (Mizuno *et. al.*, 2009). Samples of 133 ovarian cancer patients were separated into two groups (n=91 of low RANKL expression and n=42 of high RANKL expression groups) according to a median quantile expression cut-off (50%). The expression cut-off value is 0.7 FPKM (fragments per kilobase of transcript per million mapped reads). The two patient cohorts were compared by a Kaplan-Meier survival plot with 95% confidence intervals and logrank P value was calculated using the Cox regression model.

Statistical analysis of data

Microsoft Excel 2010 was used for data analysis of this study. One-way ANOVA were performed for each set of data to show that there were significant differences in mean values between treated and non-treated samples, $p < 0.05$.

4.3 RESULTS

4.3.1 Establishing a cell density-dependent malignancy model

Fig. 4.1 showed clinical data obtained from Prognoscan website on the overall survivability based on RANKL expression – a malignancy marker. Fig. 4.1A-B showed the expression value of RANKL in 133 ovarian cancer patients. The data are being separated into high and low RANKL expression levels. Fig. 4.1C showed a Kaplan-Meier plot, which represents an overall survival plot based on the expression level of RANKL. The blue line represents low expression plots and red line represents high expression plots. It is shown that patients with higher level of RANKL expression level exhibits lower overall survivability.

In order to study the relationship between malignancy and transporters, the establishment of a cell density-dependent malignancy model is needed. DU145 cells were incubated under four different cellular density, starting from 2.1, 5.3, 10.5 and 31.6 × 10^3 cells / cm^2. The change in cell density is shown morphologically in Fig. 4.2A using images from a phase contrast microscope. A steady increase in the number of cells was observed in these images. Fig. 4.2B showed the change in total cellular proteins in the four samples. The increase in amount of cellular protein showed a positive correlation with the increase in cell density. Yes-associated protein (YAP), a protein from the Hippo pathway, also showed an increase in expression level under high density (Fig. 4.2C-D). This result coincided with past studies that suggest YAP expression increases as cell density increase (Kraff *et. al.*, 2012). The expression level of RANKL protein, a malignancy marker, under these circumstances were being studied using Western blotting. It is found that the expression level of RANKL steadily increased as cell density increased (Fig. 4.2E-F). This suggest that the increase in cell density could possibly resulted in an increase in malignancy (RANKL expression). These results showed a correlation was identified between RANKL and YAP which suggest a

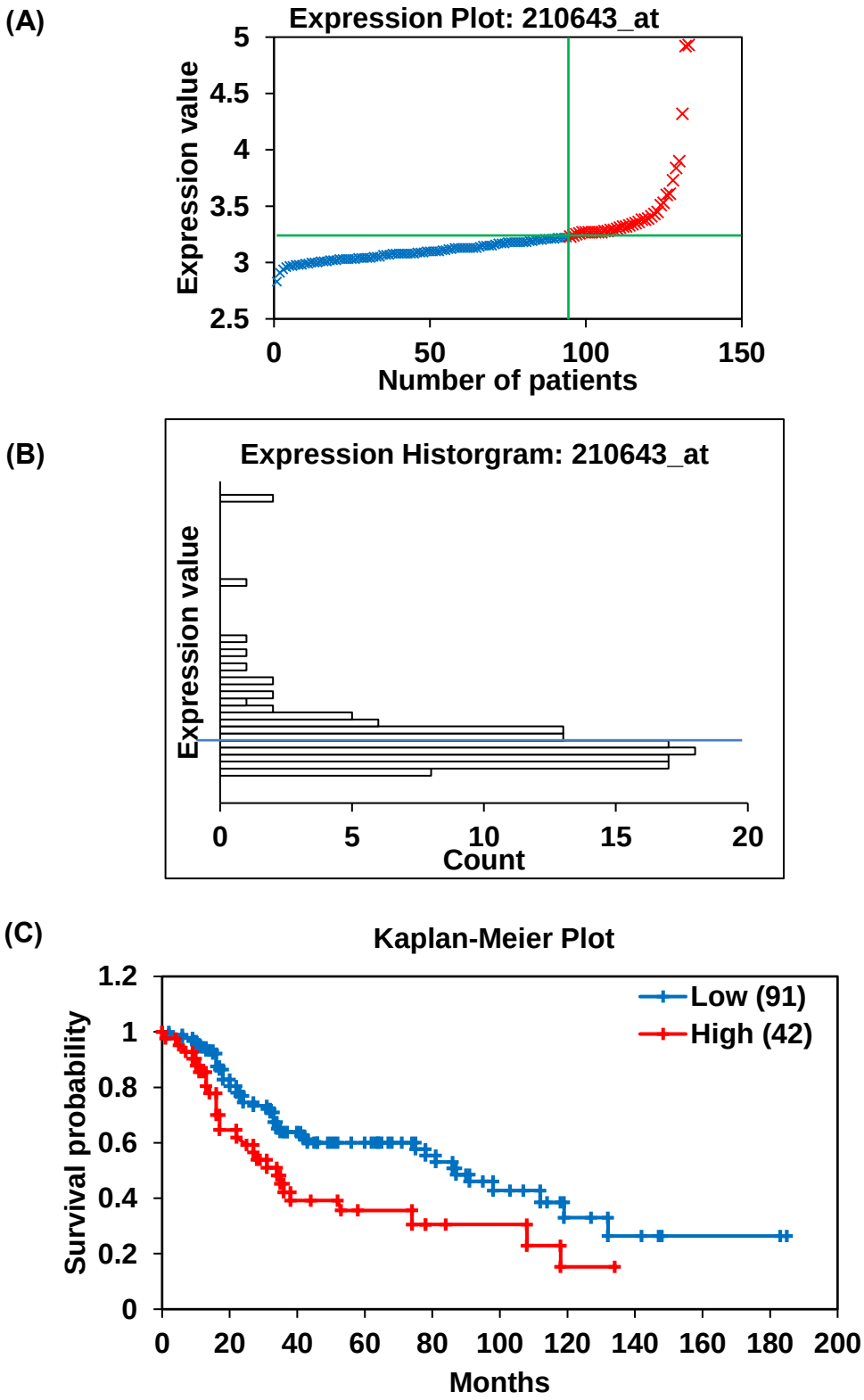

Figure 4.1 *In silico* analysis of RANKL expression on overall survival in ovarian cancer patients. (A) Attribution plot based on the 133 patients with various types of ovarian cancer. (B) Expression value of RANKL in each patient, and (C) Kaplan-Meier plot showing overall survival of cancer patients over time based on the expression level of RANKL.

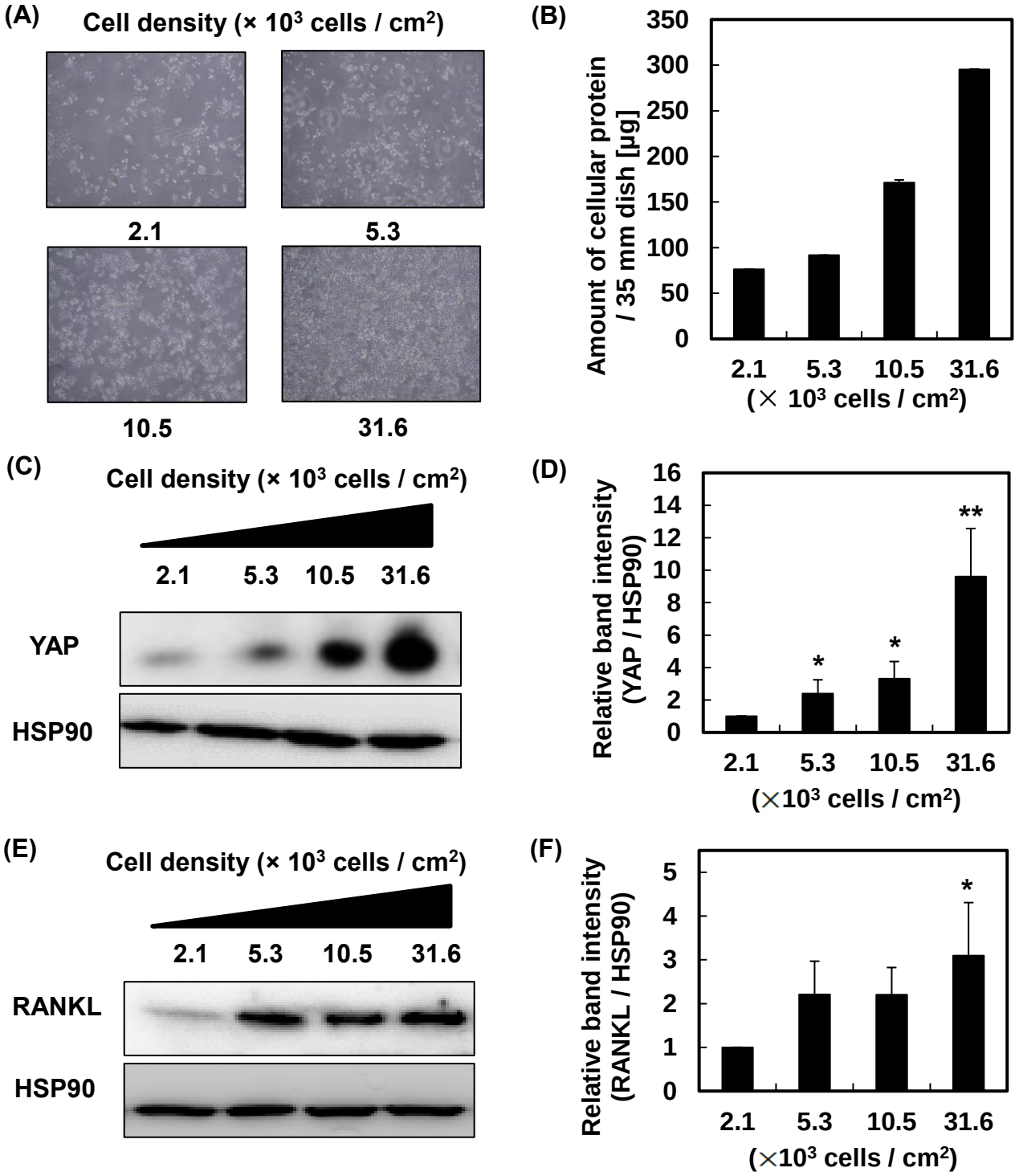

Figure 4.2 Establishment of a cell density-dependent malignancy model. Cells were seeded at 2.1, 5.3, 10.5 and 31.6 ×10^3 cells / cm^2. The changes in (A) cell morphology using phase contrast microscope and (B) protein concentrations using Bradford method were studied. (C) (D) Protein expression levels of YAP under different cell density were evaluated using Western blotting. (E) (F) Protein expression levels of RANKL under different cell density were evaluated using Western blotting. One representative blot is shown out of three independent experiments. (*, $p < 0.05$; **, $p < 0.01$. n =3).

pivotal role of YAP in regulating the expression level of RANKL.

4.3.2 Role of YAP in regulation of malignancy markers and ALA uptake transporters

Results from previous section exhibited a correlation between RANKL and YAP whereby expression levels of YAP and RANKL increases as cell density increases (Fig. 4.2). As an important protein involve in cell density, the relationship of YAP between malignancy markers and ALA uptake transporters was evaluated in this section. Fig. 4.3 showed the change in protein expression levels of YAP, malignancy markers and ALA uptake transporters following the inhibition of YAP using verteporfin. The inhibition of YAP using verteporfin was successful, as shown by significant decrease in the protein expression levels ($p < 0.005$) (Fig. 4.3A-3B). Previous study showed that the expression level of YAP decrease in a concentration dependent manner as concentration of verteporfin added increased (Wang *et. al.*, 2016). On the other hand, expression levels of RANKL showed a significant 40% decrease following the addition of verteporfin ($p < 0.05$) (Fig. 4.3C). Similar trend was observed in the expression level of receptor activator of nuclear factor κB (RANK), another malignancy marker ($p < 0.005$) (Fig. 4.3D). RANK expression was also significantly suppressed following verteporfin addition. These findings suggest that YAP played an important role in regulating cell density and malignancy markers. Interestingly, it is observed that the inhibition of YAP using verteporfin also lead to the downregulation of expression levels of ALA uptake transporters (Fig. 4.3E).

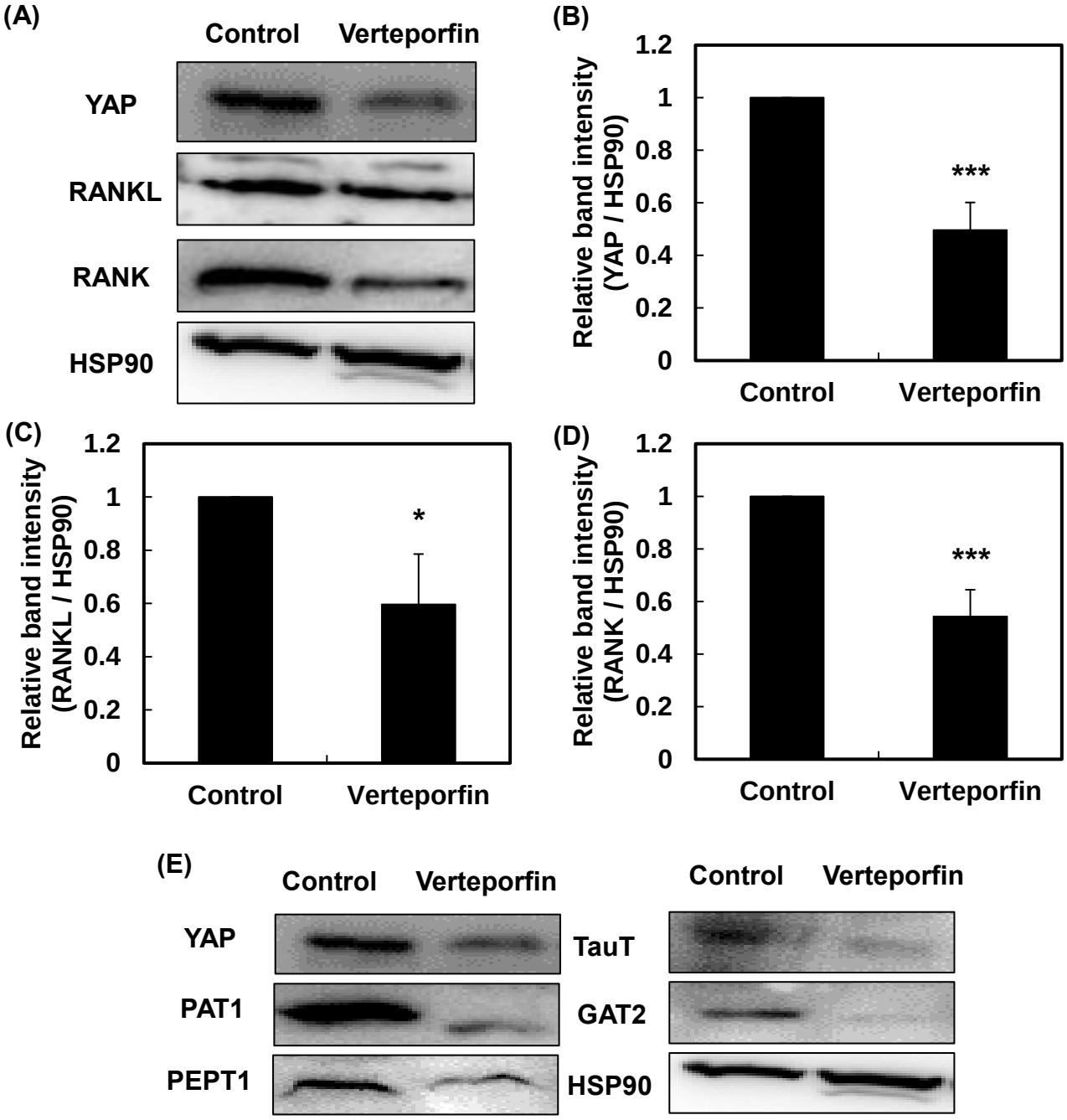

Figure 4.3 Role of YAP in the regulation of malignancy markers & ALA uptake transporters. YAP inhibition assay was carried out using 5 μM verteporfin. (A) The protein expression level of YAP and malignancy markers, RANKL and RANK, were studied using Western blotting. (B) (C) (D) Band intensity graph of expression levels of these proteins were plotted. (E) Protein expression level of YAP and various ALA uptake transporters. One-way ANOVA (Tukey's test) was performed for each set of data to show that there were significant differences in mean values between treated and untreated samples, *, $p < 0.05$; ***, $p < 0.005$. n =3. Bars represent standard deviation (SD).

4.3.3 Efficiency of ALA-PDT under different cell density

In this section, the effectiveness of ALA-PDT was studied by separating the DU145 cells into high and low cell density samples. Since expression levels of malignancy markers are higher in high cell density samples, this difference in cell density may be related to cancer malignancy. Low cell density samples were prepared at 2.1×10^3 cells / cm^2 while high cell density samples were prepared at 31.6×10^3 cells / cm^2. The cells were being incubated for 24 hours in the dark following ALA addition and light irradiation. The concentration of living cells following light irradiation were being studied using trypan blue dye. In low cell density samples, the concentration of living cells decreased by 11% following light irradiation (Fig. 4.4A). However, the number of living cells in high cell density condition decreased to about one-fifth following irradiation of light ($p < 0.0001$). This result suggest ALA-PDT is significantly more effective in cancer cells of higher cell density.

In Fig. 4.4B, the effect of cell density on the expression levels of two ALA uptake transporters, PAT1 and PEPT1 was evaluated. These findings showed that the expression levels of both transporters gradually increase as cell density increase. On the other hand, Osaki *et. al.* (2019) reported that effectiveness of ALA-PDT *in vitro* correlates with PpIX concentrations in carcinomas [23]. Therefore, the concentration of PpIX in DU145 samples under various cell density was being studied using HPLC (Fig. 4.4C). PpIX concentration was found to be significantly higher in high cell density samples ($p < 0.01$). The fluorescence intensity of PpIX under different density was also carried out using confocal microscope (Fig. 4.5). An increase in red fluorescence intensity was observed as cell density increase. These results coincided with findings from Fig. 4.4A which showed that cytotoxicity of ALA-PDT is significantly higher in high cell density samples. This result suggests the enhancement of

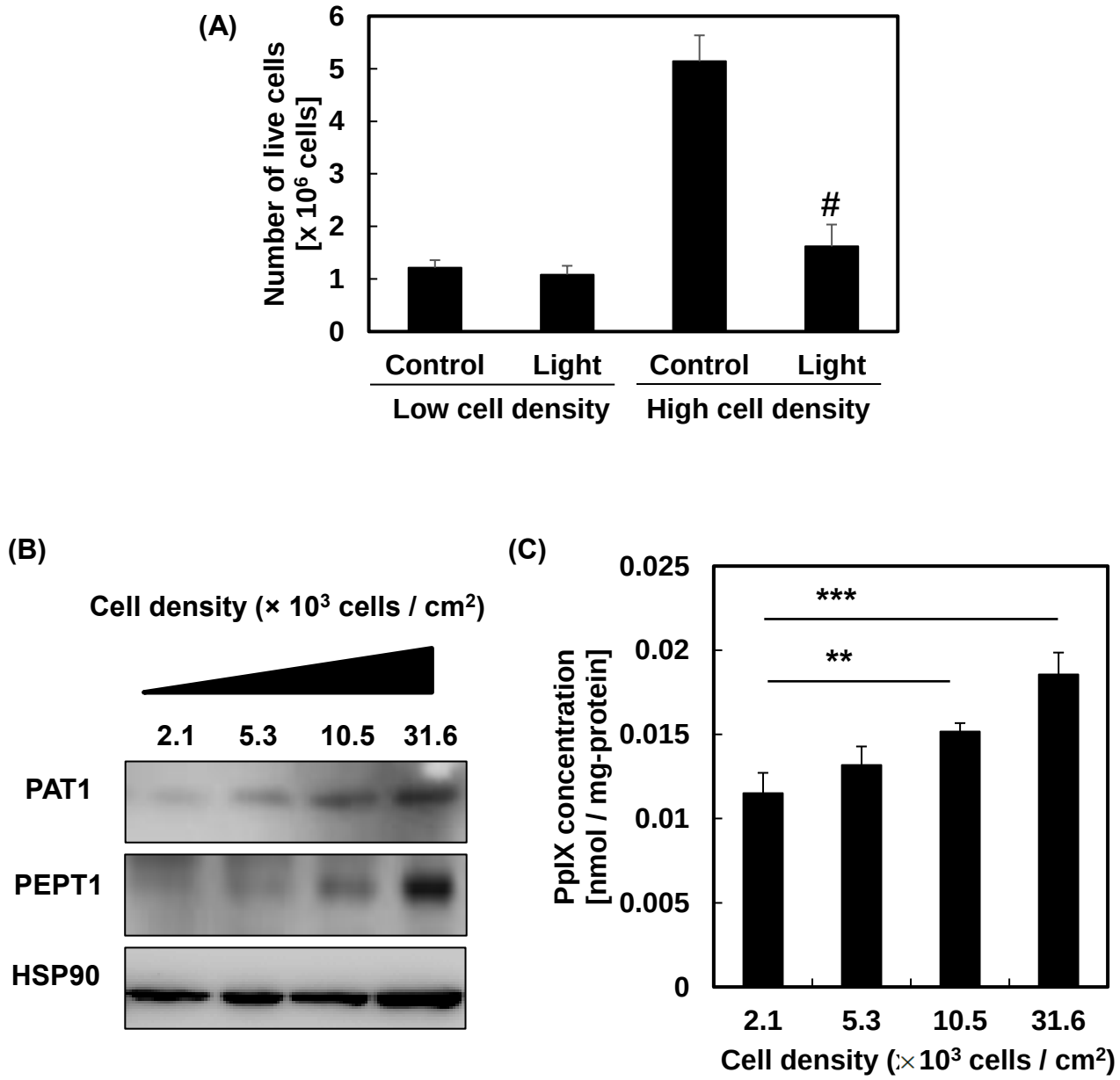

Figure 4.4 Effectiveness of ALA-PDT and PpIX accumulation under different cell density. (A) DU145 cells were seeded at high (31.6 × 10^3 cells / cm^2) and low (2.1 × 10^3 cells / cm^2) cell density for 24 hours before 4 hours of ALA administration. The samples were then directed with 5 minutes of light irradiation. Samples were then incubated for 24 hours and the number of live cells were then quantified using trypan blue solution and analysed using an automated hemocytometer. (B) Changes in expression levels of ALA uptake transporters under different cell density. (C) PpIX concentration under various cellular density (2.1, 5.3, 10.5 and 31.6 × 10^3 cells / cm^2) in DU145 cells were studied. One-way ANOVA (Tukey's test) was performed for each set of data to show that there were significant differences in mean values between treated and untreated samples, **, $p < 0.01$; ***, $p < 0.005$; #, $p < 0.0001$. n =3. Bars represent standard deviation (SD).

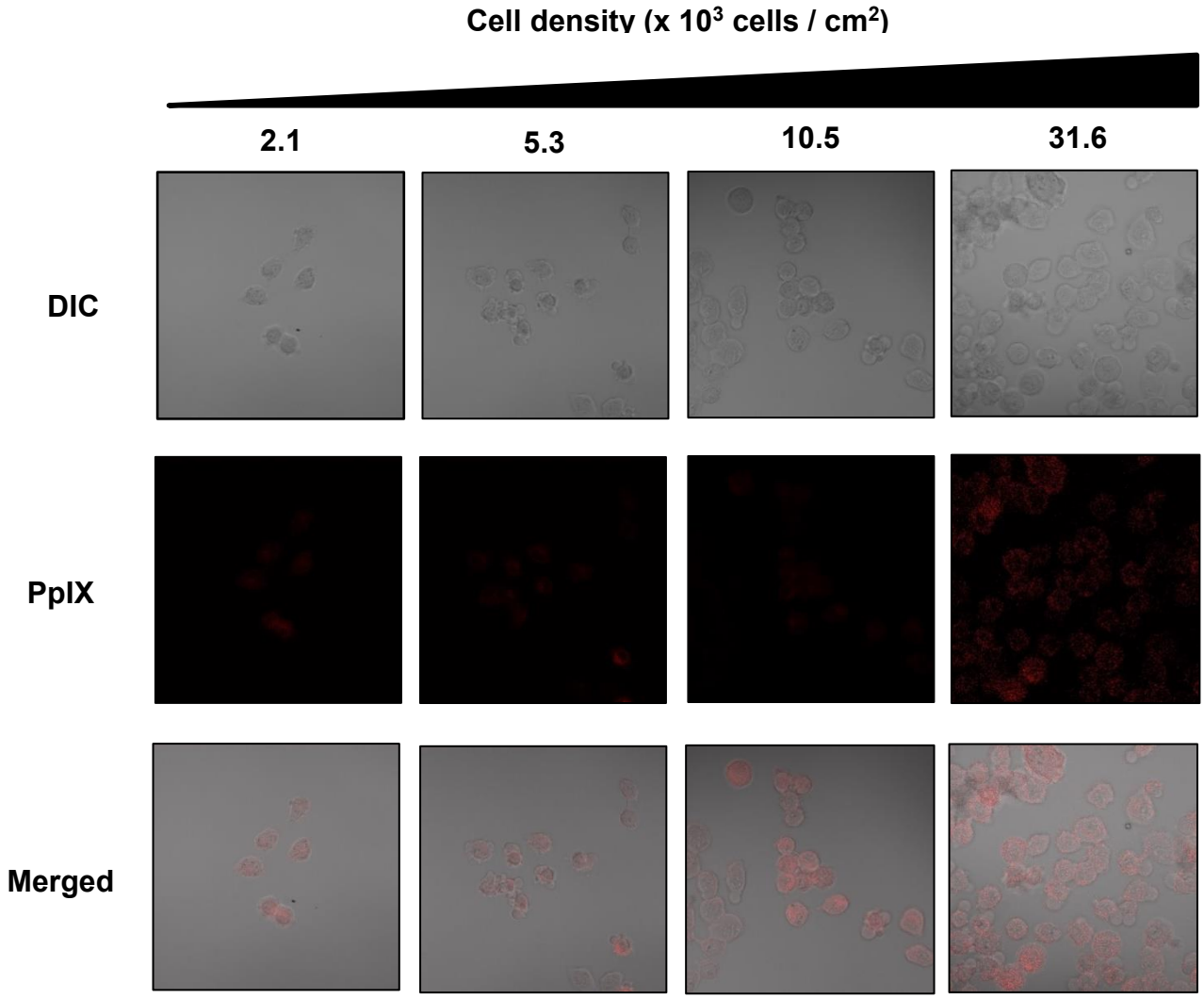

Figure 4.5 Confocal microscopy images showing PpIX fluorescence under different cell density. DU145 cells were seeded at 2.1, 5.3, 10.5 and 31.6 ×10^3 cells / cm^2 for 24 hours before 4 hours of ALA administration. Samples were then incubated for 24 hours and the samples are observed under a confocal microscope.

efficiency of ALA-PDT is a result of higher expression levels of transporters in high cell density samples.

4.3.4 Role of transporters in PpIX accumulation under different cell density

In order to identify the roles of PAT1 and PEPT1 in high and low cell density cancer cells, transporters' inhibition assays were carried out using tryptophan (PAT1 inhibitors) and ibuprofen (PEPT1 inhibitors). Inhibition of PAT1 only showed a significant decrease in the high cell density sample (Fig. 4.6A). This suggest that PAT1 is non-functional during low cell density condition, or in other words, not involved in ALA uptake. On the other hand, inhibition of PEPT1 showed a more significant decrease in the high cell density sample ($p < 0.001$) compared to low cell density sample ($p < 0.05$) (Fig. 4.6B). Similar to the PAT1 inhibition study, the result suggests that PEPT1's function in ALA uptake is significantly hindered during low cell density culture condition. This study suggest that ALA uptake is more effective in cancer cells of higher cell density due to higher expression levels of ALA uptake transporters.

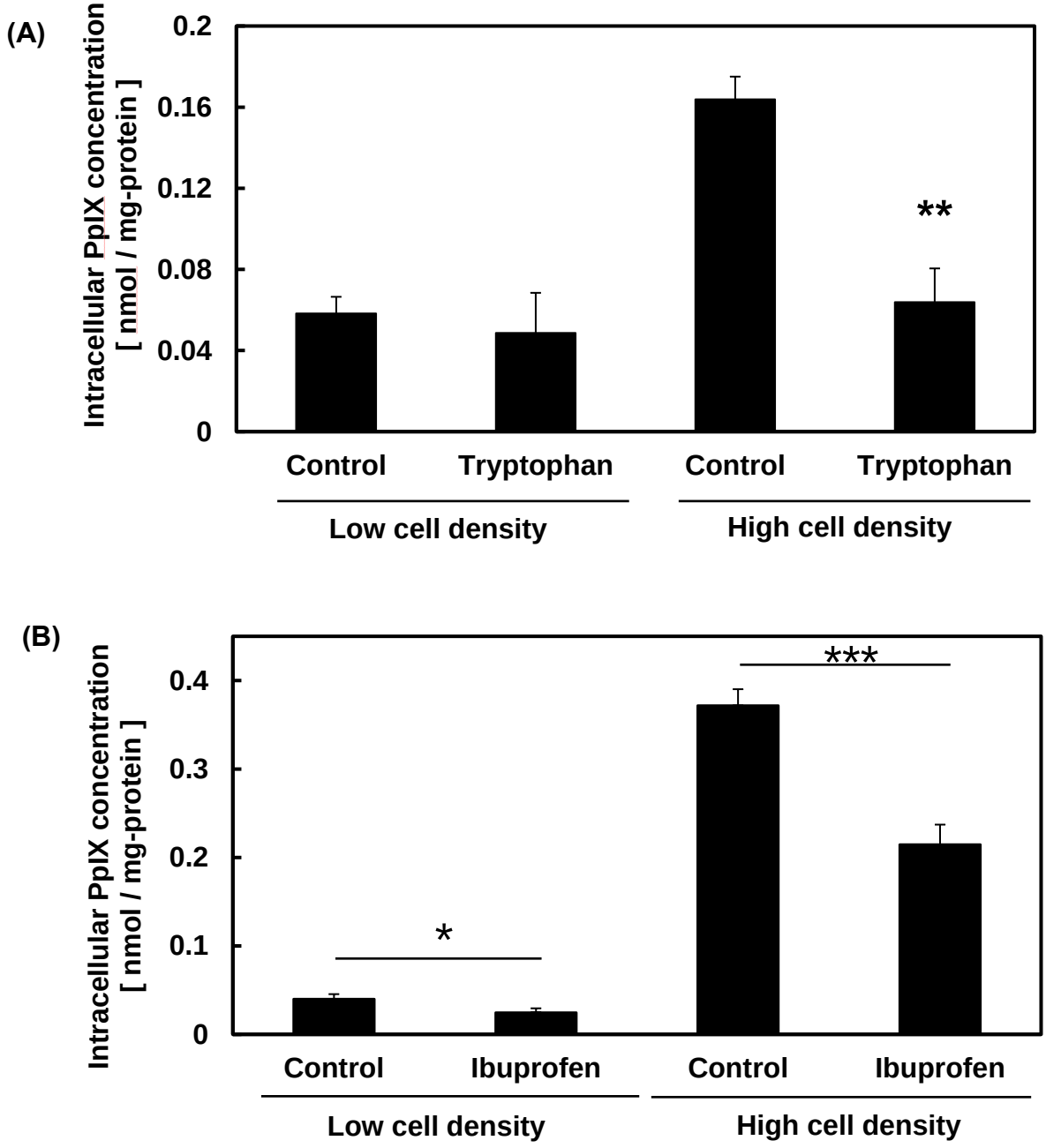

Figure 4.6 PpIX accumulation following transporter inhibition under different cell density. DU145 cells were first seeded at high (31.6×10^3 cells / cm^2) and low (2.1×10^3 cells / cm^2) cell density. (A) Tryptophan, a PAT1 inhibitor, and (B) ibuprofen, PEPT1 inhibitor, were co-administered together with 1 mM ALA. The concentration of intracellular PpIX were then studied using HPLC. One-way ANOVA (Tukey's test) was performed for each set of data to show that there were significant differences in mean values between treated and untreated samples, *, $p < 0.05$; **, $p < 0.01$; ***, $p < 0.005$. n =3. Bars represent standard deviation (SD).

4.4 DISCUSSION

Highly malignant cancers are much more difficult to treat, particularly due to their high metastatic capabilities and drug resistance characteristics (Kerbel, 1992). Therefore, it is imperative that scientists study the effect of cancer therapies on different cancer malignancy so that it could execute its cancer-killing properties at its maximum potential. In order to understand the efficiency of ALA-PDT on cell density and its possible relationship with cancer malignancy, a novel malignancy model induced by cell density was developed (Fig. 4.2). The reason behind this is that highly malignant cells have higher proliferation rate, leading to formation of highly dense lumps of cancerous cells (Jones *et. al.*, 1998). YAP is an oncogene that regulates various downstream processes, such as proliferations and metastasis, based on the cell density through cell contact inhibition (Zhao, *et. al.*, 2007; Varelas *et. al.*, 2010]. This study showed that YAP expression increased following the increase in cellular density (Fig. 4.2C). It is hypothesized that as long as nutrient and space availability are present, YAP expression and activity would continue to increase indefinitely. The increase in expression level of YAP would stop when these conditions are no longer satisfied, possibly due to the increase in frequency of cell contact inhibition and regulation of tissue growth (Zhao *et. al.*, 2007). However, there is currently no information on a precise cellular density value which may result in the occurrence of contact inhibition.

Results from Fig. 4.2 suggest the increase in expression levels of malignancy marker and YAP could be related. Next, the potential role of YAP was studied in regulating the expression of malignancy markers (Fig. 4.3). Verteporfin was used to suppress YAP expression in this study. Wang *et. al.* (2016) reported that verteporfin suppressed YAP function through the upregulation of a YAP chaperon protein known as 14-3-3σ. This study showed that inhibition of YAP using verteporfin resulted in a decrease in expression levels of malignancy markers,

RANKL and RANK (Fig. 4.3). These findings suggest the possible role of YAP in regulating malignancy in cancer cells. The effectiveness of ALA-PDT under different cell density were also being studied using trypan blue solution (Fig. 4.4A). Samples of high cell density showed a sharp decrease in concentration of live cells to only about one-fifth of the control following light irradiation ($p < 0.0001$) (Fig. 4.4A). On the other hand, only an 11% decrease in live cell concentration was observed in the low cell density samples. This result suggests that the cancer-killing effect of ALA-PDT appears to be more potent in high cell density cancer cells. The concentration of PpIX in DU145 cells under different cell density was then evaluated using HPLC. This is because PpIX levels has been known to be an indication of the effectiveness of ALA-PDT (Lai *et. al.*, 2019; Osaki *et. al.*, 2019). It is observed that PpIX level increases following the increase in cell density (Fig. 4.4C & Fig. 4.5). This finding coincided with results from Fig. 4.5A whereby ALA-PDT was observed to be more effective at high cell density condition. Several papers have reported that PpIX fluorescence increased as cell density increased *in vitro* while this effect was more profound in malignant cells compared to normal cells (Steinbach *et. al.*, 2005; Krammer *et. al.*, 1996; Moan *et. al.*, 1998). Other studies by Collaud *et. al.*, (2004) and Juzeniene *et. al.*, (2009) suggest that ALA-induced PpIX accumulation was efflux out of the cell at a higher rate when cultured in low density than in high density. The reason for this phenomenon is due to the expression level of ABCG2, a PpIX efflux transporter, was found to be significantly higher when cultured at low density compared to higher density (Nakayama *et. al.*, 2016).

Based on previous studies, the expression levels of ALA uptake transporters, namely PAT1 and PEPT1, are responsible for the change in PpIX levels due to their role in ALA uptake in DU145 cell line (Lai *et. al.*, 2019). This study showed the expression levels of these transporters gradually increase as the cell density increase (Fig. 4.4B). Previous study also

showed the involvement of these transporters in different cell lines are dependent on their expression levels and irrespective of their origins (Lai *et. al.*, 2019). Both PAT1 and PEPT1 are known to be highly expressed in DU145 cell line. Nakayama *et. al* (2016) also showed an increase in PEPT1 expression level as cell density increases in prostate cancer cell line (Krafft *et. al.*, 2012). These data suggest that ALA uptake increase due to higher expression of transporters at higher cell density, which leads to an increase in cancer-killing action of ALA-PDT in Fig. 4.4A.

Next, the roles of transporters under various cell density were determined using transporters inhibition assay (Fig. 4.6). Similar to previous studies, the inhibitors used for PAT1 and PEPT1 are tryptophan and ibuprofen respectively (Lai *et. al.*, 2019). PAT1 inhibition of samples with high cell density showed a significant decrease by 50% in intracellular PpIX levels ($p < 0.01$) (Fig. 4.6A). However, the effect of PAT1 inhibition under low cell density showed no significant changes. It is believed that PAT1 may not be functional and failed to uptake significant level of ALA during low cell density, leading to none or negligible amount of reduction in intracellular PpIX level. This result suggests that PAT1 might not be involved in ALA uptake in low cell density samples.

Inhibition of PEPT1 was carried out using the same protocol as above (Fig. 4.6B). PEPT1 inhibition showed much lesser significant decrease in intracellular PpIX level under low cell density condition ($p < 0.05$) compared to higher cell density condition ($p < 0.001$). PpIX level decreased by approximately 50% in high cell density DU145 cells following PEPT1 inhibition whereas only a slight decrease was observed in low cell density samples. PEPT1's function in ALA uptake is believed to be significantly hindered under low cell density culture condition. Based on both transporters' inhibition assay, it is believed that both transporters showed a more dominant role in ALA uptake when cultured in high cell density due to their higher

expression levels. This also suggest a possible, more dominant role in ALA uptake in cancer cells of which have higher expression level malignancy markers. It is believed that ALA-PDT is more effective when cultured under high cell density as expression levels of transporters are significantly higher.

In a nutshell, the results obtained from this study show that ALA-PDT is more effective in cancer cells of higher cell density due to the upregulation of transporters involved in ALA uptake. There is also a potential connection whereby ALA-PDT may be more effective in cancer cells of higher malignancy. In addition, it is also found that there is a possibility that YAP might play an important role in the regulation of both malignancy markers and ALA uptake transporters, although this statement requires further clarification in the future. This study showed the ALA-PDT is more effective in high cell density cancer cells due to the upregulation of ALA uptake transporters.

CHAPTER 5

SUMMARY

5.1 CONCLUSION

5.2 FUTURE CONSIDERATIONS

5.1 CONCLUSION

The main aim of this study was to study the roles of transporters involved in cellular uptake of ALA across cellular membrane in ALA-PDT *in vitro*. In summary, the findings of this study can be concluded as follows:

All four uptake transporters, namely, PEPT1, PAT1, TauT and GAT2 were involved in ALA uptake in both normal and cancerous cells based on their respective expression levels. In general, expression levels of transporters were found to correlate with their degree of involvement in cellular uptake of ALA. Higher uptake of ALA will lead to higher production of PpIX, which is important in ALA-PDT and PDD.

The expression levels of all four transporters were also found to be independent of organ origin and vary across cell lines. TMK1 and MKN45 cells did not show similar patterns of transporter expression levels despite both being gastrointestinal cell lines. Another pair of prostate cancer cell lines, DU145 and PC3, also failed to show similar trend of transporter expression levels. This finding is consistent with past knowledges whereby cancer cells are heterogenous in nature and therefore specific treatment may be required to ensure effective recovery for each respective patient (Caldas *et. al.*, 2002).

Findings from Chapter 3 showed that there is no correlation of upregulation of specific transporters between cancerous or normal cell lines of the same origin. This finding overwritten past researches whereby PEPT1 expression was believed to be only highly expressed in cancer cells but not in normal cells (Chung *et. al.*, 2013). Cancer cells contains various genetic mutations compared to normal healthy cells. In this case, it is important to identify which transporters are highly expressed only in cancer cells to allow maximum effectiveness of ALA treatment while keeping the undesirable damages to surrounding healthy cells to a minimal level. Through this process, the effectiveness

and specificity of ALA-PDD and ALA-PDT could be significantly increase to achieve maximum results without causing further damage to the cancer patient.

Results from Fig. 3.4 and 3.5 showed significant decrease in PpIX levels in lung and prostate normal cells but not in their cancerous counterparts when inhibitors of highly expressed ALA uptake transporters were added. This phenomenon can be utilized to increase specificity of ALA-PDT and PDD. Since the expression levels of ALA uptake transporters varies in normal and cancer cell lines despite having the same origin, the co-administration of transporters inhibitory drugs targeted specifically to highly expressed transporters together with ALA could be a new therapeutic option for tailor-made therapy in ALA-PDT and PDD. This method of targeting highly expressed transporters in cancer patients is believed to be able to improve the effectiveness and specificity of ALA-PDT and ALA-PDD.

Findings from Chapter 4 showed that the efficiency of ALA-PDT is found to be affected by the expression levels of ALA uptake transporters, which changes under different cell density conditions. The study was carried out using a newly established cell density-dependent malignancy model, where expression level of malignancy markers is higher in higher cell density samples. When DU145 cancer cells were cultured under high cell density samples, a higher cancer killing effect of ALA-PDT and increase in expression level of ALA uptake transporters were observed. This showed that ALA-PDT is significantly more effective in high cell density cancer cells due to the upregulation of ALA uptake transporters. In addition, this study also showed a possibility that YAP might play an important role in the regulation of both cancer malignancy markers and ALA uptake transporters.

5.2 FUTURE CONSIDERATIONS

Even though this research has successfully identified the roles of transporters involved in cellular uptake of ALA across cellular membrane in ALA-PDT, more in-depth investigations are required to study their roles under a more cancer-like environment. Two important investigations should be further considered:

Findings from Fig. 2.3 showed the amount of intracellular and extracellular PpIX vary across different cell lines. This dissertation had showed the amount of ALA uptake by the cell is important in allowing sufficient PpIX production for ALA-PDD and PDT. However, retaining a significant amount of PpIX within the cell is also an important factor in order to maximise the effect of ALA-PDD and PDT. Therefore, the difference between the production of intracellular and extracellular PpIX among each cell line should be thoroughly studied in the hope of retaining as much PpIX produced within the cell without being efflux out.

Secondly, past studies had suggested that adenosine triphosphate-binding cassette G2 (ABCG2) transporter was involved in the efflux of PpIX in cells (Zhou *et. al.*, 2005, Hagiya *et. al.*, 2012; Kobuchi *et. al.*, 2012). Therefore, inhibition of this efflux transporter is believed to be able to prevent PpIX efflux and retain the PpIX produced within the cells. A comparative study on various cell lines should be carried out to examine the expression level of ABCG2 and how they affect the efflux and accumulation of PpIX in the cells.

On the other hand, it is also important to study the expression level of ABCG2 in normal cell lines and compare their expression levels with respective cancerous counterparts. This study is essential to evaluate whether is there any potential specificity issue following the inhibition of ABCG2. Past studies have suggested that ABCG2 is

found to be highly expressed in cancer patients (Zhou *et. al.,* 2005; Kobuchi *et. al.*, 2012). Scientists believed that high expression of ABCG2 contribute to drug resistance of cancer cells. Therefore, clarifying the expression levels of normal and cancer cells could be pivotal in increasing the specificity and effectiveness of ALA-PDD and PDT.

The second future investigation is targeted on understanding the role of verteporfin, a YAP inhibitor, and its effect on the effectiveness of ALA-PDT. Under normal circumstances, the number and proliferation capability of cells are well regulated. However, this is not the case for cancer cells. Cancer cells were known to be able to proliferate indefinitely to form tumours, regardless of the cell densities, leading to the formation of tumours (Zhao *et. al.*, 2007). This indefinite proliferative capability is exceptionally prevalent in malignant cells and is generally believed to be due to the effect of YAP and Hippo pathway (Li *et. al.*, 2020).

Findings in Chapter 4 suggest the role of YAP in regulating expression levels of ALA uptake transporters and cell density. The expression level of malignancy markers is found to be higher in high density samples. Therefore, it may be important to look into how YAP regulate cell densities and cancer malignancy, leading to regulation of expression levels of transporters and the effect on ALA uptake *in vitro* and *in vivo*. As one of the major components in the Hippo pathway, the connection of YAP and other Hippo pathway components, such as LATS1 and TAZ, with the malignancy of cancer cell should be carried out. This research is important as cancer malignancy has always been closely related to the proliferative capabilities and cell density of cancer cells – both which are important roles of YAP and the Hippo pathway.

Bibliography

Abrahamse, H., & Hamblin, M. R. (2016). New photosensitizers for photodynamic therapy. *Biochemical Journal*, *473*(4), 347-364.

Addison, J. M., Burston, D., Dalrymple, J. A., Matthews, D. M., Payne, J. W., Sleisenger, M. H., & Wilkinson, S. (1975). A common mechanism for transport of di-and tri-peptides by hamster jejunum in vitro. *Clinical Science*, *49*(4), 313-322.

Adibi, S. A., & Morse, E. L. (1977). The number of glycine residues which limits intact absorption of glycine oligopeptides in human jejunum. *The Journal of clinical investigation*, *60*(5), 1008-1016.

Agostinis, P., Berg, K., Cengel, K. A., Foster, T. H., Girotti, A. W., Gollnick, S. O., Hahn., S. M., Hamblin, M. R., Juzeniene, A., Kessel, D., & Korbelik, M. (2011). Photodynamic therapy of cancer: an update. *CA: a cancer journal for clinicians*, *61*(4), 250-281.

Anderson, C. M., Jevons, M., Thangaraju, M., Edwards, N., Conlon, N. J., Woods, S., Ganapathy, V. & Thwaites, D. T. (2010). Transport of the photodynamic therapy agent 5-aminolevulinic acid by distinct H+-coupled nutrient carriers coexpressed in the small intestine. *Journal of Pharmacology and Experimental Therapeutics*, *332*(1), 220-228.

Anderson, D. M., Maraskovsky, E., Billingsley, W. L., Dougall, W. C., Tometsko, M. E., Roux, E. R., Teepe, M. C., DuBose, R. F., Cosman, D. & Galibert, L. (1997). A homologue of the TNF receptor and its ligand enhance T-cell growth and dendritic-cell function. *Nature*, *390*(6656), 175-179.

Boll, M., Foltz, M., Rubio-Aliaga, I., Kottra, G., & Daniel, H. (2002). Functional characterization of two novel mammalian electrogenic proton-dependent amino acid cotransporters. *Journal of Biological Chemistry*, *277*(25), 22966-22973.

Boonstra, E., de Kleijn, R., Colzato, L. S., Alkemade, A., Forstmann, B. U., & Nieuwenhuis, S. (2015). Neurotransmitters as food supplements: the effects of GABA on brain and behavior. *Frontiers in psychology*, *6*, 1520.

Bozell, J. J., Moens, L., Elliott, D. C., Wang, Y., Neuenscwander, G. G., Fitzpatrick, S. W., Bilski, R. J. & Jarnefeld, J. L. (2000). Production of levulinic acid and use as a platform chemical for derived products. *Resources, conservation and recycling*, *28*(3-4), 227-239.

Caldas, C., & Aparicio, S. A. (2002). Cancer: The molecular outlook. *Nature, 415*(6871), 484.

Casas, A., & Batlle, A. (2002). Rational design of 5-aminolevulinic acid derivatives aimed at improving photodynamic therapy. *Current Medicinal Chemistry-Anti-Cancer Agents*, *2*(4), 465-475.

Chen, C.-Y. A., Ezzeddine, N., & Shyu, A.-B. (2008). Messenger RNA Half-Life Measurements in Mammalian Cells. *Methods in Enzymology*, *448*, 335–357. http://doi.org/10.1016/S0076-6879(08)02617-7

Chen, G., Sircar, K., Aprikian, A., Potti, A., Goltzman, D., & Rabbani, S. A. (2006). Expression of RANKL/RANK/OPG in primary and metastatic human prostate cancer as markers of disease stage and functional regulation. *Cancer*, *107*(2), 289-298.

Chen, Z., Fei, Y. J., Anderson, C. M., Wake, K. A., Miyauchi, S., Huang, W., Thwaites, D. T. & Ganapathy, V. (2003). Structure, function and immunolocalization of a proton - coupled amino acid transporter (hPAT1) in the human intestinal cell line Caco - 2. *The Journal of physiology*, *546*(2), 349-361.

Chung, C. W., Kim, C. H., Lee, H. M., Kim, D. H., Kwak, T. W., Chung, K. D., Jeong, Y. & Kang, D. H. (2013). Aminolevulinic acid derivatives-based photodynamic therapy in human intra-and extrahepatic cholangiocarcinoma cells. *European Journal of Pharmaceutics and Biopharmaceutics*, *85*(3), 503-510.

Chung, G. G., Provost, E., Kielhorn, E. P., Charette, L. A., Smith, B. L., & Rimm, D. L. (2001). Tissue microarray analysis of β-catenin in colorectal cancer shows nuclear phospho-β-catenin is associated with a better prognosis. *Clinical Cancer Research, 7*(12), 4013-4020.

Collaud, S., Juzeniene, A., Moan, J., & Lange, N. (2004). On the selectivity of 5-aminolevulinic acid-induced protoporphyrin IX formation. *Current Medicinal Chemistry-Anti-Cancer Agents*, *4*(3), 301-316.

De Rosa, F. S., & Bentley, M. V. L. (2000). Photodynamic therapy of skin cancers: sensitizers, clinical studies and future directives. *Pharmaceutical research*, *17*(12), 1447-1455.

Delaney, G., Jacob, S., Featherstone, C., & Barton, M. (2005). The role of radiotherapy in cancer treatment. *Cancer*, *104*(6), 1129-1137.

Dolmans, D. E., Fukumura, D., & Jain, R. K. (2003). Photodynamic therapy for cancer. *Nature reviews cancer*, *3*(5), 380.

Döring, F., Walter, J., Will, J., Föcking, M., Boll, M., Amasheh, S., Clauss, W. & Daniel, H. (1998). Delta-aminolevulinic acid transport by intestinal and renal peptide transporters and its physiological and clinical implications. *The Journal of clinical investigation*, *101*(12), 2761-2767.

Dysart, J. S., & Patterson, M. S. (2005). Characterization of Photofrin photobleaching for singlet oxygen dose estimation during photodynamic therapy of MLL cells in vitro. *Physics in Medicine & Biology*, *50*(11), 2597.

Ennis, S. R., Novotny, A., Xiang, J., Shakui, P., Masada, T., Stummer, W. & Keep, R. F. (2003). Transport of 5-aminolevulinic acid between blood and brain. *Brain research*, *959*(2), 226-234.

Faria, T. N., Timoszyk, J. K., Stouch, T. R., Vig, B. S., Landowski, C. P., Amidon, G. L., Weaver, C. D., Wall, D. A. & Smith, R. L. (2004). A novel high-throughput PepT1 transporter assay differentiates between substrates and antagonists. *Molecular pharmaceutics*, *1*(1), 67-76.

Frølund, S., Marquez, O. C., Larsen, M., Brodin, B., & Nielsen, C. U. (2010). δ - Aminolevulinic acid is a substrate for the amino acid transporter SLC36A1 (hPAT1). *British Journal of Pharmacology*, *159*(6), 1339-1353.

Fukuhara, H., Yamamoto, S., Karashima, T. & Inoue, K. (2020). Photodynamic diagnosis and therapy for urothelial carcinoma and prostate cancer: New imaging technology and therapy. *International Journal of Clinical Oncology*, 1-8.

Gether, U., Andersen, P. H., Larsson, O. M., & Schousboe, A. (2006). Neurotransmitter transporters: molecular function of important drug targets. *Trends in pharmacological sciences*, *27*(7), 375-383.

Gheewala, T., Skwor, T., & Munirathinam, G. (2017). Photosensitizers in prostate cancer therapy. *Oncotarget*, *8*(18), 30524–30538. doi: http://doi.org/10.18632/oncotarget.15496

Giacomini, K. M., Huang, S. M., Tweedie, D. J., Benet, L. Z., Brouwer, K. L., Chu, X., & Hoffmaster, K. A. (2010). Membrane transporters in drug development. *Nature Reviews Drug Discovery*, *9*(3), 215.

Greenwood, E. (2002). Prognostics: Tailor-made therapy. *Nature Reviews Cancer, 2*(3), 157.

Gygi, S. P., Rochon, Y., Franza, B. R., & Aebersold, R. (1999). Correlation between protein and mRNA abundance in yeast. *Molecular and cellular biology*, *19*(3), 1720-1730.

Hagiya, Y., Adachi, T., Ogura, S. I., An, R., Tamura, A., Nakagawa, H., Okura, I., Mochizuki, T. & Ishikawa, T. (2008). Nrf2-dependent induction of human ABC transporter ABCG2 and heme oxygenase-1 in HepG2 cells by photoactivation of porphyrins: biochemical implications for cancer cell response to photodynamic therapy. *Journal of experimental therapeutics & oncology*, *7*(2).

Hagiya, Y., Endo, Y., Yonemura, Y., Takahashi, K., Ishizuka, M., Abe, F., Tanaka, T., Okura, O, Nakajima, M., Ishikawa, T. & Ogura, S. I. (2012). Pivotal roles of peptide transporter PEPT1 and ATP-binding cassette (ABC) transporter ABCG2 in 5-aminolevulinic acid (ALA)-based photocytotoxicity of gastric cancer cells in vitro. *Photodiagnosis and photodynamic therapy*, *9*(3), 204-214.

Huggett, M. T., Jermyn, M., Gillams, A., Illing, R., Mosse, S., Novelli, M., Kent, E., Bown, S. G., Pogue, B. W. & Pereira, S. P. (2014). Phase I/II study of verteporfin photodynamic therapy in locally advanced pancreatic cancer. *British journal of cancer*, *110*(7), 1698.

Hunter, G. A., Al-Karadaghi, S., & Ferreira, G. C. (2011). Ferrochelatase: the convergence of the porphyrin biosynthesis and iron transport pathways. *Journal of Porphyrins and Phthalocyanines*, *15*(05n06), 350-356.

Itoh, Y., Ninomiya, Y., Tajima, S., & Ishibashi, A. (2001). Photodynamic therapy of acne vulgaris with topical δ - aminolaevulinic acid and incoherent light in Japanese patients. *British Journal of Dermatology*, *144*(3), 575-579.

Jichlinski, P., Forrer, M., Mizeret, J., Glanzmann, T., Braichotte, D., Wagnières, G., Zimmer, G., Guillou, L., Schmidlin, F., Graber, P., van den Bergh, H. & Leisinger, H. (1997). Clinical evaluation of a method for detecting superficial transitional cell carcinoma of the bladder by light - induced fluorescence of protoporphyrin IX following topical application of 5 - aminolevulinic acid: Preliminary results. *Lasers in Surgery and Medicine*, *20*(4), 402-408.

Jones, H., Nakashima, T., Sanchez, O. H., Kozieradzki, I., Komarova, S. V., Sarosi, I., Morony, S., Rubin, E., Sarao, R., Hojilla, C. V., Komnenovic, V., Kong, Y., Dixon, S. J., Sims, S. M., Khokha, R., Wada, T. & Penninger, J. M. (2006). Regulation of cancer cell migration and bone metastasis by RANKL. *Nature*, *440*(7084), 692-696. doi: https://doi.org/10.1038/nature04524

Kennedy, J. C. & Pottier, R. H. (1992). Endogenous protoporphyrin IX, a clinically useful photosensitizer for photodynamic therapy. *Journal of Photochem Photobiol Biol*, *14*(4): 275-92.

Kerbel, R. S. (1992). Expression of multi-cytokine resistance and multi-growth factor independence in advanced stage metastatic cancer: Malignant melanoma as a paradigm. *American Journal of Pathology*, *141*(3), 519.

Klingler, F. D., & Ebertz, W. (2003). Oxocarboxylic acids. *Ullmann's Encyclopedia of Industrial Chemistry*.

Kolhatkar, V., & Polli, J. E. (2010). Reliability of inhibition models to correctly identify type of inhibition. *Pharmaceutical research*, *27*(11), 2433-2445.

Konopka, K. & Goslinski, T. (2007). Photodynamic therapy in dentistry. *Journal of Dental Research*, *86*(8), 694-707.

Koussounadis, A., Langdon, S. P., Um, I. H., Harrison, D. J., & Smith, V. A. (2015). Relationship between differentially expressed mRNA and mRNA-protein correlations in a xenograft model system. *Scientific Reports*, *5*, 10775.

Krafft, C., Belay, B., Bergner, N., Romeike, B. F., Reichart, R., Kalff, R. & Popp, J. (2012). Advances in optical biopsy – correlation of malignancy and cell density of primary brain tumors using Raman microspectroscopic imaging. *Analyst*, *137*(23), 5533-5537. doi: https://doi.org/10.1039/C2AN36083G

Krammer, B., & Plaetzer, K. (2008). ALA and its clinical impact, from bench to bedside. *Photochemical & Photobiological Sciences*, *7*(3), 283-289.

Krammer, B. & Uberrriegler, K. (1996). In vitro investigation of ALA-induced protoporphyrin IX. *J Photochem Photobiol.,* 36(2), 121-126.

Kristensen, A.S., Andersen, J., Jørgensen, T. N., Sorennsen, L., Eriksen, J., Loland, C. J., Stromgaard, K. & Gether, U. (2011). SLC6 Neurotransmitter Transporters : Structure , Function , and Regulation. *Pharmacological reviews.* 63(3):585-640.

Lai, H. W., Sasaki, R., Usuki, S., Nakajima, M., Tanaka, T., Ogura, S. (2019). Novel strategy to increase specificity of ALA-induced PpIX accumulation through inhibition of transporters involved in ALA uptake. Photodiagnosis and Photodynamic Therapy, 27, 327-335. doi: https://doi.org/10.1016/j.pdpdt.2019.06.017

Larsen, M., Holm, R., Jensen, K. G., Brodin, B., & Nielsen, C. U. (2009). Intestinal gaboxadol absorption via PAT1 (SLC36A1): modified absorption in vivo following co - administration of L - tryptophan. *British journal of pharmacology*, *157*(8), 1380-1389.

Leanne B, J., & Ross W, B. (2008). Photodynamic therapy and the development of metal-based photosensitisers. *Metal-based drugs*, *2008*.

Lee, M. J., Hung, S. H., Huang, M. C., Tsai, T. & Chen, C. T. (2017). Doxycycline potentiates antitumor effect of 5-aminolevulinic acid-mediated photodynamic therapy in malignant peripheral nerve sheath tumor cells. *PloS one*, *12*(5), e0178493. doi: https://doi.org/10.1371/journal.pone.0178493

Li, X. & Zhou, X. (2020). ALA-PDT inhibits human HSAS1 cell viability and cytokine secretion by Hippo/YAP signalling pathway. *Journal of Immunology*, *36*(8), 701-706.

Lydiard, R. B. (2003). The role of GABA in anxiety disorders. *The Journal of clinical psychiatry*, *64*, 21-27.

Meredith, D., Temple, C. S., Guha, N., Sword, C. J., Boyd, C. A., Collier, I. D., Morgan, K. M. & Bailey, P. D. (2000). Modified amino acids and peptides as substrates for the intestinal peptide transporter PepT1. *The FEBS Journal*, *267*(12), 3723-3728.

mimetic. (n.d.). *Collins English Dictionary - Complete & Unabridged 10th Edition*. Retrieved May 14, 2018 from Dictionary.com website http://www.dictionary.com/browse/mimetic

Mizuno, H., Kitada, K., Nakai, K., & Sarai, A. (2009). PrognoScan: a new database for meta-analysis of the prognostic value of genes. *BMC medical genomics*, *2*(1), 1-11.

Moan, J. & Peng, Q (2003). An outline of the hundred-year history of PDT. *Anticancer Res*. 23:3591– 3600.

Moan, J., Berg, K., Kvam, E., Western, A., Malik, Z., Rück, A., & Schneckenburger, H. (1989). Intracellular localization of photosensitizers. In *Ciba Foundation Symposium 146-Photosensitizing Compounds: Their Chemistry, Biology and Clinical Use* (pp. 95-111). John Wiley & Sons, Ltd.

Moan, J., Bech, O., Gaullier, J. M., Stokke, T., Steen, H. B., Ma, L. & Berg, K. (1998). Protoporphyrin IX accumulation in cells treated with 5-aminolevulinic acid dependence on cell density, cell size and cell cycle. *Int J Cancer*, 75(1), 134-139.

Moretti, M. B., Garcia, S. C., Perotti, C., Batlle, A., & Casas, A. (2002). δ-Aminolevulinic acid transport in murine mammary adenocarcinoma

Morgan, R. A., Dudley, M. E., & Rosenberg, S. A. (2010). Adoptive cell therapy: genetic modification to redirect effector cell specificity. *The Cancer Journal, 16*(4), 336-341.

Nishio, Y., Fujino, M., Zhao, M., Ishii, T., Ishizuka, M., Ito, H. & Taketani, S. (2014). 5-Aminolevulinic acid combined with ferrous iron enhances the expression of heme oxygenase-1. *International immunopharmacology*, *19*(2), 300-307.

Novotny, A., Xiang, J., Stummer, W., Teuscher, N. S., Smith, D. E., & Keep, R. F. (2000). Mechanisms of 5 - Aminolevulinic Acid Uptake at the Choroid Plexus. *Journal of Neurochemistry*, *75*(1), 321-328.

Ögmundsdóttir, M. H., Heublein, S., Kazi, S., Reynolds, B., Visvalingam, S. M., Shaw, M. K., & Goberdhan, D. C. (2012). Proton-assisted amino acid transporter PAT1 complexes with Rag GTPases and activates TORC1 on late endosomal and lysosomal membranes. *PloS one*, *7*(5), e36616.

Okudaira, H., Shikano, N., Nishii, R., Miyagi, T., Yoshimoto, M., Kobayashi, M., Ohe, K., Nakanishi, T., Tamai, I., Namiki, M. & Kawai, K. (2011). Putative transport mechanism and intracellular fate of trans-1-amino-3-18F-fluorocyclobutanecarboxylic acid in human prostate cancer. *Journal of Nuclear Medicine*, *52*(5), 822-829.

Osaki, T., Yokoe, I., Sunden, Y., Ota, U., Ichikawa, T., Imazato, H., Ishii, T., Takahashi, K., Ishizuka, M., Tanaka, T., Li, L., Yamashita, M., Murahata, T., Tsuka, T., Azuma, K., Ito, N., Imagawa, T. & Okamoto, Y. (2019). Efficacy of 5-Aminolevulinic Acid in Photodynamic Detection and Photodynamic Therapy in Veterinary Medicine. *Cancers*, *11*(4), 495. doi: https://doi.org/10.3390/cancers11040495

Otsuka, S. (2017). *腫瘍内低酸素環境におけるポルフィリン代謝機構の解明*。(Doctoral Dissertation) Tokyo Institute of Technology, Tokyo, Japan.

Peng, Q., Warloe, T., Berg, K., Moan, J., Kongshaug, M., Giercksky, K. E., & Nesland, J. M. (1997). 5 - Aminolevulinic acid - based photodynamic therapy. *Cancer*, *79*(12), 2282-2308.

Petroff, O. A. (2002). Book review: GABA and glutamate in the human brain. *The Neuroscientist*, *8*(6), 562-573.

Plaunt, A. J., Harmatys, K. M., Hendrie, K. A., Musso, A. J., & Smith, B. D. (2014). Chemically triggered release of 5-aminolevulinic acid from liposomes. *RSC advances*, *4*(101), 57983-57990.

Rick, K., Sroka, R., Stepp, H., Kriegmair, M., Huber, R. M., Jacob, K., & Baumgartner, R. (1997). Pharmacokinetics of 5-aminolevulinic acid-induced protoporphyrin IX in skin and blood. *Journal of Photochemistry and Photobiology B: Biology*, *40*(3), 313-319.

Rodriguez, L., Batlle, A., Di Venosa, G., MacRobert, A. J., Battah, S., Daniel, H., & Casas, A. (2006). Study of the mechanisms of uptake of 5-aminolevulinic acid derivatives by PEPT1 and PEPT2 transporters as a tool to improve photodynamic therapy of tumours. *The international journal of biochemistry & cell biology*, *38*(9), 1530-1539.

Rubio-Aliaga, I., & Daniel, H. (2002). Mammalian peptide transporters as targets for drug delivery. *Trends in pharmacological sciences*, *23*(9), 434-440.

Schewe, D. M. & Aguirre-Ghiso, J. A. (2009). Inhibition of eIF2α dephosphorylation maximizes bortezomib efficiency and eliminates quiescent multiple myeloma cells surviving proteasome inhibitor therapy. *Cancer research*, *69*(4), 1545-1552.

Scimemi, A. (2014). Structure, function, and plasticity of GABA transporters. *Frontiers in Cellular Neuroscience*, *8*, 161. http://doi.org/10.3389/fncel.2014.00161

Smith D. E., Clémençon, B. &Hediger, M. A. (2013). Proton-coupled oligopeptide transporter family SLC15: Physiological, pharmacological and pathological implications. *Molecular Aspects Medicine.* 34(2-3):323-336.

Steinbach, P., Wedmgandt, H., Baumgartner, R., Kriegmair, M., Hofstadter, F. & Knuchel, R. (1995). Cellular fluorescence of the endogenous photosensitizer proptoporphyrin IX following the exposure to 5-aminolevulinic acid. *Photochem. Photobiol*, 62(5), 887-895.

Stummer, W., Pichlmeier, U., Meinel, T., Wiestler, O. D., Zanella, F., Reulen, H. J., & ALA-Glioma Study Group. (2006). Fluorescence-guided surgery with 5-aminolevulinic acid for resection of malignant glioma: a randomised controlled multicentre phase III trial. *The Lancet Oncology*, *7*(5), 392-401.

Tamura, A., Onishi, Y., An, R., Koshiba, S., Wakabayashi, K., Hoshijima, K., Priebe. W.. Yoshida, T., Kometani, S., Matsubara, T., Mikuriya, K. & Ishikawa, T. (2007). In vitro evaluation of photosensitivity risk related to genetic polymorphisms of human ABC

transporter ABCG2 and inhibition by drugs. *Drug Metabolism and Pharmacokinetics*, *22*(6), 428-440.

Thwaites, D. T. & Anderson, C. M. H.(2007). Deciphering the mechanisms of intestinal imino (and amino) acid transport: The redemption of SLC36A1. *Biochim Biophys Acta - Biomembr.* 1768(2):179-197.

Tomi, M., Tajima, A., Tachikawa, M., & Hosoya, K. I. (2008). Function of taurine transporter (Slc6a6/TauT) as a GABA transporting protein and its relevance to GABA transport in rat retinal capillary endothelial cells. *Biochimica Et Biophysica Acta (BBA)-Biomembranes*, *1778*(10), 2138-2142.

Tran, T. T., Mu, A., Adachi, Y., Adachi, Y., & Taketani, S. (2014). Neurotransmitter Transporter Family including SLC6A6 and SLC6A13 contributes to the 5 - aminolevulinic Acid (ALA) - induced accumulation of protoporphyrin IX and photodamage, through uptake of ALA by cancerous cells. *Photochemistry and Photobiology*, *90*(5), 1136-1143.

Uptake. (2003) In *Miller-Keane Encyclopedia and Dictionary of Medicine, Nursing, and Allied Health, Seventh Edition*. Retrieved May 11 2018 from https://medical-dictionary.thefreedictionary.com/uptake

Valdés, P. A., Leblond, F., Kim, A., Harris, B. T., Wilson, B. C., Fan, X. & Simmons, N. E. (2011). Quantitative fluorescence in intracranial tumor: implications for ALA-induced PpIX as an intraoperative biomarker. *Journal of neurosurgery*, *115*(1), 11-17.

van den Boogert, J., van Hillegersberg, R., de Rooij, F. W., de Bruin, R. W., Edixhoven-Bosdijk, A., Houtsmuller, A. B., & Tilanus, H. W. (1998). 5-Aminolaevulinic acid-induced protoporphyrin IX accumulation in tissues: pharmacokinetics after oral or intravenous administration. *Journal of Photochemistry and Photobiology B: Biology*, *44*(1), 29-38.

Van Hillegersberg, R., Van Den Berg, J. W. O., Kort, W. J., Terpstra, O. T., & Wilson, J. P. (1992). Selective accumulation of endogenously produced porphyrins in a liver metastasis model in rats. *Gastroenterology*, *103*(2), 647-651.

Van't Veer, L. J., Dai, H., Van De Vijver, M. J., He, Y. D., Hart, A. A., Mao, M., & Schreiber, G. J. (2002). Gene expression profiling predicts clinical outcome of breast cancer. *Nature, 415*(6871), 530.

Varelas, X., Samavarchi-Tehrani, P., Narimatsu, M., Weiss, A., Cockburn, K., Larsen, B. G., Rossant, J. & Wrana, J. L. (2010). The Crumbs Complex Couples Cell Density Sensing to Hippo-Dependent Control of the TGF-β-SMAD Pathway. *Developmental Cell*, *19*(6), 831-844.

Wang, C., Zhu, X., Feng, W., Yu, Y., Jeong, K., Guo, W., Lu, Y. & Mills, G. (2016). Verteporfin inhibits YAP function through up-regulating 14-3-3σ sequestering YAP in the cytoplasm. *American Journal of Cancer Research*, *6*(1), 27.

Wang, I. & Wheeler, D. A. (2014). Genomic sequencing of cancer diagnosis and therapy. *Annual Review of Medicine*, *65*, 33-48.

Xie, Y., Hu, Y., & Smith, D. E. (2016). The proton - coupled oligopeptide transporter 1 plays a major role in the intestinal permeability and absorption of 5 - aminolevulinic acid. *British Journal of Pharmacology*, *173*(1), 167-176.

Yahara, T., Tachikawa, M., Akanuma, S. I., Kubo, Y., & Hosoya, K. I. (2014). Amino acid residues involved in the substrate specificity of TauT/SLC6A6 for taurine and γ-aminobutyric acid. *Biological and Pharmaceutical Bulletin*, *37*(5), 817-825.

Yang, E., van Nimwegen, E., Zavolan, M., Rajewsky, N., Schroeder, M., Magnasco, M., & Darnell, J. E. (2003). Decay Rates of Human mRNAs: Correlation With Functional Characteristics and Sequence Attributes. *Genome Research*, *13*(8), 1863–1872. http://doi.org/10.1101/gr.1272403

Yang, X., Palasuberniam, P., Kraus, D., & Chen, B. (2015). Aminolevulinic Acid-Based Tumor Detection and Therapy: Molecular Mechanisms and Strategies for Enhancement. *International Journal of Molecular Sciences*, *16*(10), 25865–25880. http://doi.org/10.3390/ijms161025865

Yonemura, Y., Endo, Y., Canbay, E., Liu, Y., Ishibashi, H., Mizumoto, A., Hirano, M., Imazato, Y., Takao, N., Ichinose, M., Noguchi, K., Li, Y., Wakama, S., Yamada, K., Hatano, K., Shintani, H., Yoshitake, H. & Ogura, S. (2017). Photodynamic detection of peritoneal metastases using 5-aminolevulinic acid (ALA). *Cancers*, *9*(3), 23.

Zhao, B., Wei, X., Li, W. H., Udan, R. S., Yang, Q., Kim, J., Xie, J., Ikenoue, T., Yu, J., Li, L., Zheng, P., Ye, K., Chinnaiyan, A., Halder, G., Lai, Z. & Zheng, P. (2007). Inactivation of YAP oncoprotein by the Hippo pathway is involved in cell contact inhibition and tissue growth control. *Genes and Development*, *21*(21), 2747-2761. doi: https://doi.org/10.1101/gad. 1602907

Zhou, Y., Holmseth, S., Guo, C., Hassel, B., Höfner, G., Huitfeldt, H. S., Danbolt, N. C. (2012). Deletion of the γ-Aminobutyric Acid Transporter 2 (GAT2 and SLC6A13) Gene in Mice Leads to Changes in Liver and Brain Taurine Contents. *The Journal of Biological Chemistry*, *287*(42), 35733–35746. doi: http://doi.org/10.1074/jbc.M112.368175

Acknowledgement

I owe the completion of this thesis to my supervisor, Assoc. Prof. Dr Ogura Shun-Ichiro. The entire progress of this project until the submission of this thesis would not be successful without his constant encouragement, guidance and support. I would like to take this opportunity to express my uppermost gratitude to him for his willingness to sacrifice their time, money and energy on me with patience, dedication and kindness throughout my entire project. It is an honour to be one of his students and I look forward for a close relationship between us in my upcoming academic career.

I would also like to thank all the staff of School of Life Science and Biotechnology especially Ms. Fukaya Yumiko, for their continuous time and effort in providing technical support to me in terms of methodology, preparation of media, and sterilization of materials. Many thanks to my fellow seniors and labmates, especially Mr. Sasaki Ryuta, Mr. Usuki Shiro and Mr. Koura Yuuki for their kind assistance, guidance and professional advice during the entire course of this project.

Credits should also be given to my beloved family who raised me to who I am, and to my friends who constantly provide me morale support and motivation. Without their constant support, love and tolerance, completing my doctoral thesis would certainly remain a dream. Each and every one mentioned above is my inspirations in the completion of my doctoral research.

Last but not least, I would also like to thank the Japanese government and University Institute of Technology for providing the chance and Monbugakusho (MEXT) scholarship to study here without worrying about financial problem. It is impossible for an international student like me which comes from an average family could afford the high living expense in Tokyo.

First-Authored Publication(s):

1. **Lai, H.W.**, Takahashi, K., Nakajima, M., Tanaka, T. & Ogura, S. (2021). Efficiency of aminolevulinic acid (ALA)-photodynamic therapy based on ALA uptake transporters in a cell density-dependent malignancy model. *Journal of Photochemistry & Photobiology B: Biology, 218*, 112191. doi: https://doi.org/10.1016/j.jphotobiol.2021.112191

2. **Lai, H.W.**, Nakayama, T. & Ogura, S. (2020). Key transporters leading to specific protoporphyrin IX accumulation in cancer cell following administration of aminolevulinic acid in photodynamic therapy/diagnosis. *International Journal of Clinical Oncology*, 1-8. doi: https://doi.org/10.1007/s10147-020-01766-y

3. **Lai, H.W.**, Sasaki, R., Usuki, S., Nakajima, M., Tanaka, T. & Ogura, S. (2019). Novel strategy to increase specificity of ALA-Induced PpIX accumulation through inhibition of transporters involved in ALA uptake. *Photodiagnosis and Photodynamic Therapy, 27*, 327-335. doi: https://doi.org/10.1016/j.pdpdt.2019.06.017